

**Potential of Natural Products as SARS-COV-2 RNA Dependent RNA
Polymerase Inhibitors: A Molecular Docking Study**

Tarekegn Tafese Yenako

Major-Advisor: Teshome Geremew (PhD)

Co-Advisor: Milkyas Endale (PhD)

A Thesis Submitted to the Department of Applied Biology

School of Applied Natural Science

Presented in Partial Fulfilment for the Requirements for Degree of Master's in
Applied Biology (Biotechnology)

Office of Graduate Studies

Adama Science and Technology University

June, 2022

Adama, Ethiopia

DECLARATION

I hereby declare that this Master's Thesis entitled "**Potential of natural products as SARS-CoV-2 RNA dependent RNA polymerase inhibitors: a molecular docking study**" is my original work. That is, it has not been submitted for the award of any academic degree, diploma, or certificate in any other university. All sources of materials that are used for this thesis have been duly acknowledged through citation.

Name of student

Signature

Date

RECOMMENDATION

We, the advisors of this thesis, hereby certify that we have read the revised version of the thesis entitled “**Potential of natural products as SARS-CoV-2 RNA dependent RNA polymerase inhibitors: a molecular docking study**” prepared under our guidance by Tarekegn Tafese submitted in partial fulfillment of the requirements for the degree of Masters of Science in Applied Biology. Therefore, we recommend the submission of the revised version of the thesis to the department following the applicable procedures.

_____	_____	_____
Co-advisor	Signature	Date

_____	_____	_____
Co-advisor	Signature	Date

APPROVAL PAGE

We, the advisors of the thesis entitled “**Potential of natural products as SARS CoV-2 RNA dependent RNA polymerase inhibitors: a molecular docking study**” and developed by Tarekegn Tafese, hereby certify that the recommendation and suggestions made by the board of examiners are appropriately incorporated into the final version of the thesis.

_____	_____	_____
Co-advisor	Signature	Date

_____	_____	_____
Co-advisor	Signature	Date

We, the undersigned, members of the Board of Examiners of the thesis by Tarekegn Tafese have read and evaluated the thesis entitled “potential of natural products as SARS-CoV-2 RNA dependent RNA polymerase inhibitors: a molecular docking study” and examined the candidate during the open defense. This is, therefore, to certify that the thesis is accepted for partial fulfillment of the requirement of the degree of Master of Science in Applied Biology.

_____	_____	_____
Chairperson	Signature	Date

_____	_____	_____
Internal Examiner	Signature	Date

_____	_____	_____
External Examiner	Signature	Date

Finally, approval and acceptance of the thesis is contingent upon the submission of its final copy to the Office of Postgraduate Studies (OPGS) through the Department Graduate committee (DGC) and School Graduate Committee (SGC).

_____	_____	_____
Department Head	Signature	Date

_____	_____	_____
School Dean	Signature	Date

_____	_____	_____
Office of Postgraduate Studies, Dean	Signature	Date

ACKNOWLEDGEMENT

First of all, I would like to thank the almighty God who helped me to reach this level. Second, I would like to express my deepest appreciation and sincere gratitude to my advisors, Dr. Teshome Geremew, and Dr. Milkyas Endale for their kind encouragement, consistent guidance, and supervision of all kinds throughout the MSc thesis research period. I have benefited a lot from the guidance of several mentors over the years. Of these, I have to acknowledge the support I got from Dr. Rajalakshmanan Eswaramoorthy (Saveetha University, India), Mr. Ashenaf Milkesa (MSc) and Mr. Mamaru Bitawu (MSc) in various software data analysis.

I would like to express my heartfelt gratitude to Adama Science and Technology University for the MSc scholarship opportunity given to me and for financially supporting me during my work.

Last but not least, I'd like to express my profound appreciation to my family, who have been at my side throughout my academic career. This long academic life was fraught with ups and downs, hope and despair, and required enormous spiritual and material support. Thank you for your unwavering support throughout this work.

TABLE OF CONTENTS

Contents.....	Pages
DECLARATION.....	i
RECOMMENDATION.....	ii
APPROVAL PAGE.....	iii
ACKNOWLEDGEMENT.....	iv
LIST OF TABLES.....	vii
LIST OF FIGURES.....	viii
LIST OF ABBREVIATIONS AND ACRONYMS.....	x
ABSTRACT.....	xii
1. INTRODUCTION.....	1
1.1. Background of the Study.....	1
1.2. Statement of the Problem.....	3
1.3. Objective of the Research.....	4
1.3.1. General Objective.....	4
1.3.2. Specific Objectives.....	5
1.4. Significance of the Study.....	5
1.5. Scope of the Study.....	6
2. LITERATURE REVIEW.....	7
2.1. COVID 19 (SARS-CoV-2).....	7
2.1.1. Structural and Genomic Organization of SARS-Cov-2.....	8
2.1.2. Viral Cell Entry, Replication, and Pathophysiology.....	10
2.2. Researches and Discovery of therapeutic agents on COVID-19.....	12
2.2.1. Role of Natural Products in Research on SARS CoV-2.....	12
2.2.4. Vaccines of COVID-19.....	14
2.3. Molecular Docking.....	15
2.3.1. Molecular Docking Studies on COVID-19.....	18
3. MATERIALS AND METHODS.....	25

3.1. Materials	25
3.1.1. Computer Software Used to Conduct the Study	25
3.1.2. Natural Products.....	26
3.1.3. Viral Receptor	28
3.2. Study Design	30
3.2.1. Retrieval of Natural Products.....	31
3.2.2. Drug Likeness, Physicochemical, and Pharmacokinetic Properties	31
3.2.3. Toxicity Predictions	32
3.2.4. Preparation of Ligands for docking	32
3.2.5. Retrieval and Preparation of Viral Receptor.....	33
3.2.6. Identification of the Active Site and Generation of the Receptor Grid	35
3.2.7. Docking Method Validation	36
3.2.8. Docking Analysis.....	36
4. RESULT AND DISCUSSION	37
4.1. Results.....	37
4.1.1. Identification of the General Characteristics of the Natural Compounds.....	37
4.1.2. Drug Likeness and Physico Chemical Properties	38
4.1.3. Pharmacokinetics	40
4.1.4. Toxicity Predictions	43
4.1.5. Binding site identification of the RdRp for docking.....	44
4.1.6. Molecular Docking and Binding Affinities	45
4.1.7. Interaction Analysis	47
4.2. Discussion	57
5. CONCLUSION AND RECOMMENDATIONS.....	61
5.1. Conclusion	61
5.2. Recommendations.....	62
RESEARCH FUND ACKNOWLEDGEMENT	63
REFERENCES.....	64
APPENDICES	i

LIST OF TABLES

Table 3. 1: List of computer software and databases.	25
Table 4. 1: General Characteristics of the natural compounds considered in this study.	37
Table 4. 2: Physicochemical properties and RO5 of test compounds.	39
Table 4. 3: Pharmacokinetics properties targeted compounds.	41
Table 4. 4: Protox II predicted organ toxicity, toxicological endpoints, and acute toxicity.	43
Table 4. 5: Binding energy and polar contact of the compounds on RdRp.	46

LIST OF FIGURES

Figure 2. 1: Schematic diagram of SARS-CoV-2.....	8
Figure 2. 2: Genomic organization of SARS-CoV-2.....	10
Figure 2. 3: Elements in protein-ligand docking (RdRp-remdesivir complex).....	17
Figure 2. 4: Natural products studied against SARS CoV-2 proteins.	24
Figure 3. 1: The structure of natural compounds considered in this study.....	28
Figure 3. 2: PDB structure of RdRp in surface and cartoon view (visualized by Pymol).....	29
Figure 3. 3: Flow chart of the employed methodology.....	30
Figure 4. 1: Good In vivo Drug absorption and Permeation Lipinski's Rule of 5.....	38
Figure 4. 2: Boiled egg model for pharmacokinetic properties.	42
Figure 4. 3: Active site RNA dependent RNA polymerase (CASTp predicted).	45
Figure 4. 4: Interaction of RdRp enzyme on Berberamine(52) [(A) 2D interactions (B) 3D interactions].....	48
Figure 4. 5: Interaction of RdRp enzyme on Dicentrin(53) [(A) 2D interactions (B) 3D interactions].....	48
Figure 4. 6: Interaction of RdRp enzyme on Coptisine(54) [(A) 2D interactions (B) 3D interactions].....	49
Figure 4. 7: Interaction of RdRp enzyme on Jatrorrhizine(55) [(A) 2D interactions (B) 3D interactions].....	49
Figure 4. 8: Interaction of RdRp enzyme on Palmatine(56) [(A) 2D interactions (B) 3D interactions].....	50
Figure 4. 9: Interaction of RdRp enzyme on Bufotenin(57) [(A) 2D interactions (B) 3D interactions].....	50
Figure 4. 10. Interaction of RdRp enzyme on Psilocybin(58) [(A) 2D interactions (B) 3D interactions].....	51
Figure 4. 11: Interaction of RdRp enzyme on Biscryptolepine(60) [(A) 2D interactions (B) 3D interactions].....	51
Figure 4. 12: Interaction of RdRp enzyme on CPD61 [(A) 2D interactions (B) 3D interactions].	52

Figure 4. 13: Interaction of RdRp enzyme on CPD62 [(A) 2D interactions (B) 3D interactions].	52
Figure 4. 14: Interaction of RdRp enzyme on CPD63 [(A) 2D interactions (B) 3D interactions].	53
Figure 4. 15: Interaction of RdRp enzyme on CPD64 [(A) 2D interactions (B) 3D interactions].	53
Figure 4. 16: Interaction of RdRp enzyme on CPD65 [(A) 2D interactions (B) 3D interactions].	54
Figure 4. 17: Interaction of RdRp enzyme on CPD66 [(A) 2D interactions (B) 3D interactions].	54
Figure 4. 18: Interaction of RdRp enzyme on CPD67 [(A) 2D interactions (B) 3D interactions].	55
Figure 4. 19: Interaction of RdRp enzyme on CPD68 [(a) 2D interactions (b) 3D interactions].	55
Figure 4. 20: Interaction of RdRp enzyme on CPD69 [(A) 2D interactions (B) 3D interactions].	56
Figure 4. 21: Interaction of RdRp enzyme on CPD70 [(A) 2D interactions (B) 3D interactions].	56
Figure 4. 22: Interaction of RdRp enzyme on CPD71 [(A) 2D interactions (B) 3D interactions].	57

LIST OF ABBREVIATIONS AND ACRONYMS

ACE	Angiotensin Converting Enzyme
ADT	Auto Dock Tool
BBB	Brain Blood Barrier
BCV	Bovine Corona Virus
CASTP	Computed Atlas of Surface Topography of proteins
CDC	Center for Disease Control
CNS	Central Nervous System
COVID-19	Corona Virus Disease-2019
CYPE	Cytochrome P450 enzyme
DMV	Double Membrane Vesicle
FDA	Food and Drug Agency
HCV	Hepatitis C Virus
MDS	Molecular Dynamics Simulation
MERS	Middle East Respiratory Syndrome
MGL	Molecular Graphics Laboratory
NSP	Nonstructural Protein
ORF	Open Reading Frame
PCID	PubChem Compound ID
PDB	Protein Data Bank
PDBQT	Protein Data Bank Partial Charge Type
PEDV	Porcine Epidemic Diarrhea Virus

PSM	Plant Secondary Metabolite
RBD	Receptor Binding Domain
RdRp	RNA dependent RNA polymerase
RMSD	Root Mean Square Deviation
RTC	Replication Transcription Complex
SARS	Severe Acute Respiratory Syndrome
SDF	Structure Data File
SMILES	Simplified Molecular Input Line Entry System
TMPRSS2	Trans membrane Protease Serine 2
TPSA	Topological Polar Surface Area
WHO	World Health Organization

ABSTRACT

COVID-19 is a transmissible respiratory disease caused by severe acute respiratory syndrome coronaviruses 2 (SARS CoV-2) which emerged in December 2019 in Wuhan, China. Several attempts have been done to examine the potential of natural compounds to prevent the multiplication of SARS-CoV-2 since the outbreak of the pandemic. The present study aimed to evaluate the potential of twenty selected natural products from published literature as SARS-CoV-2 RNA-dependent RNA polymerase inhibitors using a molecular docking approach. Out of them, nine compounds were published previously for their promising antiviral drug-like activity by various investigators whereas the remaining eleven were new and isolated from different Ethiopian flora in the applied chemistry department of ASTU. To test if these compounds meet the criteria for use as active drugs in humans, a rule of five (Ro5) was calculated. Remdesivir, an FDA-approved emergency medication, was utilized as a control. The docking evaluation, physicochemical, pharmacokinetic properties, and toxicity profiles were computed using Autodoc vina 4.2, SwissADME, and Protox II webservers, respectively. Among the examined compounds, nicotflorin(59) violates Lipinski's rule of five out of twenty compounds and hence docking evaluation proceeded for the remaining 19 natural products. The docking results showed that biscryptolepin(60), berbamin(52), CPD63, Jatrorrhizine(55), Dicentrin(53), CPD61, and CPD66, CPD69, and CPD70, displayed better binding affinity with ΔG values of -9.0, -8.8, and -7.7, , -7.4, -7.1, -6.8 kcal/mol, respectively, compared to remdesivir (-6.7 kcal/mol) suggesting the potential of these compounds as SARS CoV-2 RNA dependent RNA polymerase inhibitors. The toxicological endpoints prediction study result showed the LD50 values ranged from 96-89470 mg/Kg. Acute toxicity predictions showed that the compounds under consideration are not fatal; rather, they can be classified as nontoxic to highly toxic classes, with dicentrin(53), coptisine (54), and palmatine(56) active for all predicted toxicological endpoint and psilocybin(58), biscryptolepine (60), CPD61, CPD62, CPD68, and CPD69 with no predicted toxicological endpoints. Overall, the results of the present study revealed that four of the studied compounds i.e. Biscryptolepine(60) and CPD61(C₁₅H₁₄O₆) with zero toxicological endpoints, and CPD63 (C₁₈H₁₇NO₂), and CPD70(C₁₄H₈N₂O with one toxicological are promising compounds as SARS CoV-2 RNA dependent RNA polymerase inhibitors hence further experimental in vitro and in vivo therapeutic examination on COVID-19 is recommended.

Key words: Molecular Docking, Natural Products, SARS-CoV-2.

CHAPTER ONE

1. INTRODUCTION

1.1. Background of the Study

The coronavirus disease 2019 (COVID-19) is a contagious respiratory disease caused by severe acute respiratory syndrome coronaviruses 2 (SARS CoV-2) that causes illness in humans. In December 2019, the first human cases of COVID-19, a coronavirus disease, were reported in Wuhan, China (WHO, 2020a). Coronaviruses are positive-sense single-stranded RNA viruses with medium size viruses ranging from 26 to 32 kb in length. They belong to the Nidovirales order of RNA viruses (Su *et al.*, 2016). They are major viral pathogens that cause viral pneumonia in both animals and humans. Coronaviruses (CoV) are classified into four genera: alpha, beta, gamma, and delta. Alpha and beta are responsible for seven coronaviruses that cause diseases in humans, whereas gamma and delta are pathogens that affect animals rather than humans. SARS-CoV-2 is a novel beta coronavirus and the seventh coronavirus discovered to cause disease in humans (Zhu *et al.*, 2020). SARS-CoV-2 is genetically similar to SARS-CoV with an 80 percent sequence similarity (Lu *et al.*, 2020).

COVID-19 has been characterized as a pandemic by World Health Organization in March 2020. Globally, as of 11 May 2022, there have been 516,476,402 confirmed cases of COVID-19, including 6,258,023 deaths, reported to WHO while in Ethiopia, as of 11 May 2022, there have been 470,760 confirmed cases of COVID-19 with 7,510 deaths, reported to WHO (WHO, 2022). People with COVID-19 experience a wide range of symptoms, from mild to severe, including fever, dry cough, tiredness, loss of taste or smell, and shortness of breath. Symptoms may appear 2-14 days after exposure to the virus. The virus can spread from an infected person's mouth or nose in small liquid particles when they cough, sneeze, speak or breathe (CDC, 2022a).

The current worldwide COVID-19 epidemic is endangering people's daily life. SARS-CoV-2 has been spreading swiftly over the world since its first appearance in December 2019. Scientific and medical communities from all around the world have risen to combat the virus, and after a year of the breakout, several vaccinations have been developed from different corners of the world. However, it has been noted that a variant of concern is causing reinfection in previously

vaccinated and infected people (Rahman *et al.*, 2022). Therefore, further study is required to battle this pandemic.

Recently, the development of therapeutic agents against SARS-CoV-2 has also been applied for bioinformatics study known as molecular docking via simulation approaches. Employing this approach several natural compounds have been investigated against SARS CoV-2 (Chakravarti *et al.*, 2021). Several existing drugs are also studied through molecular docking and showed promising inhibitory effects on selected viral enzymes and are repurposed for emergency use. For example, nelfinavir and remdesivir were predicted to be COVID 19 drug candidates as inhibitors of the viral enzymes responsible for viral replication such as main protease (Mpro)(Hu *et al.*, 2021) and RdRp (Poustforoosh *et al.*, 2021) respectively. Besides approved antiviral drugs, natural products under research and development have shown considerable inhibitory effects on many key proteins of SARS-CoV-2 (Abubakar *et al.*, 2021).

Nowadays, medicinal plants have played a pivotal role in primary health care and are rich in novel bioactive compounds. Studies revealed that drug development from natural sources has shown that natural products or natural product-derived drugs comprised about 28% of all new drugs entering the market (Rashid, 2013). Plants produce secondary metabolites due to a prominent function such as protection against predators and microbial pathogens, repellence to herbivores and microbes, defense against abiotic stress (e.g., UV-B exposure), for the communication of the plants with other organisms, and are insignificant for growth and developmental processes (Dias *et al.*, 2012; Cragg and Newman, 2013). In recent years, medicinal plants have become popular for treating several diseases due to their efficacy and cost-effectiveness. Systematic studies involving pharmacological activities and the mechanism of action of bioactive molecules derived from herbal medicine provide the vital knowledge required to design new medications (Ramawat, 2009).

Conventional approaches to natural products were a mix of chemical analysis and structure-function relationship analysis. Recently, new concepts of *in silico* computational approaches/molecular docking have evolved for drug prediction based on drug candidate–ligand/receptor interaction (Kim, 2021). *In silico* computational simulation is an investigation performed by computer programs. *In-silico* study is thought to have the potential to speed the rate of discovery while reducing the need for expensive lab work and clinical trials (Müller *et al.*,

2018). One way to achieve this is by producing and screening drug candidates more effectively by studying their interaction with target proteins through a bioinformatics study known as molecular docking.

1.2. Statement of the Problem

The COVID-19 epidemic continues to harm communities, including those living in poverty, older people, people with disabilities, youth, and indigenous peoples (WHO, 2020a). The COVID-19 pandemic has resulted in a tremendous loss of human life globally and poses an unparalleled threat to public health. Scientists and medics have been rushing to study this novel virus to identify efficient therapeutic drugs and vaccinations, given the prospect of a pandemic.

Within less than a year after the outbreak of the COVID-19 pandemic, numerous research teams rose to the challenge and discovered vaccines against SARS-CoV-2, the virus that causes COVID-19. Different existing viral medications are also re-proposed against the virus. However, a variant of concern has been reported to be more infectious, and more likely to produce re-infections or breakthroughs in individuals who have been vaccinated or previously infected. These variants are more likely to induce severe illness, escape detection by an immune response developed by the vaccine, or withstand antiviral therapy. Laboratory studies suggest that some immune responses elicited by existing vaccinations may be less effective against some of these variants(Kim, 2021).

Repurposed therapeutic drugs and vaccinations help to alleviate the pandemic scenario. Nonetheless, low availability, unprecedented side effects of the drugs, and ethical questions about immunizations make global implementation difficult. Furthermore, the problem can be aggravated by virus mutation, which can result in drug-resistant mutants, making anti-viral medications useless. In addition to this, safety issues regarding some of the available vaccines are also research focus areas. In this regard, vaccines such as mRNA-related, thrombocytopenia, and adenoviral vector vaccines are reported to cause health problems such as myocarditis, thrombosis, and Guillain-Barre syndrome after being delivered respectively(Edwards and Orenstein, 2022). Therefore, more research works are ongoing to stop this epidemic, including the development of specialized medicinal drugs. In this context, natural products can be used to

explore possible therapies since they are easily available, abundant, and safe, and may not pose an adverse effect on health. SARS COV-2 RNA polymerase RNA-dependent enzyme has no similarity with any host cell proteins because of this it has been a target for antiviral agent investigation (Venkataraman *et al.*, 2018).

From a rational point of view, any disease by itself is a problem of the world so any investigation that searches for any therapeutic regimens is considered significant. Investigations for therapeutic agents, drugs, or vaccines require educated personnel and the economy. So even if we have the expertise, the economy is the problem to do investigation in the conventional approach. Conventional approach (lab experimentation) in searching for therapeutic drugs is time-consuming and expensive, so in this dilemma bioinformatics as an emerging technology is relieving these problems, by providing basic information on disease genome, structure and pathology and even its backbone in screening for drugs against the disease. RdRp of SARS-CoV-2 plays the main role in genome replication of SARS-CoV-2, any therapeutic agents targeting it would be very important in COVID-19 combatting, however, fewer investigations have been done targeting it (Dong *et al.*, 2021). Thus this study was designed to examine the drug ability potential of selected natural products targeting RNA-dependent RNA-polymerase of SARS-CoV-2.

1.3. Objective of the Research

1.3.1. General Objective

- The general objective of this study is to evaluate the potential of selected natural products as SARS-CoV-2 RNA-dependent RNA polymerase inhibitors using molecular docking analysis.

1.3.2. Specific Objectives

The specific objectives of this study were:

- To determine the binding affinity and interaction mechanism between selected natural products and RNA-dependent RNA polymerase.
- To determine drug-likeness, physicochemical and pharmacokinetic properties of compounds under study.
- To identify the active site of RNA-dependent RNA polymerase for molecular docking.
- To analyze the inhibitory effect of the select natural products on SARS-CoV-2
- To propose a promising inhibitory candidate from selected natural compounds.

1.4. Significance of the Study

COVID 19 is a catastrophic global health issue, and the virus is developing resistance to certain existing medicines, therefore developing a new therapy is critical. In this context, the *in silico* approach is important since it is faster and less expensive compared to experimental investigations. Because of the time-consuming development of antiviral drugs and the availability of high-speed computer methodologies, using *in silico* methods provides a flexible way to find viable coronavirus therapeutics.

Natural products are safe and easily accessible for the development of therapeutic agents against COVID-19, in the current alarming situation. Thus, the present study will provide drug-like natural products from an *in-silico* examination that can be further investigated *in-vivo* experimental as potential compounds against SARS-CoV-2.

1.5. Scope of the Study

The present study was designated for *in-silico* discovery of drug-like therapeutic agents considering natural products may have an inhibitory effect on COVID-19. The methodology of the study focused on the molecular docking of these natural products (one from fungi, eighteen from plants, and one from animals) on the selected enzyme of SARS CoV-2, namely RNA-dependent RNA polymerase. The study was delimited to the computer-based evaluation of inhibitory activities of selected natural compounds on the enzyme.

CHAPTER TWO

2. LITERATURE REVIEW

2.1. COVID 19 (SARS-CoV-2)

The China Health Authority notified the WHO on December 31, 2019, about multiple instances of pneumonia with an unknown cause in Wuhan city, central China (Harapan *et al.*, 2020). The cases had been reported since December 8, 2019, but unknowingly many peoples with the virus were working at the local Huainan Seafood Wholesale Market in Wuhan city (Lu *et al.*, 2020). On January 7, a new coronavirus, named as 2019-nCoV by the World Health Organization, was identified in a patient's throat swab sample (Hui *et al.*, 2020). The Coronavirus Study Group by WHO named this pathogen as severe acute respiratory syndrome coronavirus 2 (SARS-CoV-2) and the condition as coronavirus disease 2019 (COVID-19) (WHO, 2020b).

Burrell *et al.* (2016) explained that SARS-CoV-2 belongs to the Coronaviridae family and the Nidovirales order. Coronaviridae family is classified into four genera: Aalphacoronavirus includes human coronavirus (HCoV)-229E and HCoV-NL63; Betacoronavirus includes HCoV-OC43, SARS-HCoV, HCoV-HKU1, and Middle Eastern respiratory syndrome coronavirus (MERS-CoV); Gammacoronavirus includes viruses isolated from whales and birds, and Deltacoronavirus includes viruses isolated from pigs. SARS-CoV-2 is an enveloped, single-stranded, and positive-sense RNA virus (+ssRNA) that belongs to the Betacorona virus which also includes SARS-CoV and MERS-CoV, two extremely dangerous viruses (Kramer *et al.*, 2006).

Lu *et al.* (2020) defined that SARS-CoV-2 is genetically distinct from SARS-CoV (with about 79 percent similarity) and MERS-CoV, according to phylogenetic analysis of the virus's genome. It is closely related (with 88 percent similarity) to two bat-derived SARS-like coronaviruses collected in eastern China in 2018. A further investigation using the genome sequences of SARS-CoV-2, RaTG13, and SARS-CoV discovered that the virus is more closely related to Bat-CoV RaTG13, a bat coronavirus previously discovered in Yunnan, China with 96.2 percent total genome sequence similarity(Zhou *et al.*, 2020).

SARS-CoV-2 considered a new virus infecting human beings belongs to beta coronavirus. People of all ages are susceptible to the virus. But COVID-19 is more likely to make older people very sick. When older persons with COVID-19 become severely ill, they may require hospitalization, intensive care, or a ventilator to help them breathe, or they may even die (CDC, 2021). People in their 50s are at higher risk, as are those in their 60s, 70s, and 80s. People aged 85 and up are the ones who are most prone to become seriously ill (CDC, 2021). People aged over 65-year-olds account for more than 81 percent of COVID-19 mortality. The number of fatalities among adults over the age of 65 is 97 times more than the number of deaths among those aged 18 to 29 (CDC, 2022b). Other factors, such as having certain underlying medical disorders such as heart failure, coronary artery disease, cardiomyopathies, obesity, diabetes, and possibly high blood pressure (hypertension) can also increase your chances of being very sick with COVID-19 (CDC, 2022b).

2.1.1. Structural and Genomic Organization of SARS-Cov-2

Morphologically, all coronaviruses are enveloped with crown-like particles enclosing a positive-sense RNA genome. The lipid bilayer envelope that encapsulates the viral particle, is derived from the host cell membrane and contains three structural proteins: membrane (M), envelope (E), and spike (S). The other viral structural protein, nucleoprotein (N), is found inside and is closely linked to the viral genomic RNA (Kumar *et al.*, 2020) (Figure 2.1).

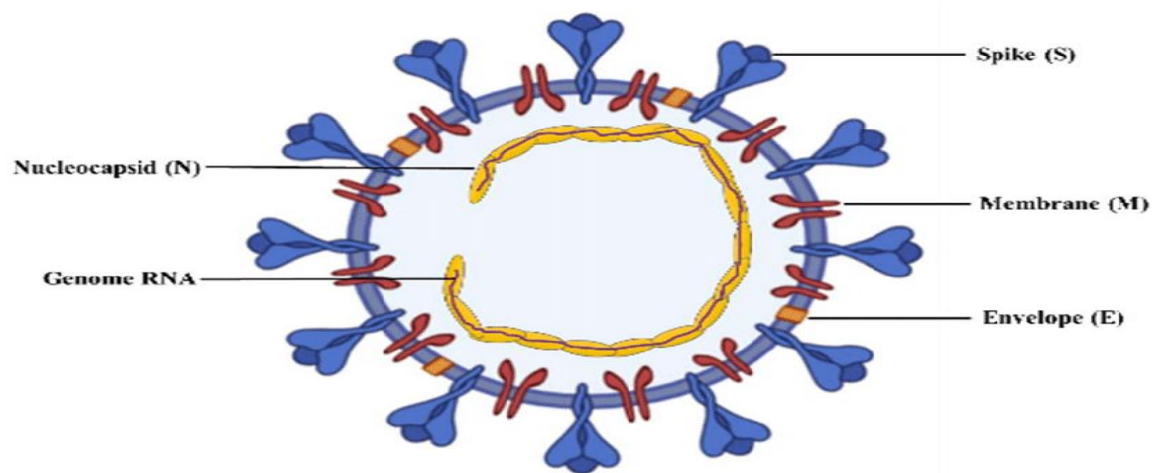


Figure 2. 1: Schematic diagram of SARS-CoV-2 (Okpara and Jamabo, 2020).

In total SARS-CoV-2 has twenty-nine proteins. All those proteins have a great research interest to understand the virus life cycle, how it enters host cells, stimulates the immune system, and consequently which of those proteins can be targeted by a treatment or used to develop therapeutic agents and vaccines. Among the 29 proteins of SARS-COV-2, four are structural proteins, sixteen are nonstructural proteins, and the rest (nine) are accessory proteins.

Structural proteins are essential in many steps of the infection, they are implied in viral genome production, replication, and the virion-receptor attachment that will promote virus entry into the host, proliferation, and spread of the infection. These structural proteins in SARS CoV-2 are spike glycoprotein, nucleocapsid protein, envelope protein, and membrane protein (Satarker and Nampoothiri, 2020). The nine structural proteins SARS CoV-2 are designated as NSP1, NSP2, NSP3, NSP4, NSP5, NSP6, NSP7, NSP8, NSP9, NSP10, NSP11, NSP12, NSP13, NSP14, NSP15, and NSP16. The end of the SARS-CoV-2 genome encodes for 9 additional proteins called accessory proteins. These are Orf3a, Orf3b, Orf6, Orf7a, Orf7b, Orf7b, Orf8, Orf9b, and Orf9c(10) (Fig 2.2) with the specific function and responsibility in viral activities (Marchan, 2020).

The SARS-CoV-2 genome is approximately 30 kb in length and is composed of 13–15 open reading frames (ORFs) grouped in a 5–3' order. The first ORF from the 5' ends encodes occupies 67% of the SARS-CoV-2 genome, and encodes polyprotein 1a (pp1a) and polyprotein 1 ab (pp1ab) precursor polyproteins, which are further cleaved into a non-structural protein in the SARS-CoV-2 genome (NSP1-16) (Wu *et al.*, 2020) (Figure 2.2). These non-structural proteins include multiple enzymes such as papain-like protease (NSP3), chymotrypsin-like main protease (3CL protease, NSP5), and RdRp (NSP12), helicase (nsp13), and exoribonuclease (NSP14) are required for the virus life cycle (Gordon *et al.*, 2020). The ORF from 3'-terminus encodes for four structural proteins: membrane glycoprotein (M), envelope (E), nucleocapsid (N), spike (S), and eight accessory proteins: 3a, 3b, p6, 7a, 7b, 8b, 9b, and 9c(10) (Figure 2.2) (Atanasov *et al.*, 2021).

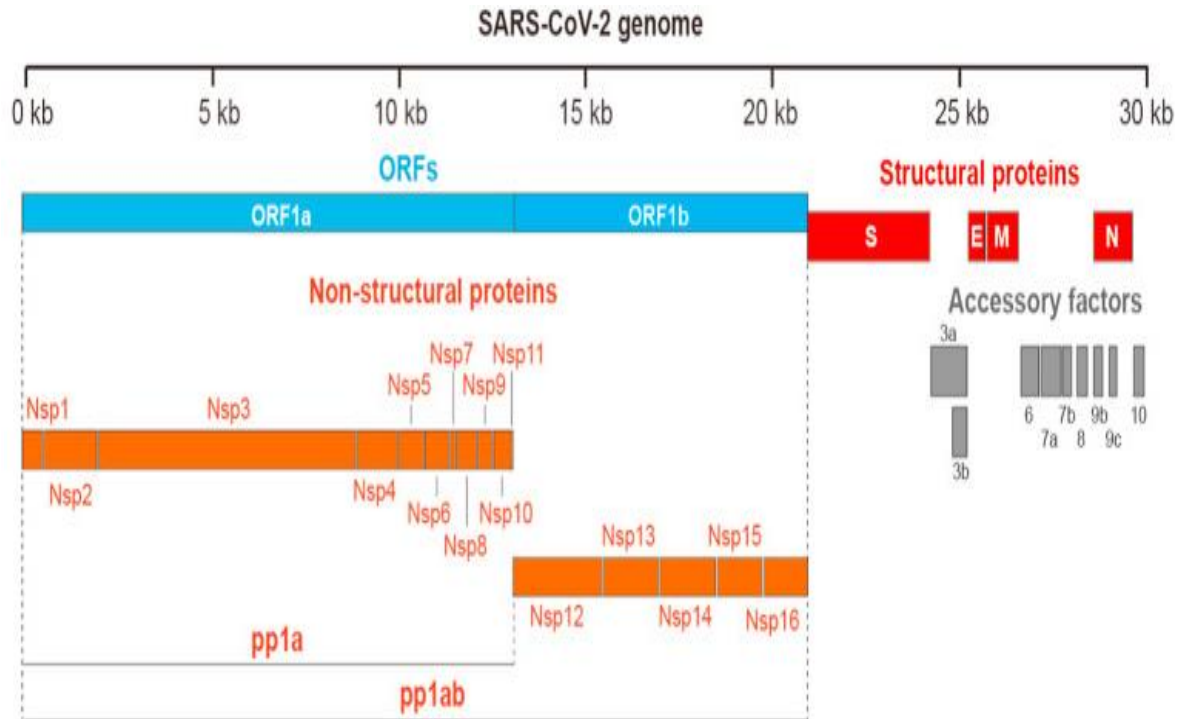


Figure 2. 2: Genomic organization of SARS-CoV-2(Thoms *et al.*, 2020).

2.1.2. Viral Cell Entry, Replication, and Pathophysiology

Corona virus spike proteins play an important role in virus attachment and entry into target cells. Entry requires the involvement of two spike protein subunits, each of which performs a different function, they are S1 and S2. Through the receptor-binding domain, the S1 subunit facilitates ACE2 attachment. The S2 subunit, which contains the fusion peptide and trans membrane domains, is responsible for viral and host cell membrane fusion (Hoffmann *et al.*, 2020). Polyproteins are translated after the viral RNA is released into the host cell. Nonstructural proteins (NSPs) are required for viral RNA replication, whereas structural proteins are important for virion assembly, and are encoded by the corona virus genomic RNA. First, the polyproteins pp1a and pp1ab are translated, and then the Papain-like protease (PLpro, Nsp3) and 3C-like protease (3CLpro) break them to generate functional NSPs like Helicase or the RNA-dependant-RNA polymerase (RdRp)(Shin *et al.*, 2018).

The replication of structural protein is carried out by RdRp (Nsp12). Ribosomes, which are attached to the endoplasmic reticulum, translate structural proteins S, Envelope (E), and

Membrane (M). The viral RNA is reproduced and hidden from the host's innate immune system in double-membrane vesicles (DMVs) formed by the ER. Nsp3 creates pores via which viral RNA exits DMVs to be assembled into a virion. Nucleocapsid proteins (N) are assembled from genomic RNA and stay in the cytoplasm. When the virus enters the cytoplasm, it releases its RNA genome, which is first translated to form the viral polyproteins pp1a and 1ab, and then cleaved into smaller products by virus-encoded proteases. The viral polymerase uses discontinuous transcription to transcribe a sequence of sub genomic mRNAs, which are ultimately translated into viral structural proteins. The N protein binds to genomic RNA, while the S, E, and M proteins are inserted into the viral envelope in the ER and Golgi apparatus. Then the virions are released from the infected cell through exocytosis and search for another host cell.

Angiotensin-converting enzyme 2 (ACE-2) is the receptor for both SARS-CoV and SARS-CoV-2 (Bindom and Lazartigues, 2009; Imai *et al.*, 2010). ACE2 is a key enzyme in the renin-angiotensin system (RAS), which regulates fluid and salt balance as well as blood pressure regulation (Kuba *et al.*, 2006). Eventually, the invasion of SARS-CoV-2 detracts the ACE2 functioning, causing an increase in blood pressure, blood vessel disruption, and organ inflammation. Although corona viruses primarily affect the respiratory system, they can also have an impact on organs such as the renal, central nervous system (CNS), cardiovascular (CV) systems, and gastrointestinal tract (GI) (Peiris *et al.*, 2003; To *et al.*, 2004). The organs that are most impacted by SARS-CoV-2 exhibit high levels of ACE2, indicating that these organs have a high affinity for SARS-CoV-2 acquisition as a result of ACE2 (Letko *et al.*, 2020)

SARS-CoV-2, in particular, prefers to infect the respiratory tract. The primary targets of SARS-CoV-2 are alveolar type II cells (AT2) in the lungs since they exhibit high amounts of ACE2 (Verdecchia *et al.*, 2020). In healthy alveoli, oxygen is absorbed, whereas carbon dioxide is exhaled. However, due to the presence of SARS-CoV-2, ACE2 is inhibited from regulating the protein angiotensin II (ANG II), resulting in severe damage to the blood vessels of the lungs and, blocking the exchange of oxygen and carbon dioxide. As a result, difficulty in breathing and improper functioning of the lungs, bronchitis, edema, alveolar collapse, and acute respiratory distress syndrome develop (Huang *et al.*, 2020; Tan *et al.*, 2021).

2.2. Researches and Discovery of therapeutic agents on COVID-19

Since the emergence of COVID-19, the novel disease and the virus that causes it have gotten a lot of interest throughout the world. Scientists and medical communities throughout the world have been working hard to study this new emerging disease and its epidemiology to design treatment regimens, identify viable therapeutic drugs, and produce vaccinations. Thousands of journal papers were published electronically, and the number of published articles has increased each week since the emergence of the virus. The majority of these articles are focusing on the elucidation of virus structure, virus transmission mechanisms/dynamics, antiviral agents, and precise diagnostics for virus detection. The scientific community, including both academic and industrial institutions as well as doctors, is extremely interested in identifying novel strategies to stop the spread of this pandemic disease and prevent further infection and transmission. Approximately 80% of SARS patents are dedicated to the development of therapeutics, 35% are connected to vaccines, and 28% are related to diagnostic agents or procedures (Liu *et al.*, 2020).

2.2.1. Role of Natural Products in Research on SARS CoV-2

Natural products have long been regarded as valuable sources of medicinal agents. Because of their intricacy, these agents are remarkably low molecular weight compounds capable of evoking enzyme activity (Malami *et al.*, 2016). They are often used arbitrarily as anti-viral drugs and immune boosters in the absence of defined therapies. Most natural compounds have long been recognized to have significant anti-viral activity, and SARS-CoV-2 is no exception. Natural products have been demonstrated to be effective against MERS-CoV and SARS-CoV infections. Besides licensed antiviral drugs, natural compounds under research and development have shown considerable inhibitory effects on many key proteins from related coronaviruses such as SARS-CoV and MERS-CoV. Since there is a significant level of sequence homology between SARS-CoV and SARS-CoV-2, inhibitors against enzymes/proteins of SARS-CoV may also be relevant to SARS-CoV-2 (Kim *et al.*, 2020).

In silico studies have revealed that several natural products have a high affinity for and inhibit the virus's non-structural proteins, including, PLpro, Mpro, and RdRp, as well as structural

proteins like spike (S) protein (Chakravarti *et al.*, 2021). Among the different classes of natural products flavonoids, alkaloids, terpenoids, steroids, and coumarins, glycosides are well studied against antiviral activities (Abubakar *et al.*, 2021). Some natural products from these classes are presented below in figure 2.4.

Flavonoids are abundant in a wide range of fruits and vegetables, including citrus fruits and tomatoes (Tutunchi *et al.*, 2020). Flavonoids are hydroxylated phenolic Phyto-molecules that belong to secondary metabolites from the plant, fruits, vegetables, roots, and other plant products like tea and wine. Flavonoids classified into subclasses include anthocyanins, chalcones, dihydrochalcones, dihydroflavonols, flavan-3-ols, flavanones, flavones, flavonols, flavanonols, and isoflavonoids (Tazzini, 2014).

Some flavonoids such as kaempferol, chrysin, and quercetin act against both human and bovine coronaviruses (BCV). The afaflavin also inhibits BCV, whereas quercetin 7-rhamnoside inhibits non-respiratory coronavirus porcine epidemic diarrhea virus (PEDV). Multiple polyphenols effectively inhibit MERS-CoV cysteine proteases including 3CLpro and papain-like protease (PLpro).

Flavonoids have been suggested as a safe alternative treatment method for coronavirus. Found inhibiting the coronavirus life cycle at various phases of viral infection. Blocks essential coronavirus enzymes as drug targets as proven by complementary approaches through both *in silico* virtual screenings and *in vitro* experiments. Different reports show that flavonoids have the potential in mitigating SARS-CoV-2 viral infection via binding to spike protein and modulation of ACE2 (Tutunchi *et al.*, 2020).

Alkaloids are a kind of plant secondary metabolite (PSM) with at least one nitrogen atom in its structure. Higher terrestrial plants, fungi (Hesse, 2002), and mammals produce alkaloids (Fattorusso and Tagliatela-Scafati, 2007). Various studies show that alkaloids act as DNA intercalating agents. DNA intercalating agents on DNA base pairs or paired regions of RNAs. From alkaloid subclasses, Isoquinoline, quinolone, and β -carboline alkaloids possess intercalating characteristics and they have shown potent antiviral activity. Recent research found that cepharanthine (**1**), a naturally occurring alkaloid, may bind to spike protein and disrupt the viral interaction with ACE2 protein (Ohashi *et al.*, 2020). A nonproteinogenic alkaloid called

nicotianamine (2) was shown to have a similar impact on ACE2 in another investigation(Chen and Du, 2020).

Terpenoids, also known as isoprenoids, are a group of natural chemicals made up of isoprene (5C- compound) units. Wen *et al.* (2007) investigated the antiviral properties of over 200 naturally occurring terpenoids and lignoids. Quinone methide triterpenes obtained from *Tripterygium regelii*, such as celastrol (3), pristimerin (4), tingenone (5), and iguesterin (6) (Figure 2.3), inhibited the SARS-CoV major protease. Tanshinone (7), which comprises the abietane diterpene moiety and was isolated from *S. multiorrhiza*, inhibited SARS-CoV main protease and PL protease specifically (Takahashi *et al.*, 2015).

Steroids and steroid glycosides are other families of natural compounds having SARS CoV-2 enzyme modulatory activities. For example, a study by Liu *et al.* (2019) found that ginsenoside (8), a tetracyclic triterpenoid saponin, increases ACE2 levels and protects against Ang II-mediated kidney damage. Coumarins, which are naturally occurring phenolic chemicals, have also been demonstrated to inhibit SARS CoV-2.

2.2.4. Vaccines of COVID-19

Vaccines are considered as the most promising strategy for preventing the COVID-19 pandemic. Globally, many COVID-19 vaccines are available. Before the World Health Organization approved it for use COVID-19 vaccine development must go through the regular preclinical and clinical stages. The development process might take years, and safety standards have remained strict. There are phases; phase I, Phase II, and Phase III in the development of the COVID-19 vaccine. Phase III trials provide preliminary estimates of vaccination effectiveness.

The surface spike protein of the virus is the main antigenic target for COVID-19 vaccinations which induces membrane fusion by binding to the angiotensin-converting enzyme 2 (ACE2) receptor on host cells (Zhou *et al.*, 2020). Antibodies that bind to the SARS-CoV-2 spike protein's receptor-binding domain can block the virus from attaching to the host cell and neutralize it.

CoronaVac (Sinovac), BBIBP-CorV/HB02, Covaxin, COVI-VAC, BNT162b2(Pfizer-BioNTech vaccine), mRNA-1273 (Moderna vaccine), Ad26.COVS.S, ChAdOx1, Gam-COVID-Vac, Ad5-

nCoV, Novavax, ZyCoV-D (Zydus Cadila), DelNS1-2019-nCoV-RBD-OPT are available, and candidate COVID-19 vaccines. They are RNA, replication-incompetent vector, recombinant protein, inactivated, and DNA vaccines developed by both traditional and modern approaches (Edwards and Orenstein, 2022).

Even if these vaccines are playing a crucial role in combating COVID-19 there is a safety issue related to some of them. For example, with mRNA vaccines, there is a danger of myocarditis and pericarditis; with the vaccine known as thrombocytopenia, there is a risk of thrombosis; and with adenoviral vector vaccines, there is a risk of Guillain-Barre syndrome. Individuals also show a wide range of adverse reactions after receiving the vaccination (Edwards and Orenstein, 2022).

2.3. Molecular Docking

Molecular docking is a technique for analyzing the conformation and orientation of molecules into the binding site of a macromolecular target (Morris and Lim-Wilby, 2008). Docking is a computational process for finding a suitable ligand that matches the protein's binding site both energetically and geometrically. In other words, it is the study of how two or more molecules, such as a ligand and a protein, interact with one another (Azam and Abbasi, 2013). It predicts the favored structural orientation, binding affinity, and interaction between ligand and protein. It is an effective and competent tool for structural molecular biology and rational computer-aided (*in-silico*) drug design (Kuntz, 1992). Docking can be used to do virtual screening on large libraries of compounds, rank the result, and provide structural theories about how the ligands block the target, which is extremely useful for lead optimization.

The application of computational approaches in drug discovery has been exposed to considerable research over the last decade to understand the development of intermolecular complexes. It is well understood that correct drug activity is caused by the molecular binding of one molecule (ligand) to the pocket of another molecule (receptor), which is typically a protein (Azam and Abbasi, 2013). Molecular docking has proven to be a highly efficient approach for discovering new drugs that target proteins.

There are two basic types of molecular docking such as protein-protein docking is the process of bringing two proteins together and ligand-protein docking is the interaction between a tiny molecule and a protein.

Protein-protein docking includes two protein molecules that are simulated to interact with one another by computer software. Protein-protein docking is more rigid than ligand-protein docking. It is the prediction of a protein-protein complex's structure based on the structures of the component proteins as it would occur in a living organism (Vakser, 2014).

Protein-Ligand docking is a widely used computer modeling approach for predicting the conformation of a receptor-ligand complex. Proteins and ligands docking technique is often separated into two stages: rigid-body docking and flexible docking (Hernández-Santoyo *et al.*, 2013).

Protein-ligand docking is of particular relevance rather than protein-protein docking due to its use in the pharmaceutical sector (Kanehisa *et al.*, 2006). It is the search for accurate ligand conformations inside a given receptor structure, where the receptor is often a protein and the ligand is a small molecule. Below in Figure 2.4 the remdesivir and RdRp docking complex from the current study is presented as an example to show the protein-ligand docking element and how the ligand could be docked into the active site of the protein.

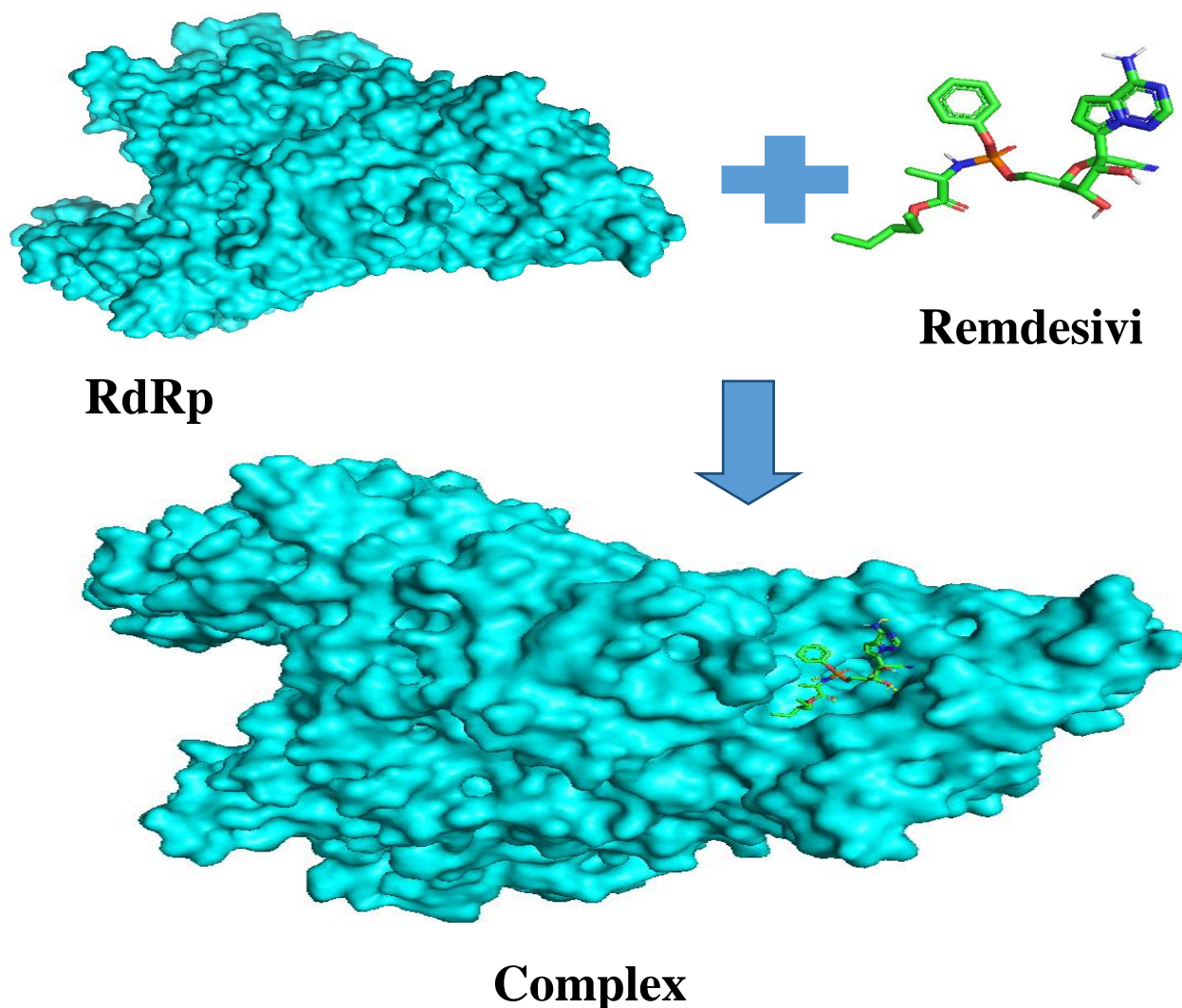


Figure 2. 3: Elements in protein-ligand docking (RdRp-remdesivir complex).

Docking procedures are generally a combination of search algorithms and a scoring function. Today there are large number numbers of computer programs with their search algorithms and scoring functions. Search algorithms predicted the best posing which is binding orientation and conformations of the ligand on the binding site of protein (Sousa *et al.*, 2006). Monte Carlo methods, Genetic algorithms, Fragment-based methods, Point complementary methods, Distance geometry methods, Tabu searcher, and Systematic searches are some common search algorithms (Kaapro and Ojanen, 2002). The scoring functions are used to differentiate between the active and random compounds. In general, scoring functions are used to estimate binding free energies in ligand-protein docking (Bissantz *et al.*, 2000). A variety of molecular docking software is used in the pharmaceutical industry. AutoDock, AutoDockVina, GOLD, FlexX, FRED, DOCK, and

ICM are the most popular and widely used molecular docking software (Azam and Abbasi, 2013).

AutoDock Vina (Vina), along with AutoDock4 (AD4), AutoDockGPU, AutoDockFR, and AutoDock-CrankPep, is one of the greatest docking engines in the AutoDock Suite, and undoubtedly one of the most extensively used and successful docking engines. This is mostly due to its ease of use and speed (up to 100x faster than AD4) when compared to the other docking engines in the suite and elsewhere, as well as the fact that it is open-source (Ccsb-Scripps, 2021b). The other quality is that Vina uses the Broyden-Fletcher-Goldfarb-Shanno algorithm, which enhances the average accuracy of binding mode predictions substantially above AutoDock (Trott and Olson, 2010).

2.3.1. Molecular Docking Studies on COVID-19

Basu *et al.* (2020) conducted a study entitled “molecular docking study of potential phytochemicals and their effects on the complex of SARS-CoV2 spike protein and human ACE2”. In this study, five phytochemicals from the flavonoid and anthraquinone subclass were docked against spike the protein of SARS-CoV2 with its human receptor ACE2 molecule and the result revealed that hesperidin (**9**), with binding energy -8.99 kcal/mole modulates the binding energy of ACE2 and spike protein compared with chloroquine and hydrochloroquine -8.98 and -7.82 respectively which results in the unstable bound structure of ACE2 and spike protein and they suggested it as competent natural products to treat COVID-19.

Tallei *et al.* (2020) conducted a study on the potential of plant bioactive compounds as SARS-CoV-2 Main Protease (M(pro)) and Spike (S) Glycoprotein Inhibitors on twenty-one plant bioactive compounds using AutoDock Vina (AV) targeting M(pro) and Spike glycoprotein. The result revealed that hesperidin (**9**), nabiximols (**10**), pectolinarin (**11**), epigallocatechin gallate (**12**), and rhoifolin (**13**) (Figure 2.4) displayed promising binding energy such as -10.4 , -10.2 , -9.8 , -9.8 kcal/mol, on pike protein and -8.3 , -8.0 , -8.2 , -7.8 kcal/mol on M (pro) respectively compared to nelfinavir (-8.8 and -8.2 kcal/mol), chloroquine (-7.3 and -6.6 kcal/mol), and hydroxylchloroquine sulfate (-6.1 and -5.3 kcal/mol) as spike glycoprotein and M(pro) inhibitors.

Garg *et al.* (2020) conducted molecular docking analysis of selected phytochemicals against SARS-CoV-2 M (pro) receptor on 38 selected natural products reported from five plants viz., *Azadirachta indica*, *Curcuma longa*, *Zingiber officinale*, *Ocimum basilicum*, and *Panax ginseng* against SARS-CoV-2 M (pro). The study revealed that out of 38 compounds; gedunin(**14**), epoxyazadiradione(**15**), nimbin(**16**), and ginsenosides(**8**) have the potential to inhibit M(pro) activity, and their binding energies are - 9.51 kcal/mol, - 8.47 kcal/mol, - 8.66 kcal/mol and - 9.63 kcal/mol, respectively, obtained using autodock vina compared to the N3 (Control) with - 8.13 kcal/mol binding energy.

Vincent *et al.* (2020) conducted molecular docking studies on the anti-viral effects of compounds from Kabasura Kudineer, a polyherbal formulation from India's Siddha system of medicine, on SARS-CoV-2 3CLpro". The study considered 145 plant compounds that are effective against fever, cough, sore throat, and shortness of breath. They docked them to 3CLpro using the docking tool iGEMDOCK v2.0. The result revealed that acetoside(**17**) (-153.06), luteolin 7-rutinoside (**18**) (-134.6) rutin (**19**) (-133.06), chebulagic acid (**20**) (-124.3), syrigaresinol(**21**) (-120.03), acanthoside(**22**) (-122.21), violanthin (**23**) (-114.9), andrographidine(**24**) (-101.8), myricetin (**25**) (-99.96), gingerenone -A(**26**) (-93.9), tinosporinone(**27**) (-83.42), geraniol(**28**) (-62.87), and nootkatone (**29**) (-62.4) showed the best binding energy in kcal/mol.

Zothantluanga (2021) conducted molecular docking simulation studies, toxicity studies, bioactivity prediction, and structure-activity relationships on 16 flavonoids of which rutin(**19**) as a potential inhibitor of SARS-CoV-2 3CL pro" displaying the highest binding affinity (kcal/mol) 8.5, -9.3, -8.7 and -9.7 towards chain A, chain B, chain C, and chain D of SARS-CoV-2 3CL pro compared to 3WL as a standard which showed -7.3, -7.5, -7.4, and -7.3 toward chain A, B, C and D respectively.

Lokhande *et al.* (2021) conducted molecular docking and simulation studies on SARS-CoV-2 Mpro. In this study, they evaluated antiviral compounds that target HIV Protease, HCV Protease, and Reverse transcriptase using FlexX docking tool. Their study revealed that mitoxantrone(**30**), leucovorin(**31**), birinapant(**32**), and dynasore(**33**) are potent compounds that showed better binding affinity toward Mpro with -43.5854 kcal/mol, -37.6167 kcal/mol, -35.2785 kcal/mol and 35.0468 kcal/mol compared to Cefotenin, 34.8902 kcal/mol and boceprevir, 30.7442 kcal/mol.

Alfaro *et al.* (2020) conducted a study on the potential of tropane alkaloids from *Schizanthus porrigens* as inhibitors of SARS-CoV-2 papain-like protease using molecular docking analysis identification of potential inhibitors and the findings indicate that Schizanthine Z (**34**) has a relatively high affinity with -7.5 kcal binding energy toward the papain-like protease of SARS-CoV-2 compare to reference ligand (lopinavir -7.0 kcal/mol).

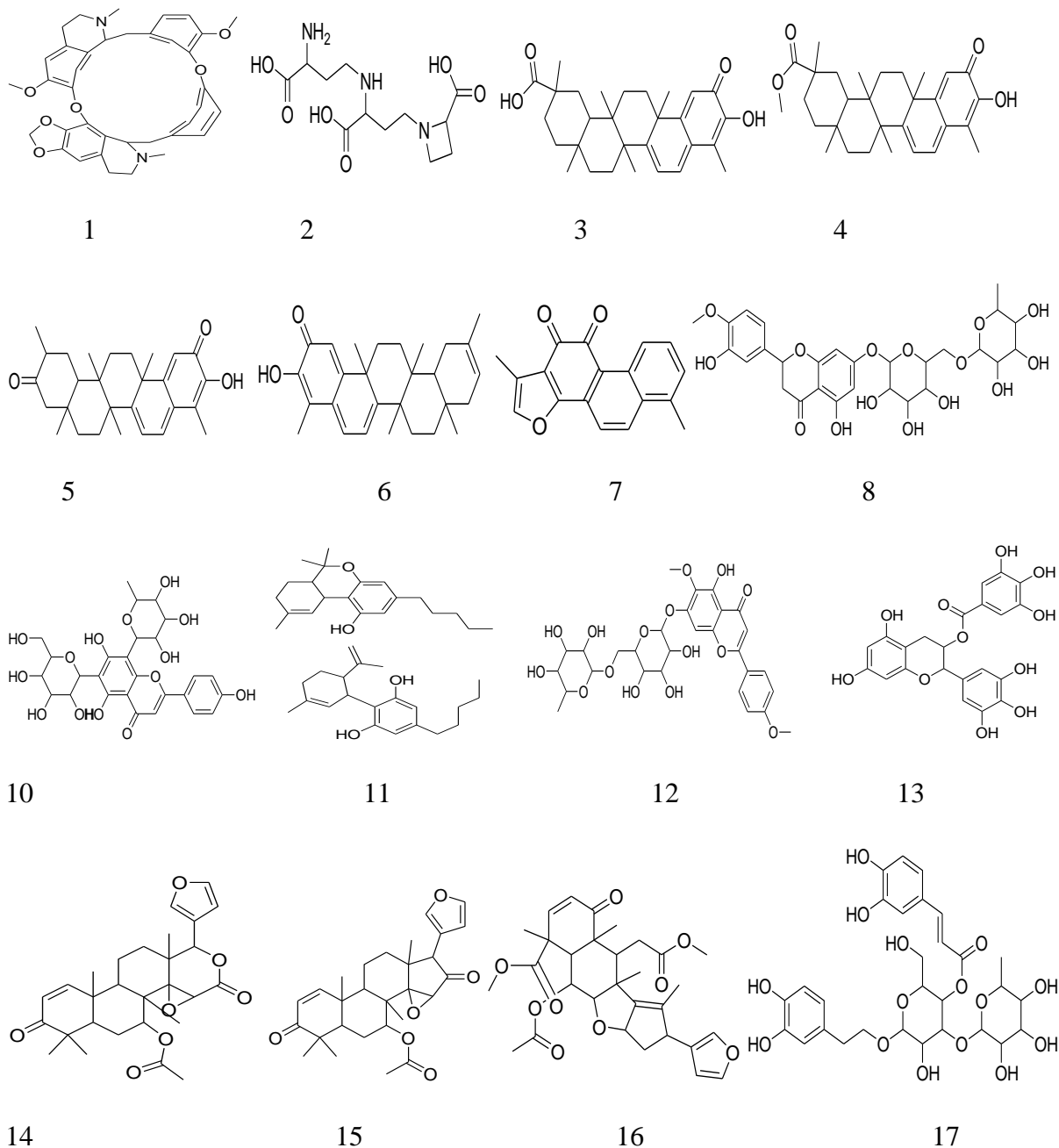
Pandeya *et al.* (2020) have done a molecular docking study on alkaloids from *Argemone mexicana* as RNA-dependent RNA polymerase inhibitors using molecular docking studies. Argemexicaine A (**35**), Argemexicaine B (**36**), Protopine (**37**), Allocryptopine (**38**), and (\pm) 6-Acetyldihydrochelerythrine (**39**) were docked against RdRp using the Autodock tools (ADT) v1.5.4 and autodock vina 4.2 programs. The study revealed that Protopine (-6.07 kcal/mol), Allocryptopine (-5.75 kcal/mol), and (+/-) 6- Acetyldihydrochelerythrine (-5.66 kcal/mol) have a high binding affinity toward RdRp.

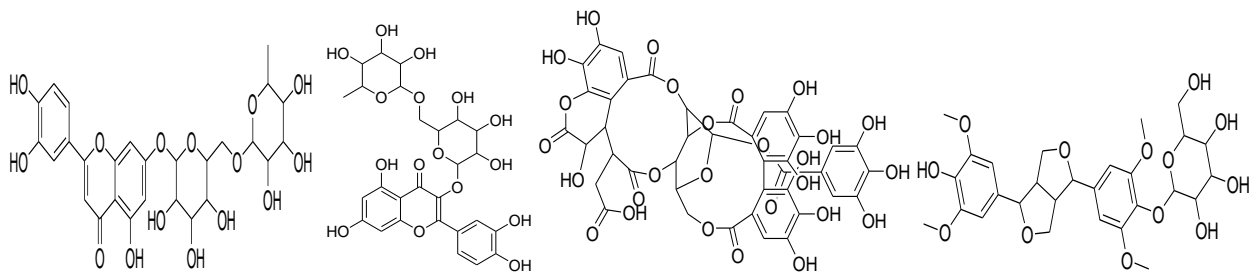
Saha *et al.* (2021) conducted potential RNA Dependent RNA polymerase inhibitors as prospective drugs against COVID-19 considering 248 natural products docked against RdRp and the result revealed that Tellimagrandin I(**40**), SaikosaponinB2(**41**), Hesperidin(**9**), and (-)-Epigallocatechin Gallate (**12**) (Figure 2.6) showed a promising binding affinity with a docking score of -9.6 kcal/mol, -8.9 kcal/mol, -8.6 kcal/mol, and -8.1 kcal/mol, respectively, and have best docking score when compared to two control, favipiravir (5.7 kcal/mol, and remdesivir -6.9 kcal/mol).

Selvaraj *et al.* (2021) conducted molecular docking analysis of compounds from *Plectranthus amboinicus* against SARS-CoV-2 linked RNA-dependent RNA polymerase (RdRp) of which rutin(**19**), Luteolin(**43**) Salvianolic acid A(**44**), Rosmarinic acid(**45**), and p-Coumaric acid(**46**) has a high binding affinity toward RdRp with -8.1kcal/mol, -7.5 kcal/mol, -7.2 kcal/mol, -6.8 kcal/mol, and -6.7 kcal/mol docking score respectively.

Wu *et al.* (2021) evaluated the potential of 480 polyphenols as potential inhibitors of SARS-CoV-2 RNA-dependent RNA polymerase (RdRp) of which RdRp-cyanidin 3-O-rutinoside(**47**) (-107.68 kcal/mol), RdRp-petunidin 3,5-O-diglucoside(**48**) (-99.18 kcal/mol), and RdRp-delphinidin 3-O-rutinoside(**49**) (-90.70 kcal/mol), have best predicted binding energies compared to four compounds remdesivir-TP (-55.00 kcal/mol), theaflavin 3,30-digallate (TF3) (-77.89 kcal/mol), swertiapuniside (-39.42 kcal/mol), and ATP (-57.83 kcal/mol) as a control group.

Lucas-Gómez *et al.* (2020) conducted the potential of betalains(**50**) and alfa-bisabolol(**51**) (Figure 2.6) against protein Nsp-12 of SARS-CoV. The docking result revealed that betalains (-10.112583 kcal/mol) and alf-bisabol (-6.545075 kcal/mol) had large negative binding energy than the control (RemTP) (-16.27044kcal/mol). They recommended that betalains may have minor inhibitory effects, on the SARS-CoV NSP-12 protein.



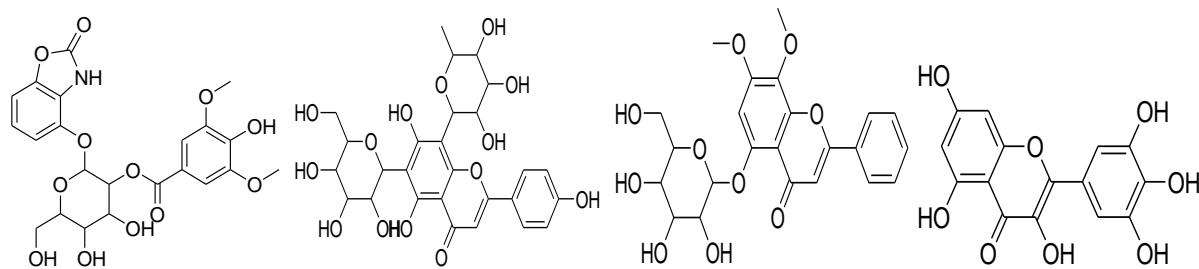


18

19

20

21

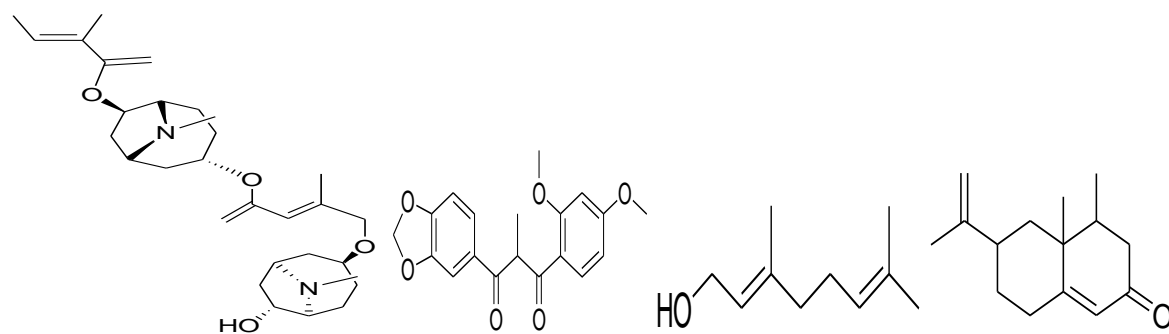


22

23

24

25

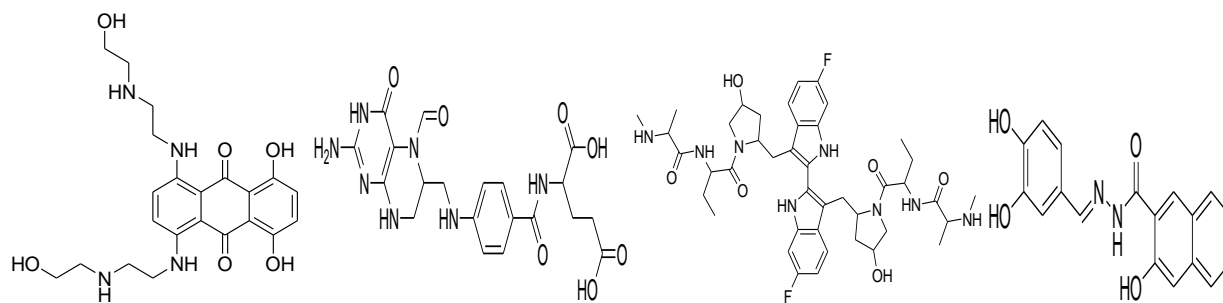


26

27

28

29

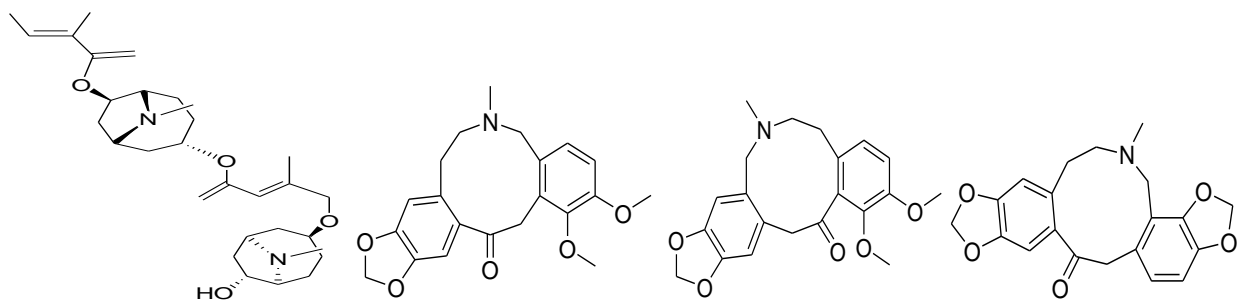


30

31

32

33

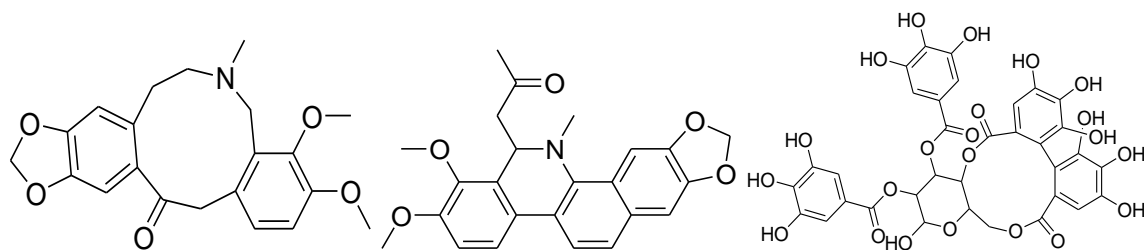


34

35

36

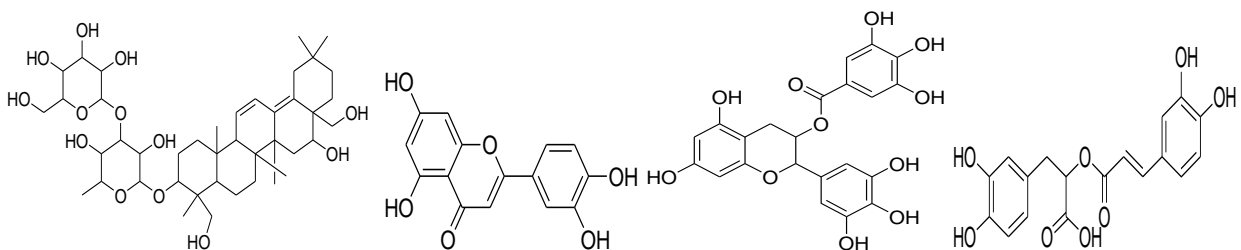
37



38

39

40

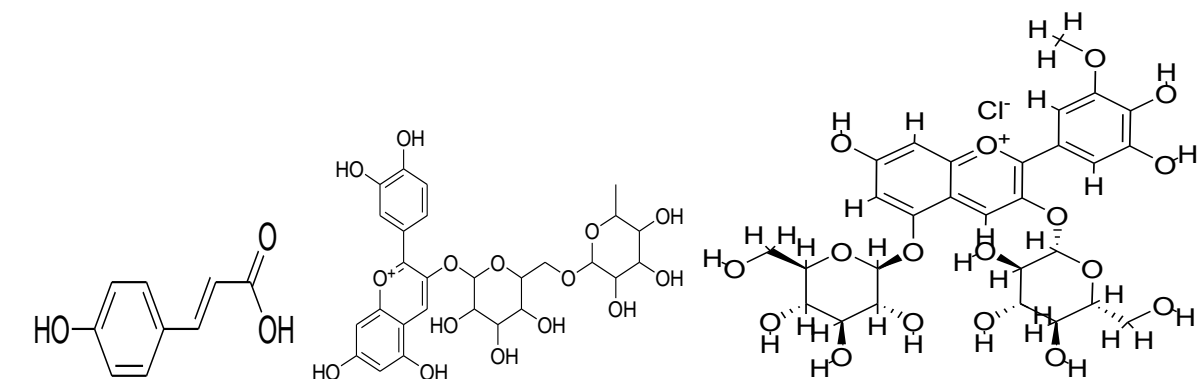


41

42

43

44



45

46

47

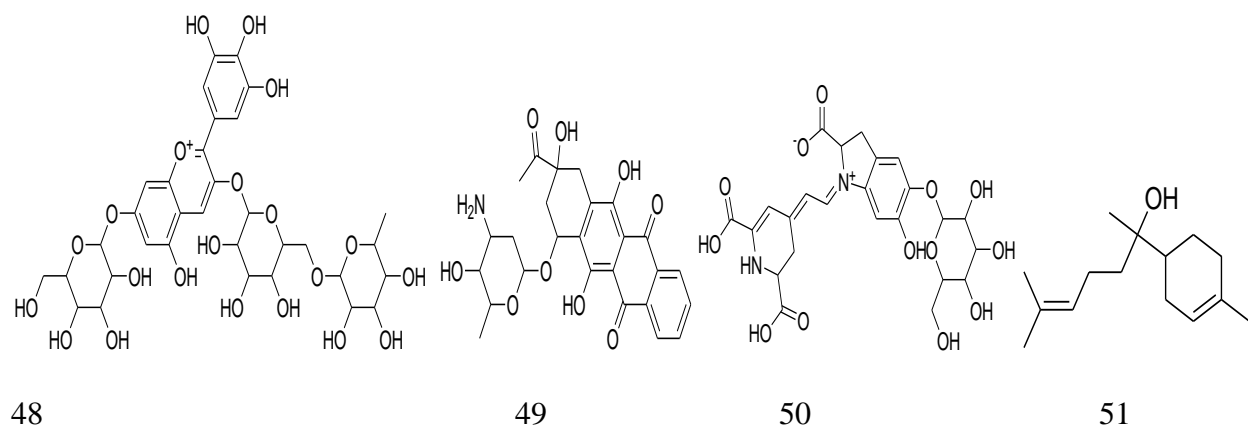


Figure 2. 4: Natural products studied against SARS CoV-2 proteins.

CHAPTER THREE

3. MATERIALS AND METHODS

3.1. Materials

3.1.1. Computer Software Used to Conduct the Study

Since the study employed the dry lab method, it needs an internet connection and computer, unlike the wet lab method. Hence, the study was conducted with the advanced software applications of bioinformatics including offline tools, online tools, and different databases were used. This as a backdrop is requested a quality computer and high-speed Wi-Fi connection. Computer (Dell: CoreI-7, 16 GB RAM), and Wi-Fi connection server of computer science and engineering laboratory were used. There were several computer programs available to accomplish the tasks under the molecular docking study. But, for the current study, the software and databases mentioned below in Table 3.1 were used due to their advance, accessibility, and easiness.

Table 3. 1: List of computer software and databases.

Offline tools	Online tools	Database
➤ MGL 1.5.7	<input type="checkbox"/> SWISS ADME	
➤ ChemDraw ultra 8	<input type="checkbox"/> SWISS MODEL	❖ PDB
➤ Open Babble 2.3.1	<input type="checkbox"/> ProtoxII	❖ PubChem
➤ SPBDV 4.10	<input type="checkbox"/> CASTp web server	
➤ Autodock-Vina 4.2		
➤ Pymol 2.5.2		
➤ BIOVIA ds 2021		

Offline tools molecular graphics laboratory (MGL) 1.5.7 (Morris and Lim-Wilby, 2009) for parameter preparation and Auto Dock Vina 4.2 (Trott and Olson, 2010) for docking were downloaded from www.scripps.edu. ChemDraw ultra 8 (Mendelsohn, 2004) for ligand structure preparation was downloaded from www.perkinelmerinformatics.com. Open Babble (O'Boyle *et al.*, 2011) for conversion of data file format was downloaded from www.openbable.org. Swiss

PDB viewer (SPBDV 4.10) (Guex and Peitsch, 1997) for energy minimization was downloaded from www.scripps.edu. Pymol 2.5.2 (Schrödinger and DeLano, 2020) software for a complex generation was downloaded from www.pymol.org, and BIOVIA discovery Studio visualizer 2021 (SYSTÈMES, 2016) for interaction analysis was downloaded from www.accelerys.com.

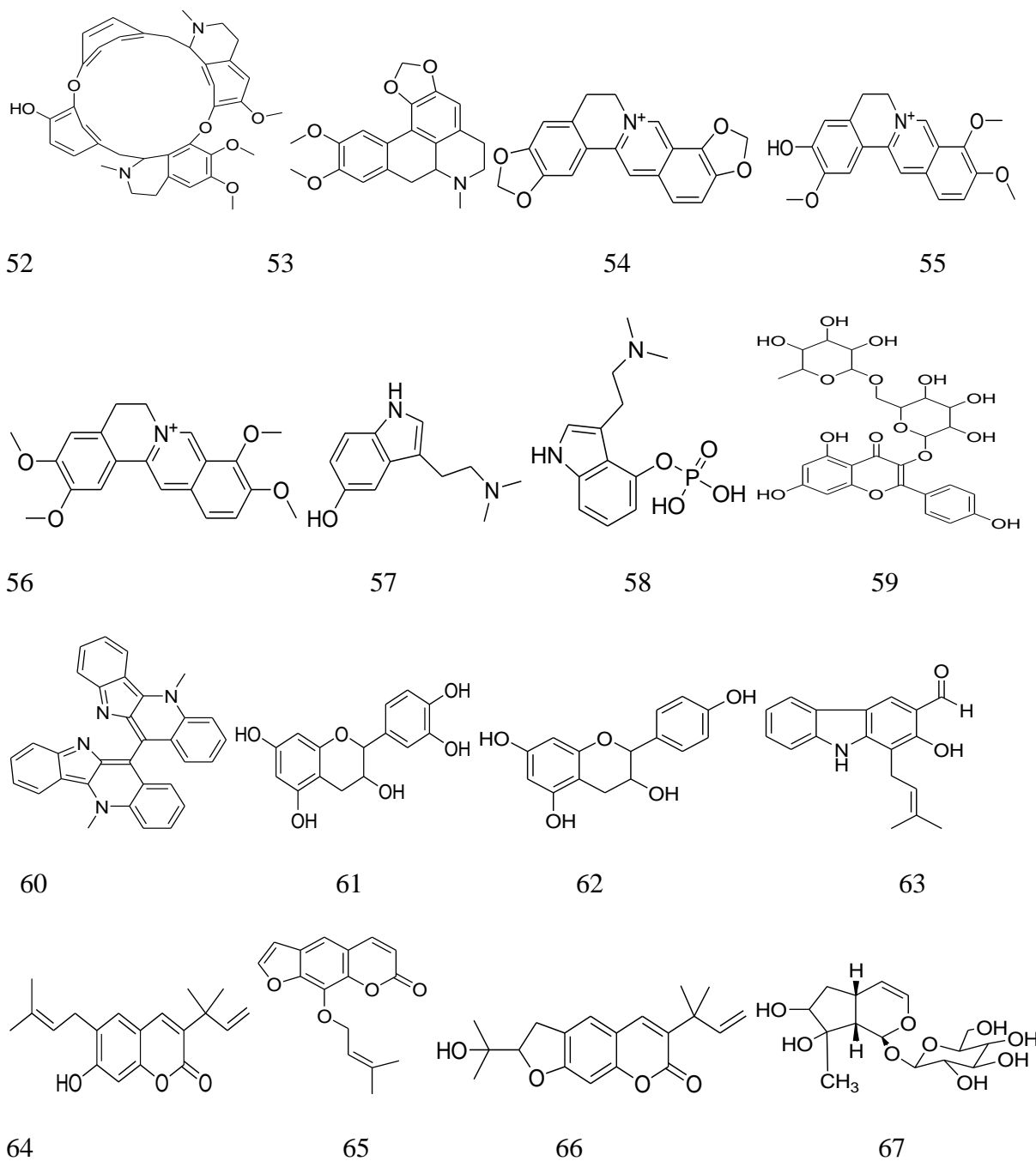
The online tool, CASTp webserver (Tian *et al.*, 2018) was used to identify the binding site of the target protein. Swiss ADME (Daina *et al.*, 2017) and SWISS-MODEL (Guex and Peitsch, 1997) are bioinformatics software used to study the physicochemical and pharmacokinetic properties of the ligands and the generation of protein structure respectively. Protox II (Banerjee *et al.*, 2018) is also an online package for toxicity profile prediction of the drugs. Protein Data Bank (Berman *et al.*, 2003) and PubChem (Kim *et al.*, 2021) are online databases which used to retrieve 3D protein and ligand structure respectively.

3.1.2. Natural Products

Twenty natural products were considered in this study to test their inhibitory potential against the RdRp enzyme of SARS CoV-2. All are published by different investigators for a different purposes but nine of them were published for their antiviral activity and the remaining eleven were new and not evaluated for any antiviral activities and have been isolated from Ethiopian plants in ASTU. The former nines are chosen based on their promising antiviral activities and the later elevens were selected based on their structural similarity and being the same class as those nine, to test if they have any inhibiting effect on the selected enzyme. One drug, RdRp inhibitor namely, remdesivir was chosen as a control.

Nine compounds with promising antiviral activities are berbamine(**52**) and dicentrine(**53**)(Wink, 2007), Coptisine(**54**), Jatrorrhizine(**55**), and Palmatine(**56**)(Schmeller *et al.*, 1997), having a potential to reduce viral replication on previous SARS-CoVs by intercalating nucleic acid, bufotenin (**57**) and psilocybin(**58**) from fungi and animal respectively (Hesse, 2002), nicotiflorin (**59**) (Da Silva *et al.*, 2020) and biscryptolepine(**60**) (Borquaye *et al.*, 2020), and eleven new isolated from Ethiopian plants are two flavans(**61** and **62**) from the stem bark of *Embelia schimperi* (Guyasa Babe *et al.*, 2018), four coumarins and carbazole alkaloids(**63**, **64**, **65** and **66**) from the roots of *Clausena anisata* (Tamene Dandena and Endale Milkyas, 2019), two iridoid

glycosides(**67** and **68**) from the root of *Acanthus sennii* (Assefa Etagegnehu *et al.*, 2016), three indole alkaloids(**69**, **70**, and **71**) from roots of *Brucea antidysentrica* (Alemu Tewabech *et al.*, 2020). Their chemical structures are listed below in Figure 3.1 by numbering(**52-71**) and were sketched using chemdraw ultra 8.



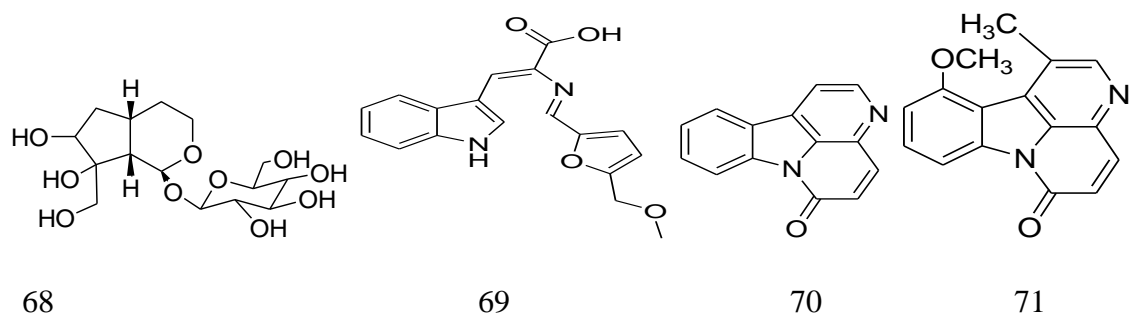


Figure 3. 1: The structure of natural compounds considered in this study.

The numbers (52 to 71) stand for **52** = berbamine, **53** = dicentrin, **54** = Coptisine, **55** = Jatrorrhizine, **56** = Palmatine, **57** = bufotenin, **58** = psilocybin, **59** = nicotiflorin, **60** = biscryptolepine **61** = 3,4-dihydro-2-(3,4-dihydroxyphenyl)-2H-chromene-3,5,7-triol, **62** = 3,4-dihydro-2-(4-hydroxyphenyl)-2H-chromene-3,5,7-triol, **63** = 2-hydroxy-1-(3-methylbut-2-enyl)-9H-carbazole-3-carbaldehyde, **64** = 7-hydroxy-6-(3-methylbut-2-enyl)-3-(2-methylbut-3-en-2-yl)-2H-chromen-2-one, **65** = 9-(3-methylbut-2-enyloxy)-7H-furo[3,2-g]chromen-7-one, **66** = 2,3-dihydro-2-(2-hydroxypropan-2-yl)-6-(2-methylbut-3-en-2-yl)furo[3,2-g]chromen-7-one, **67** = 2-((1S,4aR,7aS)-1,4a,5,6,7,7a-hexahydro-6,7-dihydroxy-7-methylcyclopenta[c]pyran-1-yloxy)-tetrahydro-6-(hydroxymethyl)-2H-pyran-3,4,5-triol, **68** = 2-((1S,4aS,7aS)-octahydro-6,7-dihydroxy-7 (hydroxymethyl)cyclopenta[c]pyran-1-yloxy)-tetrahydro-6-(hydroxymethyl)-2H-pyran-3,4,5-triol, **69** = (2Z,2E)-2-((5-(methoxymethyl)furan-2-yl)methyleneamino)-3-(1H-indol-3-yl)acrylic acid, **70** = 6H-indolo[3,2,1-ij][1,5]naphthyridin-6-one, **71** = 11-methoxy-1-methyl-6H-indolo[3,2,1-ij][1,5]naphthyridin-6-one. Numbering starts from 52 because it was continued from the compounds in the literature review.

3.1.3. Viral Receptor

The genome of SARS-CoV-2 encodes 27 proteins, including an RNA-dependent RNA polymerase (RdRP) and four structural proteins. Among them, RNA-dependent RNA polymerase (RdRp) (106 KDa) is a multifunctional enzyme found in retroviruses that is essential for genome replication and transcription (Te Velthuis *et al.*, 2010). RNA-dependent RNA-polymerase is moreover proposed to be the target of a class of antiviral drugs. It has been the topic of major accessory scientific investigations (Yin *et al.*, 2020). The reason for this is that RdRp has no similarity to the host cell protein, consequently, this minimizes the adverse effect of drugs on the host cell. These are the rationales to select RdRp as the target for the current study.

The structure of RdRp is composed of four chains on three subunits with different sequence lengths (amino acids) as shown in Figure 3.2 below corresponding to nsp12 (chain A) with 192 amino acids shown in green color, nsp7 (chain B) contains 83 amino acids, and nsp8 (chain C, blue and D, green) made up 198 amino acids. The structure was solved using electron microscopy with a resolution of 2.95.

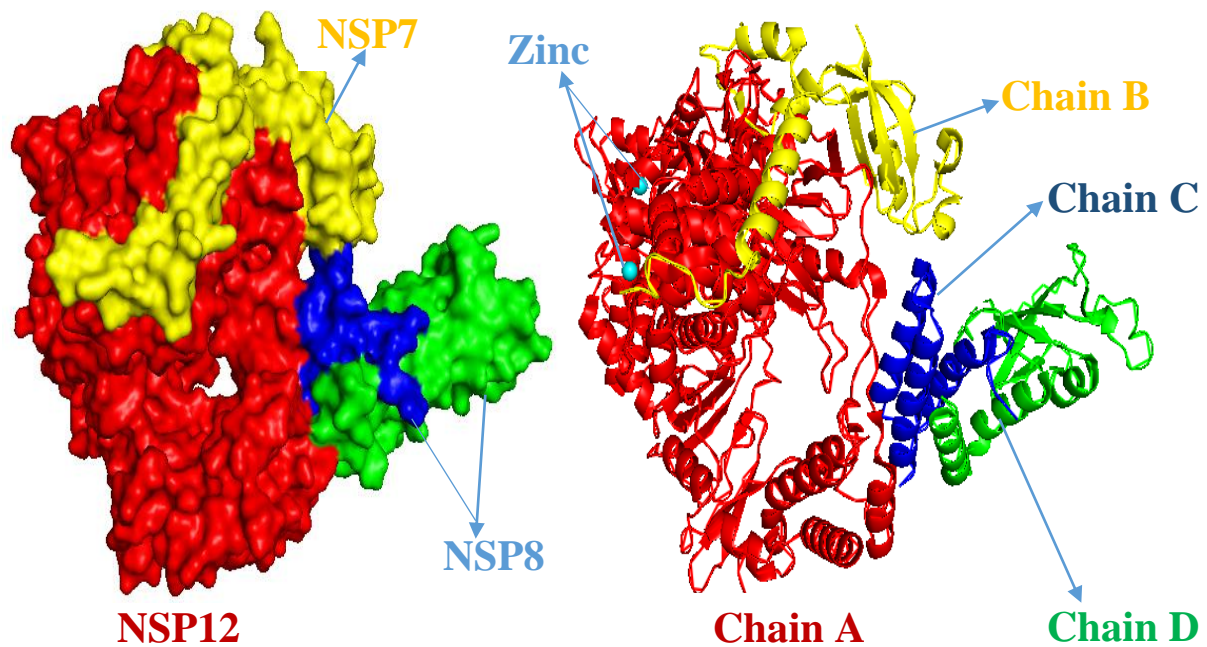


Figure 3. 2: PDB structure of RdRp in surface and cartoon view (visualized by Pymol).

3.2. Study Design

In general molecular docking, study design includes a selection of ligands and receptors as the primary step and followed by the structural and parameters preparation concerning the docking program under use. Figure 3.3 presents a brief view of the methods employed in this study.

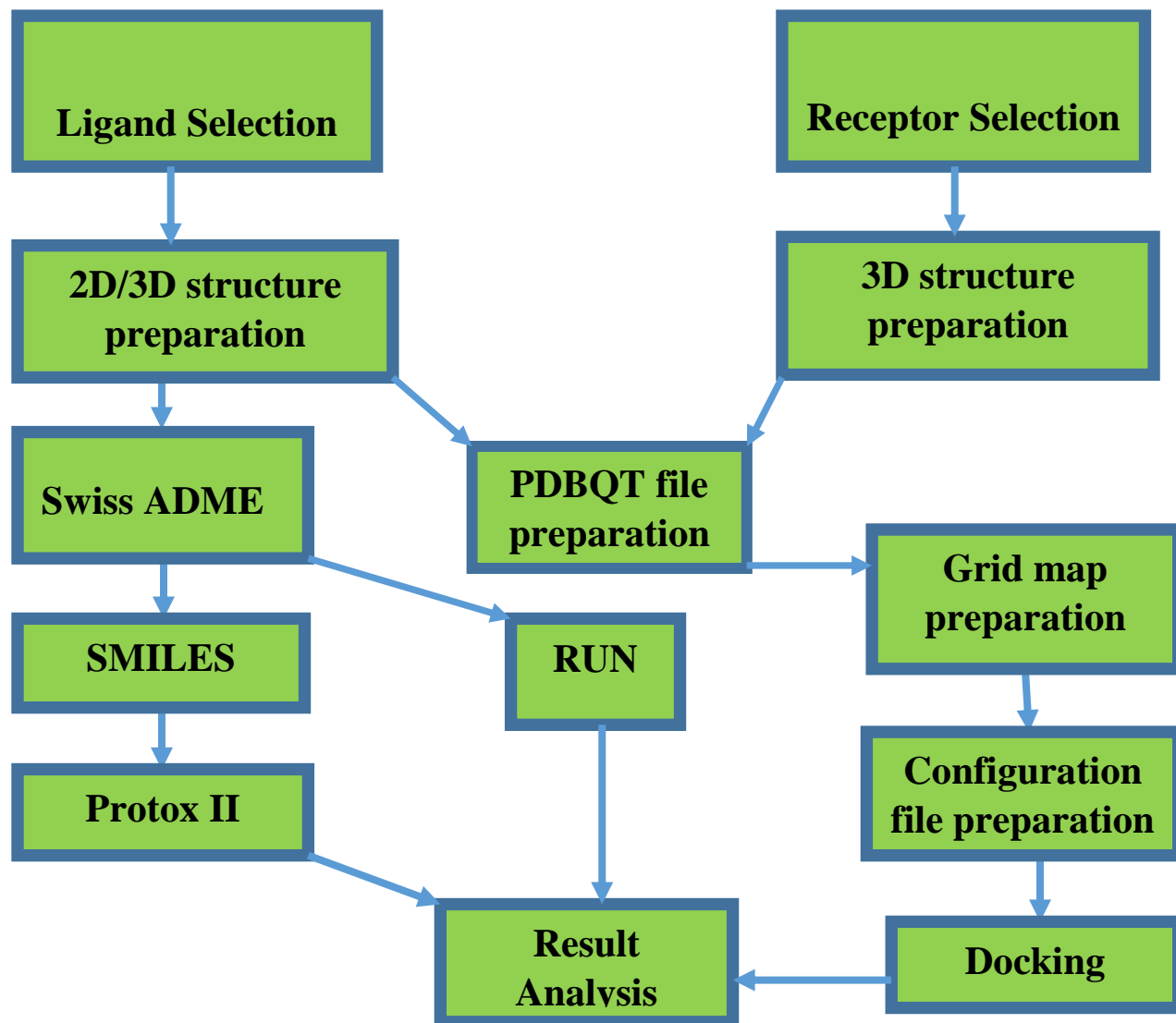


Figure 3. 3: Flow chart of the employed methodology.

3.2.1. Retrieval of Natural Products

Nine compounds that were selected from literature and control (remdesivir) were obtained from PubChem. Their 3D structure was downloaded from the PubChem in structural data file (SDF) format. The search was performed by typing their name in the search box. Their two-dimensional structure for the ADME and toxicological property evaluation was drawn by Chemdraw Ultra 8 using their canonical SMILES.

The chemical structure of the remaining eleven compounds was published only as an image file in different patents, they do not have 2D/3D structures in any molecular databases so their chemical structure was prepared by ChemDrawn ultra 8.

3.2.2. Drug Likeness, Physicochemical, and Pharmacokinetic Properties

Computer-aided drug-likeness, physicochemical and pharmacokinetic properties, and toxicity prediction studies of the given chemical have attracted the attention of the medical industry as a new way to predict possible drug candidates. In this study *in-silico* drug-likeness, physicochemical and pharmacokinetic properties (ADME), of twenty natural compounds were investigated using SwissADME.

Drug likeness properties were investigated based on Lipsink's rule of 5 which states that any therapeutic agent to be applied orally should not violate more than one of the following criteria: molecular mass of the molecules should be less than 500 Da, the number of hydrogen bond donors should less than 5, number of hydrogen bond acceptors should be less than 10, and lipophilicity log P not greater than 5 (Lipinski *et al.*, 1997). Physicochemical properties (molar refractivity, topological polar surface area, number of hydrogen bond donors/acceptors), lipophilicity (logp), and pharmacokinetics properties (GI absorption, BBB permeation, P-GP substrate, inhibition of cytochrome-P enzymes, skin permeation (log Kp)) are all important parameters for predicting drug absorption and distribution within the body (Pathak *et al.*, 2017). In the current study, these physicochemical and pharmacokinetic parameters of test compounds were evaluated on the Swiss ADME webserver.

SwissADME software (www.swissadme.ch) of the Swiss Institute of bioinformatics (<http://www.sib.swiss>) was accessed on a web server that displays the Submission page of SwissADME in Google was used to estimate individual ADME behaviors of the compounds.

The input zone itself contains a molecular sketcher based on Chem Axons Marvin JS (<http://www.chemaxon.com>) that allowed the user to draw and edit 2D chemical structures. The structures were transferred as a list to the right-hand side of the submission page, which is the actual input for computation. The list is made to contain one input molecule per line with several inputs, defined by a simplified molecular-input line-entry system (SMILES), and the results are presented for each molecule in tables, graphs, and also an excel spreadsheet. The SwissADME output file comprises one panel per molecule for clear output and export, the panel comprises all the information of the molecules. The task was performed by submitting the 2D structure of the 20 compounds. After the 2D structure was submitted through ChemAxon's Marvin JS structure drawing tool, the server requested to generate canonical SMILES and then allowed to examine the parameters.

3.2.3. Toxicity Predictions

Toxicity profiles including four toxicological endpoints such as hepatotoxicity, carcinogenicity, immunotoxicity, and mutagenicity, and the level of toxicity (LD50, mg/Kg) of the study compounds were evaluated using a ProTox-II server (Drwal *et al.*, 2014). This job was done using the canonical SMILES which were previously generated and saved from the Swiss ADME predictor. After the server was opened toxic prediction option was commanded and the box to submit canonical SMILES was generated, then the SMILES were submitted. Finally, toxicological end points (mutagenicity, immunotoxicity, carcinogenicity) were selected and a tool was run to predict.

3.2.4. Preparation of Ligands for docking

The compounds which fulfill Lipinski's rule of five for drug-likeness were docked against RdRp. All compounds of the study except nicotiflorin fulfill the criteria of Ro5. Hence their chemical structures were prepared for docking as follows. Since the chemical (2D/3D) structure of the eleven new compounds was not published in any molecular data base Chemdrawn two dimensional structure of them was converted into 3D using ChemDraw ultra 8. ChemDraw 2D structure is not energy favorable. Hence, 2D structures of the eleven compounds were energy minimized by using again ChemDraw 3D ultra 8. To do this, the structure was submitted to

ChemDraw 3D ultra 8 from the menu, and calculations | MM2 | Minimize Energy were chosen as the job type. Display every iteration was checked. Then the minimum RMS gradient was kept as default at 0.100 and allowed the program to run. Finally, an energy-minimized compound structure was generated.

Both Pub-Chem downloaded (SDF) of the former nine compounds and ChemDrawn (cdx) structure of the later eleven compounds are then converted into PDB file format using Open Bable.

Then the compounds (PDB) were submitted to the MGL one by one through the ligand menu, then the gasteiger charges were added and non-polar hydrogen atoms were merged out automatically. The torsion angle of the ligand was adjusted automatically as TORSDOF. TORSDOF denotes the number of torsional degrees of freedom in the ligand. It is used to calculate the free energy shift caused by the loss of torsional degrees of freedom during binding(Huey *et al.*, 2012). Finally, the prepared compound file was saved as PDBQT.

3.2.5. Retrieval and Preparation of Viral Receptor

The three-dimensional structure of the protein RdRp of SARS-CoV-2 (PDB ID: 7BTF) was retrieved from the Protein Data Bank (www.rcsb.org/pdb).

The PDB file of RdRp was missing several residues at the end and beginning. Protein will lose its stability if any residues are missed from its place. So, adding missing residue is important in molecular docking and molecular dynamic simulations to analyze the structure and interactions (Manhas, 2016).

The missing residue of the PDB file of protein was added through homology modeling on the SWISS-MODEL web server (<https://swissmodel.expasy.org>) (Ishikawa, 2017). After the webserver launched, modeling was done using the build user template option, it started with modeling the user template, then the full sequence (FASTA format) of the target protein was submitted in the target sequence box, and the PDB file of the target protein containing missing residue to be repaired was added as a template to be built. Then by running build a model job, repaired the 3D structure of the target protein was built as the new model and the PDB format was downloaded (Ishikawa, 2017).

Energy minimization is also required for protein since the newly generated structure of the protein is not energy favorable (Manhas, 2016). Energy minimization repairs distorted geometries of protein by moving atoms to release internal restraints. Hence, energy minimization of the newly generated structure RdRp was performed using the Swiss PDB viewer (SPDB V4.10). To do this, the newly generated model of RdRp (PDB) was submitted to SPDB V4.10 through the file menu, by selecting open PDB file as job type, select all surface was commanded from select menu, then from tools, minimize energy was computed. Computation was done *in a vacuum* with the GROMOS 96 43B1 (Guex and Peitsch, 1997). Then finally energy minimized structure of RdRp was saved in PDB file format by saving the current layer from the file menu.

Then energy minimized RdRp structure was again treated by MGL to remove het atoms(water, and zinc atoms), to add hydrogen and charges, and finally to prepare PDBQT for docking (Ccsb-Scripps, 2021a). The very first step of preparing protein for virtual screening computation includes the removal of water molecules from the binding site, water molecules are not often important in the binding of the target and ligand (Wong and Lightstone, 2011). Therefore, they have to be removed to make calculations easier and to free the binding site protein. The water molecules may interfere with the search and can lead to the false-negative result, or impractical numbering possibilities if they are left untreated. The other standard procedure is removing co-crystallized ligands attached to a receptor molecule to make pocket free. Then the next step was adding polar hydrogen atoms and Kollman charges to the protein because generally, the PDB file lacks hydrogen atoms, and also charges are not recorded in a crystal structure but the docking software requires the hydrogen atoms to be in place and charges to be assigned to run circulation which is required for appropriate treatment of electrostatics during docking.

Kollman charges are template values for each amino acid that were derived from the corresponding electrostatic potential using quantum mechanics. Adding Kollman charges are important to consider electrostatic interactions. If no charges are added to the protein, then all the electrostatic interactions between protein and ligand are absent and the van der Waals interactions will become dominant. Furthermore, docking algorithms require each atom to have a charge and an atom type that describes its properties. So finally all the het atoms (water molecules and zinc ion) were removed, and polar hydrogens and Kollman charges were added and saved as PDBQT (Ccsb-Scripps, 2021a).

3.2.6. Identification of the Active Site and Generation of the Receptor Grid

RdRp has no experimentally identified active site. The structure also has no co-crystallized native ligand except two-zinc atoms. So different literature survey was done to find the active site of RdRp. In addition, an online bioinformatics tool, the CASTp webserver (<http://sts.bioe.uic.edu>) was used to predict and cross-check the surveyed result (Tian *et al.*, 2018).

Then docking was carried out on the grid map which was prepared around predicted active site residues. The search was carried out on the active site by building a grid box with a volume that is big enough to cover the entire active site residue of the protein (Huey *et al.*, 2012). For this purpose, a 3-D map of the grid box was prepared on the target protein using the grid widget option of MGL. To do this after the prepared PDBQT file of the RdRp is submitted to the MGL, the grid box was chosen as the job type, when the grid box is selected, the grid options widget displays the current total number of grid points per map. This contains three thumbwheel widgets that help to change the number of points in the x, y, and z dimensions. The default parameters are 40, 40, and 40 which makes the total number of grid points per map 68921 because AutoGrid always adds one in each dimension. This specifies the size of each grid map: $(n_x + 1) \times (n_y + 1) \times (n_z + 1)$, where n_x is the number of grid points in the x-dimension, n_y is in the y-dimension, and n_z is in the z-dimension. The thumbwheel allows the user to alter the spacing between grid points. Some additional entries and thumb wheels allow adjusting the location of the grid's center. The number of points in each dimension can be set to a maximum of 126. AutoGrid requires an even number of grid points to be adjusted. It then adds one point in each dimension, because AutoGrid and AutoDock require a central grid point. Another thumbwheel can be used to change the distance between grid points. The default value is 0.375 between grid points, which is simply one-quarter the length of a single carbon-carbon bond. When investigating a large volume, grid spacing values of up to 1.0 can be employed. For this study large volume of a grid was needed since the size of RdRp is large and the active site unknown. The box was prepared in equal width with the size of the receptor (RdRp) to give the full freedom to the ligand likely to be docked to all parts of the receptor. Grid box size of $66 \times 60 \times 66$ Å points, makes the total number of grid points per map 273829 with a grid spacing of 0.75.0 Å considered.

3.2.7. Docking Method Validation

First, the docking of the receptor was performed with the control to validate the method by dock score from previous MD studies on the same target (RdRp) using the same approaches. The method is said to be valid if the docking score of control from both studies is relative and the RMSD value obtained is $\leq 2 \text{ \AA}$, So that docking of the compound under study can be carried out with the target protein in the same grid box area (Bell and Zhang, 2019). In the current study, the docking score of the control (remdesivir) was used to validate the method by comparing the value from the literature.

In addition, we re-docked the ligands to their corresponding targets at the experimentally identified sites to validate their binding sites and to evaluate if our approach works. The fact that the binding energy of the ligands when bound to these sites is very low indicates that our approach is indeed justifiable.

3.2.8. Docking Analysis

After all, parameters are required to conduct docking such as target.pdbqt file, ligand.pdbqt, grid map, and configuration file are prepared, and docking was performed using Autodock Vina. Vina. The configuration file was prepared in notepad, and each specification, protein name, ligand name, grid dimension, exhaustiveness, and energy range, were typed and saved with the name "config.cfg." Finally, the prepared ligands, receptors, and configuration files were submitted into the Vina folder, Vina program was run through the command prompt.

The results of the docking calculation were generated as output.txt and log.txt. Output.txt contains the best nine conformations of the ligand and log.txt contain the docking score/ ΔG of each conformation. The docking conformation of the ligands was selected by choosing the pose with the highest affinity (the largest negative Gibbs' free energy of binding/ G). Then, for the further interaction study ligand-receptor complex was generated by Pymol and the interaction was visualized by BIOVIA discovery studio 2021.

CHAPTER FOUR

4. RESULT AND DISCUSSION

4.1. Results

4.1.1. Identification of the General Characteristics of the Natural Compounds

In the current study, twenty natural products were screened to evaluate their inhibitory potential on RdRp of SARS CoV-2. They are from different classes of compounds with different characteristics (Table 4.1).

Table 4. 1: General Characteristics of the natural compounds considered in this study.

CPDS	Pubchem ID	Molecular formula	Canonical SMILES
Berbamine(52)	275182	C ₃₇ H ₄₀ N ₂ O ₆	COc1c(OC)cc2c3c1Oe1cc4c(cc1OC)CCN(C4Cc1ccc(Oc4cc(CC3N(CC2)C)ccc4O)cc1)C
Dicentrin(53)	101300	C ₂₀ H ₂₁ NO ₄	COc1cc2c(cc1OC)CC1c3c2c2OCOe2cc3CCN1C
Coptisin(54)	72322	C ₁₉ H ₁₄ NO ₄ ⁺	C1Oc2c(O1)cc1c(c2)CC[n+]2c1cc1ccc3c(c1c2)OCO3
Jatrorrhizine(55)	72323	C ₂₀ H ₂₀ NO ₄ ⁺	COc1cc2c(cc1O)CC[n+]1c2cc2ccc(c(c2c1)OC)OC
Palmatine(56)	19009	C ₂₁ H ₂₂ NO ₄ ⁺	COc1cc2CC[n+]3c(c2cc1OC)cc1c(c3)c(OC)c(cc1)OC
Bufotenin(57)	10257	C ₁₂ H ₁₆ N ₂ O	CN(CCc1c[nH]c2c1cc(O)cc2)C
Psilocybin(58)	10621	C ₁₂ H ₁₇ N ₂ O ₄ P	CN(CCc1c[nH]c2c1c(ccc2)OP(=O)(O)O)C
Nicotiflorin(59)	5318767	C ₂₇ H ₃₀ O ₁₅	Oc1ccc(cc1)c1oc2cc(O)cc(c2c(=O)c1OC1OC(COC2OC(C)C(C(C2O)O)O)C(C(C1O)O)O)O
Biscryptolepine(60)	10457065	C ₃₂ H ₂₂ N ₄	Cn1c2ccccc2c(c2c1c1ccccc1n2)c1c2ccccc2n(c2c1nc1c2ccc1)C
CPD61	-	C ₁₅ H ₁₄ O ₆	Oc1cc2OC(c3ccc(c(c3)O)O)C(Cc2c(c1)O)O
CPD62	-	C ₁₅ H ₁₄ O ₅	Oc1ccc(cc1)C1Oe2cc(O)cc(c2CC1O)O
CPD63	-	C ₁₈ H ₁₇ NO ₂	O=Cc1cc2c(c(c1O)CC=C(C)C)[nH]c1c2cccc1
CPD64	-	C ₁₉ H ₂₂ O ₃	C=CC(c1cc2cc(CC=C(C)C)c(cc2oc1=O)O)(C)C

CPD65	-	C ₁₆ H ₁₄ O ₄	<chem>CC(=CCOc1c2occc2cc2c1oc(=O)cc2)C</chem>
CPD66	-	C ₁₉ H ₂₂ O ₄	<chem>C=CC(c1cc2cc3CC(Oc3cc2oc1=O)C(O)(C)C)(C)C</chem>
CPD67	-	C ₁₅ H ₂₄ O ₉	<chem>OCC1OC(O[C@@H]2OC=C[C@@H]3[C@H]2C(C)(O)C(C3)O)C(C(C1O)O)O</chem>
CPD68	-	C ₁₅ H ₂₆ O ₁₀	<chem>OCC1OC(O[C@@H]2OCC[C@@H]3[C@H]2C(O)(CO)C(C3)O)C(C(C1O)O)O</chem>
CPD69	-	C ₁₈ H ₁₆ N ₂ O ₄	<chem>COCc1ccc(o1)/C=N/C(=C\c1c[nH]c2c1cccc2)/C(=O)O</chem>
CPD70	-	C ₁₄ H ₈ N ₂ O	<chem>O=c1ccc2c3n1c1cccc1c3ccn2</chem>
CPD71	-	C ₁₆ H ₁₂ N ₂ O ₂	<chem>COc1cccc2c1c1c(C)nc3c1n2c(=O)cc3</chem>

CPDS= compounds, SMILES= simplified molecular-input line-entry system

4.1.2. Drug Likeness and Physico Chemical Properties

Lipinski's rule of five (Ro5) is the criteria to identify whether a small molecule has drug-likeness properties or the potential to be a drug (Figure 4.1).

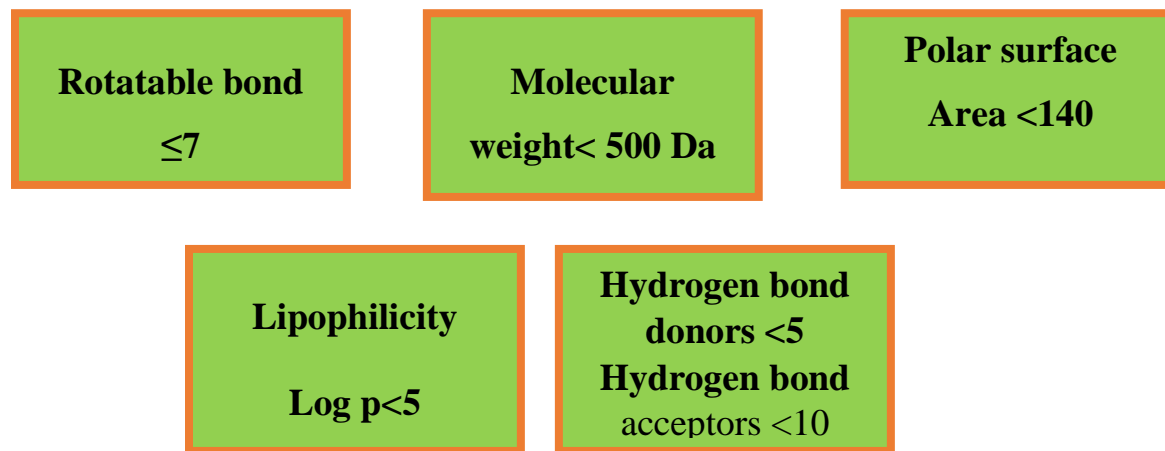


Figure 4. 1: Good In vivo Drug absorption and Permeation Lipinski's Rule of 5

Drug likeness properties of all 20 natural compounds were evaluated on the Swiss ADME webserver. Ro5 was evaluated based on the physicochemical properties of the compounds. Most of the compounds evaluated in this study do not violate the Ro5. However, nicotiflorin does not meet the Ro5 (Table 4.2). The physicochemical properties section comprises clean molecular and physicochemical characteristics like molecular formula, molecular weight, number of rotatable bonds, number of H-bond acceptors, number of H-bond donors, molar refractivity, and total polar surface area (TPSA) respectively. All predicted physicochemical properties of test compounds in the current study are presented in Table 4.2.

Table 4. 2: Physicochemical properties and RO5 of test compounds.

Compounds	NRB	MW	MLOGP	NHBD	NHBA	MR	TPA	Violations	Meet Ro5
Berberamine(52)	3	608.72	3.55	1	8	181.6	72.86	1	yes
Dicentrin(53)	2	339.39	2.38	0	5	98.02	40.16	0	yes
Coptisin(54)	0	320.32	2.37	0	4	87.95	40.8	0	yes
Jatrorrhizine(55)	3	338.38	1.78	1	4	97.33	51.8	0	yes
Palmatine(56)	4	352.4	2.01	0	4	101.8	40.8	0	yes
Bufotenin(57)	3	204.27	1.22	2	2	62.6	39.26	0	yes
Psilocybin(58)	5	284.25	0.27	3	5	73.25	95.6	0	yes
Nicotiflorin(59)	6	594.52	-3.43	9	15	139.36	249.2	3	no
Biscryptolepine(60)	1	462.54	5.34	0	2	151.01	35.64	1	yes
CPD61	1	290.27	0.24	5	6	74.33	110.38	0	yes
CPD62	1	274.27	0.79	4	5	72.31	90.15	0	yes
CPD63	3	279.33	2.66	2	2	86.94	53.09	0	yes
CPD64	4	298.38	3.51	1	3	91.83	50.44	0	yes
CPD65	3	270.28	2.14	0	4	77.5	52.58	0	yes
CPD66	3	314.38	2.74	1	4	91.05	59.67	0	yes
CPD67	3	348.35	-2.59	6	9	77.67	149.07	1	yes
CPD68	4	366.36	-3.22	7	10	79.3	169.3	1	yes

CPD69	6	324.33	0.37	2	5	91.07	87.82	0	yes
CPD70	0	220.23	2.41	0	2	67.66	34.37	0	yes
CPD71	1	264.28	2.34	0	6	79.12	43.6	0	yes

NRB= number of rotatable bonds, MW= molecular weight, MLOGP= Lipophobicity, NHBD= number of hydrogen bond donors, NHBA= number of hydrogen bond acceptors, MR= molecular refractivity, TPSA= total polar surface area

4.1.3. Pharmacokinetics

Pharmacokinetic properties (absorption, distribution metabolism, and excretion) of target compounds were examined on the Swiss ADME webserver. This section is comprised of a major descriptor of ADME including GI absorption, BBB permeant, P-GP substrate, Cytochrome p450 (CYP) isoenzymes inhibitors (CYP1A2 inhibitor, CYP2C19 inhibitor, CYP2C9 inhibitor, CYP2D6 inhibitor, CYP3A4 inhibitor), and log Kp (cm/s) (Table 4.3).

Swiss ADME adopts a support vector machine algorithm (SVM) for the datasets of known substrates/non- substrates or inhibitors/non-inhibitors for binary classification. When the tool examines, the resultant molecule will return “Yes” or “No” if the molecule under investigation is expected to be a substrate for both P-GP and CYP respectively. Skin permeation (log Kp) is another parameter of pharmacokinetics that measure a molecule’s skin permeability in centimeter per second.

The pharmacokinetics performed using SwissADME showed a high level of GI absorption with Berbamine(52), Dicentrin(53), Coptisin(54), Jatrorrhizine(55), Palmatine(56), Bufotenin(57), Psilocybin(58), CPD61, CPD62, CPD63, CPD64, CPD65, CPD66, CPD69, CPD70, and CPD71 and high BBB permeant with Dicentrin(53), Coptisin(54), Jatrorrhizine(55), Palmatine(56), Bufotenin(57), Nicotiflorin(59), CPD63, CPD64, CPD65, CPD66, CPD70, CPD71 respectively.

Table 4. 3: Pharmacokinetics properties targeted compounds.

CPDs	GI absorption	BBB permeant	P-gp substrate	CYP1A2 inhibitor	CYP2C19 inhibitor	CYP2C9 inhibitor	CYP2D6 inhibitor	CYP3A4 inhibitor	log Kp (cm/s)
52	High	No	No	No	No	No	No	No	-5.51
53	High	Yes	Yes	Yes	Yes	Yes	Yes	Yes	-6.07
54	High	Yes	Yes	Yes	No	No	No	Yes	-5.78
55	High	Yes	Yes	Yes	No	No	Yes	Yes	-5.94
56	High	Yes	Yes	No	No	No	Yes	Yes	-5.79
57	High	Yes	No	Yes	No	No	No	No	-5.8
58	High	No	No	No	No	No	No	No	-9.16
59	Low	No	Yes	No	No	No	No	No	-9.91
60	Low	No	No	No	No	No	No	No	-4.61
61	High	No	Yes	No	No	No	No	No	-7.82
62	High	No	Yes	No	No	No	No	No	-7.46
63	High	Yes	No	Yes	Yes	Yes	Yes	No	-4.48
64	High	Yes	No	Yes	Yes	Yes	No	No	-4.26
65	High	Yes	No	Yes	Yes	Yes	No	No	-5.46
66	High	Yes	No	Yes	Yes	Yes	Yes	No	-5.47
67	Low	No	Yes	No	No	No	No	No	-9.98
68	Low	No	Yes	No	No	No	No	No	-10.53
69	High	No	No	Yes	No	Yes	No	No	-6.43
70	High	Yes	No	Yes	No	No	No	No	-5.93
71	High	Yes	No	Yes	No	No	No	Yes	-5.95
Control	Low	Yes	Yes	No	No	No	No	Yes	-8.62

GI passive absorption and prediction for brain access of molecules are also presented by the passive diffusion BOILED-Egg Model (Brain or Intestinal Estimated permeation predictive model). The description exists in a region of agreeable properties for GI absorption on a plot of two computed descriptors; ALOGP versus PSA respectively. GI absorption, BBB permeation, and PG-P substrate of the twenty study compounds are presented in BOILED-Egg Model (Figure 4.2). The white region is the space of the molecules with a greater extent of absorption by the GI tract, and the yellow region (yolk) is the space with the highest probability to permeate to the brain. The compound out of the white and yellow region are poorly absorbed and least permeate of BBB. This boiled-egg model also predicted whether compounds were substrates of P-glycoprotein (PGP). Red dots (PGP⁻) represent compounds that are not substrates of the PGP CNS efflux transporter, while, blue dots (PGP⁺) represent compounds that are substrates of PGP and predicted to pass through the CNS (Panyatip *et al.*, 2020). All the study compounds are presented on the graph by numbering. The coding of compounds (52-71) is represented as molecule 1-20, where CPD52 = molecule 1, and the rest continued in the same manner.

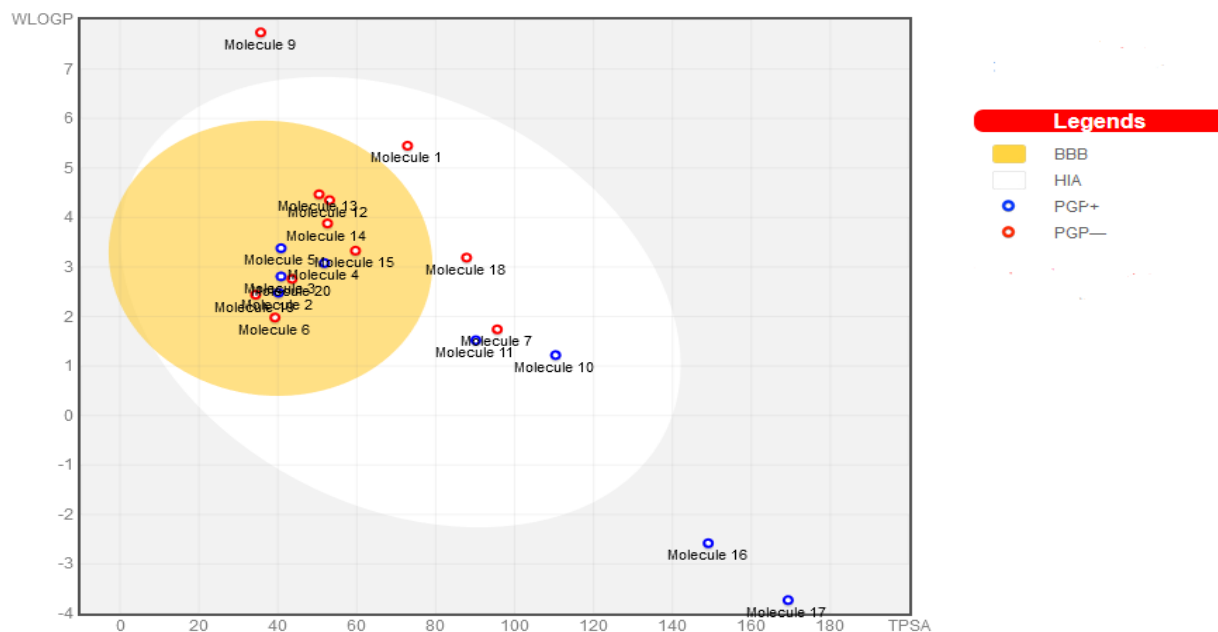


Figure 4. 2: Boiled egg model for pharmacokinetic properties.

4.1.4. Toxicity Predictions

One of the most important considerations when choosing a therapeutic candidate is the absence of toxicity (Sadeghi *et al.*, 2021). In this study, the organ toxicity (hepatotoxicity) and toxicological endpoints (carcinogenicity, immunotoxicity, mutagenicity, and cytotoxicity), Lethal dose (LD50), and acute toxicity classes were evaluated for all the test natural compounds using Protox II. The prediction results are presented below in table 4.4.

Table 4. 4: Protox II predicted organ toxicity, toxicological endpoints, and acute toxicity.

CPDs	Hepatotoxicity	Carcinogenicity	Immunotoxicity	Mutagenicity	Cytotoxicity	LD50(mg/Kg)	ATC
52	inactive	inactive	active	active	active	1700	4
53	inactive	active	active	active	active	89470	3
54	inactive	active	active	active	active	200	3
55	inactive	inactive	active	active	inactive	200	3
56	inactive	active	active	active	active	200	3
57	inactive	inactive	active	inactive	inactive	787	4
58	Inactive	inactive	inactive	inactive	inactive	96	3
59	inactive	inactive	active	inactive	inactive	5000	5
60	inactive	inactive	inactive	inactive	inactive	675	4
61	inactive	inactive	inactive	inactive	inactive	10000	6
62	inactive	inactive	inactive	inactive	inactive	2500	5
63	inactive	inactive	inactive	active	inactive	1000	4
64	inactive	inactive	inactive	active	inactive	2905	5
65	inactive	inactive	active	active	inactive	480	4
66	inactive	inactive	inactive	active	inactive	1500	4
67	inactive	inactive	active	inactive	inactive	2000	4
68	inactive	inactive	inactive	inactive	inactive	29700	6
69	inactive	inactive	inactive	inactive	inactive	1680	4
70	active	inactive	active	inactive	inactive	1190	4
71	inactive	inactive	active	active	inactive	3000	5
Control	inactive	inactive	inactive	inactive	inactive	1000	4

CPDs = Compounds, LD50 = Lethal Dose, ACT = Acute Toxicity Class

4.1.5. Binding site identification of the RdRp for docking

The catalytic site of RdRp for test compound docking was identified using an online bioinformatics tool known as CASTp 3.0. CASTp 3.0 predicted the 12 pockets as a binding site with different pocket ID, volume, and surface but the pocket ID with the large volume and surface area is considered as the best active site for docking study. The predicted active site with volume of 6565549 Å³ and surface area of 3694.224 Å² shown in (Figure 4.3) with red color contains active site residues from chain A and B such as A: ASP161, TYR163, ASP164, VAL166, GLU167, PHE429, LYS430, GLU431, GLY432, SER433, VAL435, GLU436, LEU437, LYS438, HIS439, HIS439, PHE440, PHE441, PHE442, ASP452, TYR455, TYR456, TYR479, ILE494, VAL495, ASN496, ASN497, LEU498, ASP499, LYS500, SER501, ALA502, LYS511, ALA512, TYR516, THR540, MET542, ASN543, LEU544, LYS545, TYR546, ALA547, ILE548, SER549, ALA550, LYS551, ARG553, ALA554, ARG555, THR556, VAL557, ALA558, GLY559, VAL560, ILE562, THR565, ASN568, ARG569, HIS572, GLN573, LEU576, LYS577, ALA580, ARG583, GLY584, ALA585, THR586, VAL588, ILE589, GLY590, THR591, SER592, LYS593, PHE594, TYR595, GLY597, TRP598, ASN600, MET601, THR604, VAL605, SER607, GLY616, TRP617, ASP618, TYR619, PRO620, LYS621, CYS622, ASP623, ARG624, MET626, GLU665, LYS676, THR680, SER681, SER682, GLY683, ASP684, ALA685, THR686, ALA688, TYR689, ASNA691, ARG750, PHE753, SER754, MET755, MET756, LEU758, SER759, ASP760, ASP761, ALA762, VAL763, PHE793, SER795, ALA797, LYS798, CYS799, TRP800, HIS810, GLU811, PHE812, CYS813, SER814, GLN815, HIS816, PRO832, ASP833, ARG836, ILE837, ALA840, PHE843, VAL844, ASP845, ILE847, VAL848, LEU854, GLU857, ARG858, VALA860, SER861, LEU862, ILE864, ASP865, TYR903, MET906, LEU907, ASP910, THR912, SER913, TYR915, PHE920, ALA923, MET924, THR929, VAL930, LEU931, GLN932 B: SER1, MET3, SER4, LYS7, LEU40, LEU41, ALA42, LYS43.

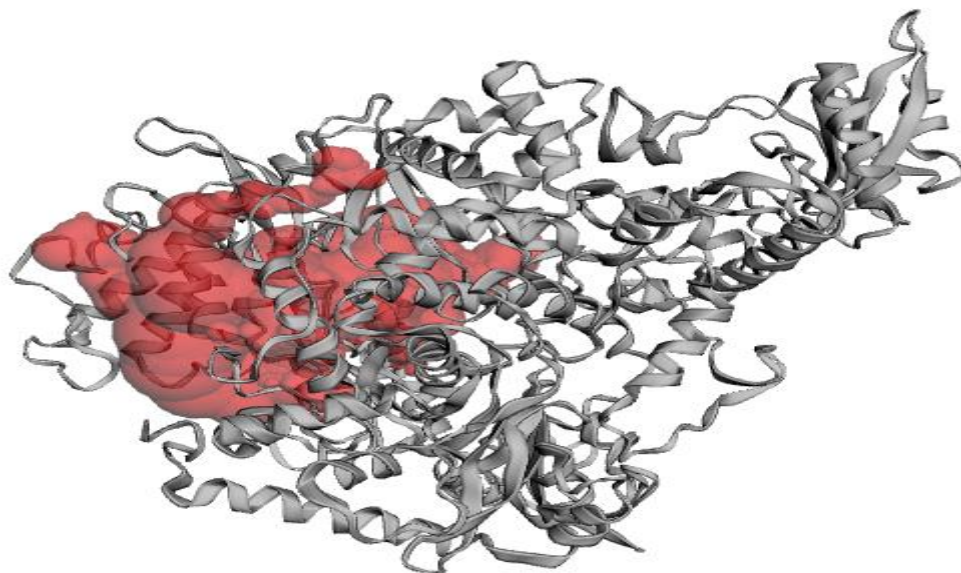


Figure 4. 3: Active site RNA dependent RNA polymerase (CASTp predicted).

4.1.6. Molecular Docking and Binding Affinities

For each test compound, AV generated nine poses at the binding site of the RdRp with different binding energy and RMSD value (Appendix 1). But according to Trott and Olson (2010) more negative binding energy value suggests a better binding affinity between drugs and a protein. Based on this, the first pose with more negative binding energy and zero RMSD value was chosen for further investigation. The results showed that biscriptolepin(60) (-8.8) berbamin(52) (-9.0), CPD63(-7.7), Jatrorrhizine(55) (-7.4), (Dicentrin(53) (-7.1) and CPD66, CPD69, and CPD70 (-6.8), CPD62 and CPD7(6-.6), CPD64 (-6.5) CPD68 (-6.3), CPD65 (-6.2), Palmatine (56) (-6.1), CPD67 psilocybin (58) (-5.9) , and bufotenin (57) (-5.3) as RdRp inhibitors in descending order. Gibbs's free binding energy and polar interaction of the selected compounds on RdRp are presented below in Table 4.5.

Table 4. 5: Binding energy and polar contact of the compounds on RdRp.

Compounds	Binding energy (kcal/mol)	Polar contact	
		Residues (H-bonds)	Bond length
Berbamine(52)	-8.8	ARG-249	3.01
		THR-319	3.66
		ARG-457	3.12
Dicentrin(53)	7.1	ASN-414,	2.71
		SER-15	3.53
		GLN-18	3.48
Coptisin(54)	-8.0	PHE-396	2.70
		ASN-628	2.46
Jatrorrhizine(55)	-7.4	ARG-349	2.32
		ARG-457	3.57
Palmatine(56)	-6.1	ASP-760	3.39
Bufotenin(57)	-5.3	THR-246	2.58
		THR-319	3.53
Psilocybin(58)	-5.9	GLU-436,	3.30
		GLU-431	3.47
		ALA-42	1.80
		ASP-760	2.47
		ASP-761	2.38
		THR-252	2.13
Biscryptolepine(60)	-9.0	TYR-265	2.43
		ARG-249	2.22
		THR 319	2.31
		PRO-412	2.63
CPD61	-7.1	TYR-546,	2.11
		ASN-414	2.93
CPD62	-6.6	SER-433	2.33
		ASP-879	3.23
CPD63	-7.7	ASN-414	1.92
CPD64	-6.5	LYS-7	2.48

CPD65	-6.2	SER-913	2.74
CPD66	-6.8	-	
CPD67	-6.1	TRP-617	2.82
		ASP-761	2.70
		LYS-798	2.80
		GLU-811	1.88
CPD68	-6.3	TRP-617	2.73
		TYR-619	2.09
		ASP-760	2.14
		ASP-761	2.20
		SER-814	2.11
CPD69	-6.8	-	
CPD70	-6.8	PHE-396	2.15
		ARG-624	1.97
CPD71	-6.6	ASP-760	3.49
		ARG-624	3.73
		ASP-208	2.65
Remdesvir	-6.7	ASN-209	1.87
		THR-206	2.18
		THR-51	2.34

4.1.7. Interaction Analysis

For the interaction analysis of the top pose from the docking result, the RdRp-Ligand complex was prepared using PyMol and the interaction of all poses was visualized using BIOVIA discovery studio software. The interactions between the RdRp enzyme and 19 natural compounds and control are shown below in Figures 4.4-4.22. The 2D and 3D structures of the complex, each compound, and RdRp were presented in the figures. As shown in the two-dimensional structure the complexes were stabilized by different types of chemical bonds. Major types of interactions were van der Waals, hydrophobic (alkyl and pi-alkyl), polar (conventional and carbon-hydrogen bond), and electrostatic interactions. Vander Waals interactions were common in all 19 RdRp-Ligand complexes, which hold the neighboring amino acid residues

Coptisine(54)

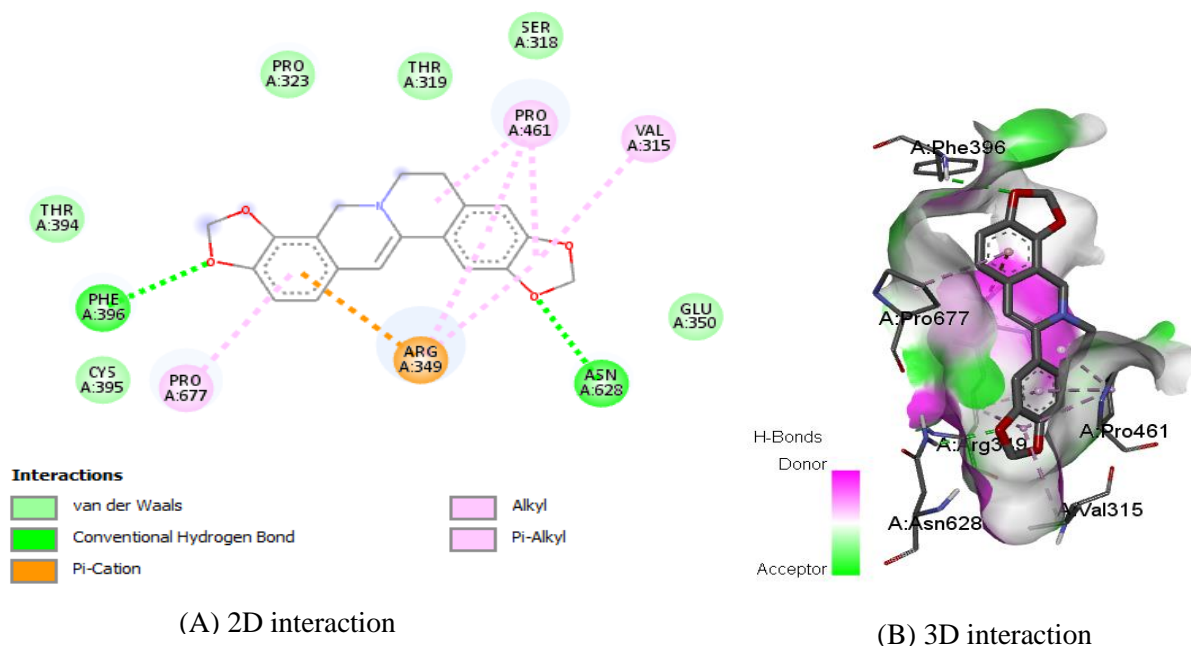


Figure 4. 6: Interaction of RdRp enzyme on **Coptisine(54)** [(A) 2D interactions (B) 3D interactions].

Jatrorrhizine(55)

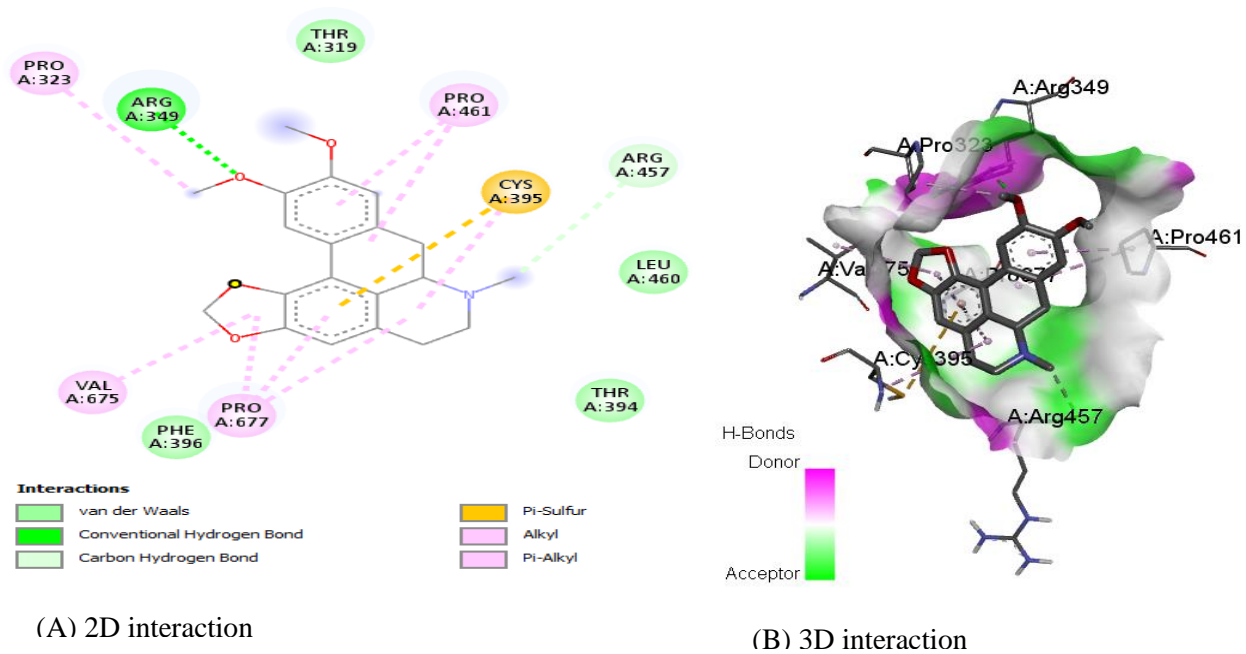
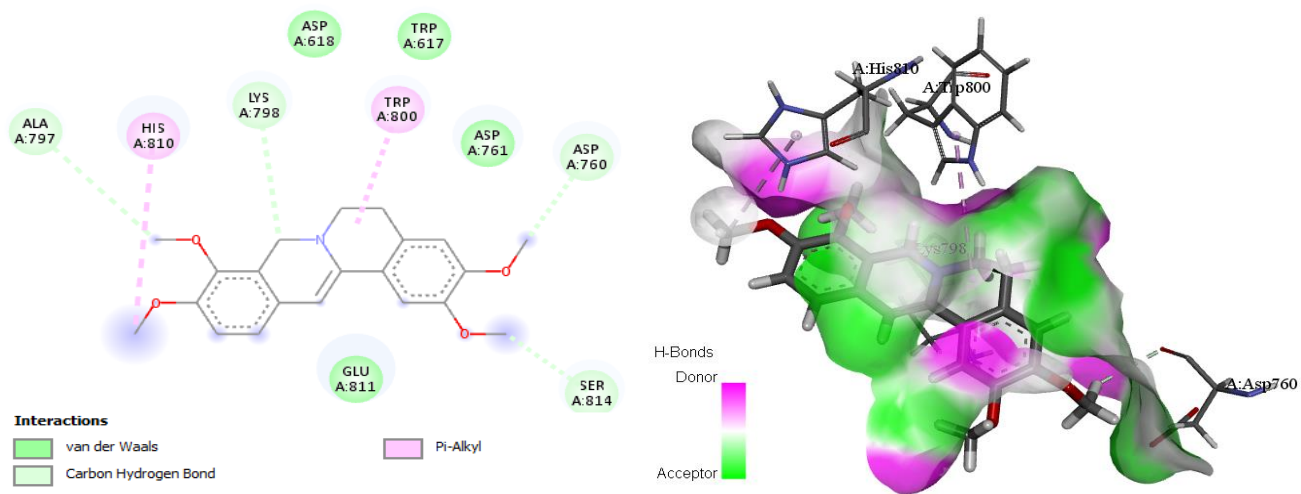


Figure 4. 7: Interaction of RdRp enzyme on **Jatrorrhizine(55)** [(A) 2D interactions (B) 3D interactions].

Palmatine(56)

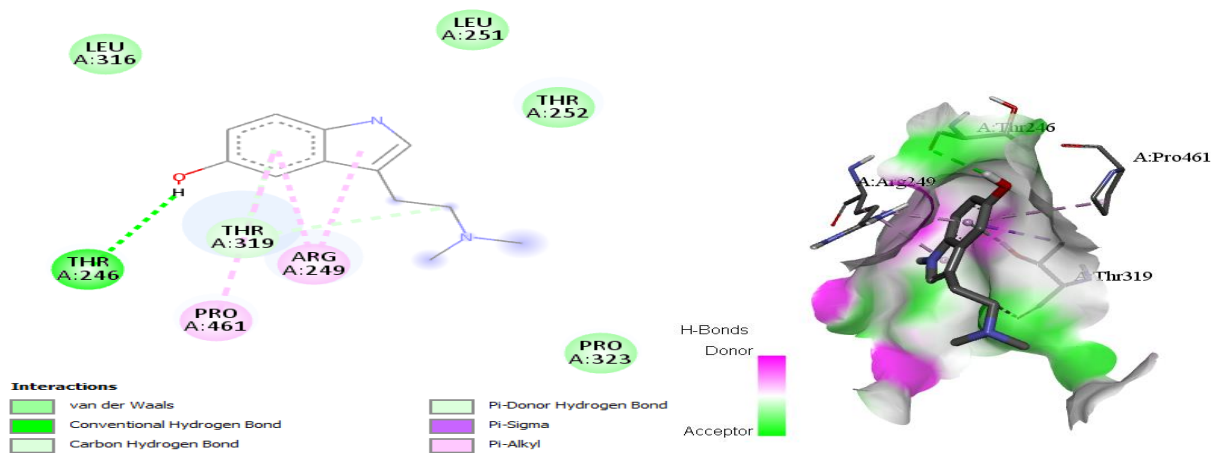


(A) 2D interaction

(B) 3D interaction

Figure 4. 8: Interaction of RdRp enzyme on **Palmatine(56)** [(A) 2D interactions (B) 3D interactions].

Bufotenin(57)



(A) 2D interaction

(B) 3D interaction

Figure 4. 9: Interaction of RdRp enzyme on **Bufotenin(57)** [(A) 2D interactions (B) 3D interactions].

Psilocybin(58)

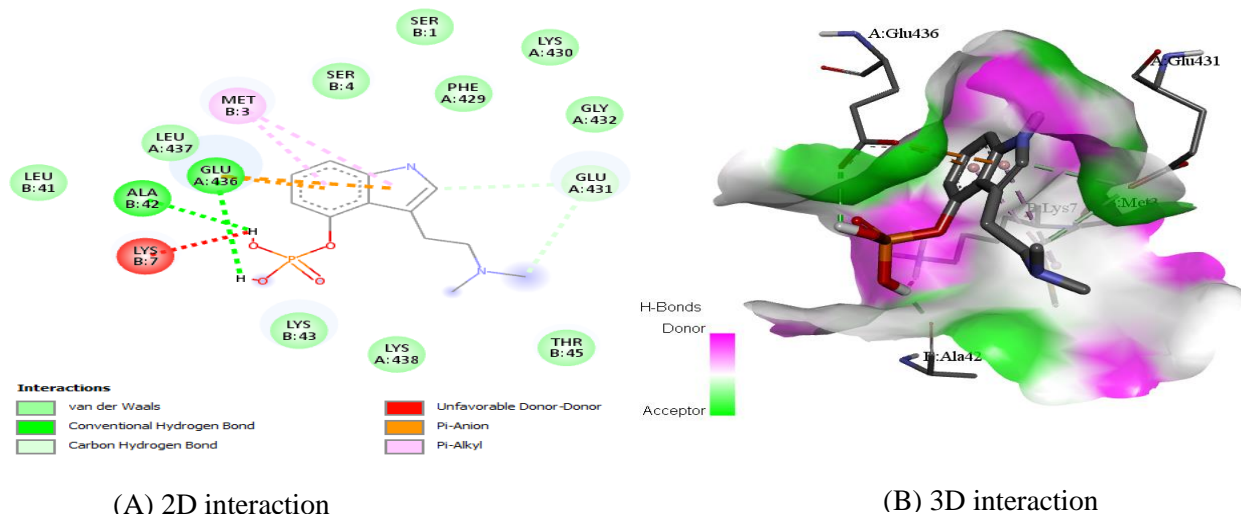


Figure 4. 10. Interaction of RdRp enzyme on **Psilocybin(58)** [(A) 2D interactions (B) 3D interactions].

Biscryptolepine(60)

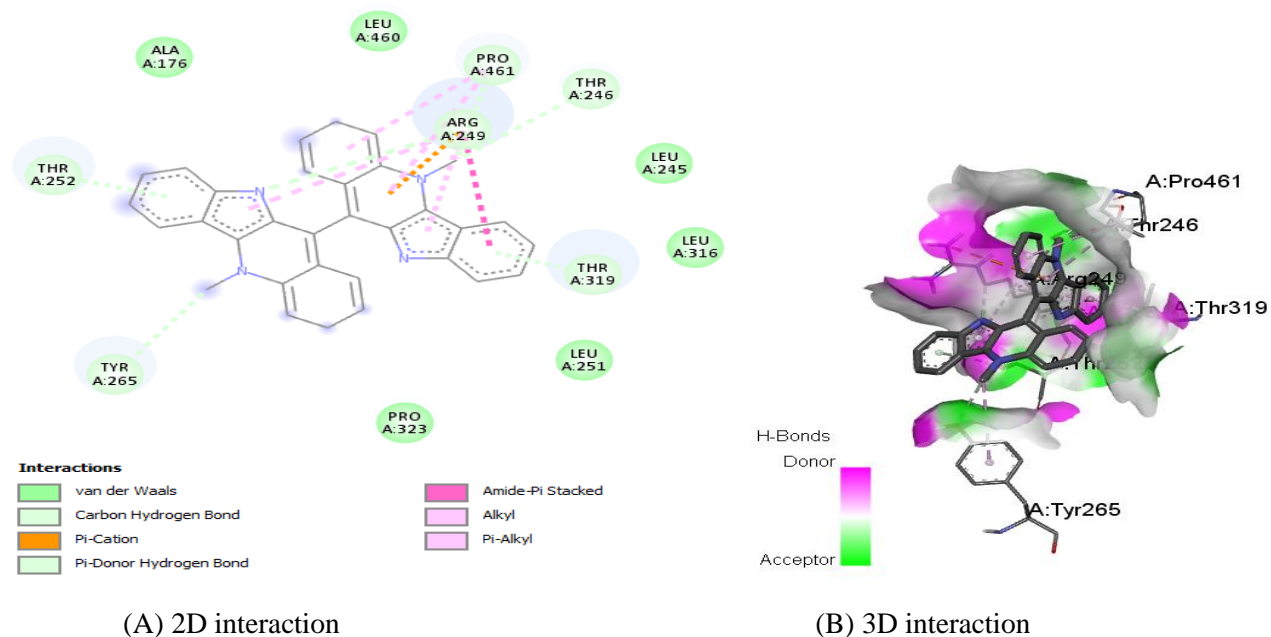


Figure 4. 11: Interaction of RdRp enzyme on **Biscryptolepine(60)** [(A) 2D interactions (B) 3D interactions].

CPD61

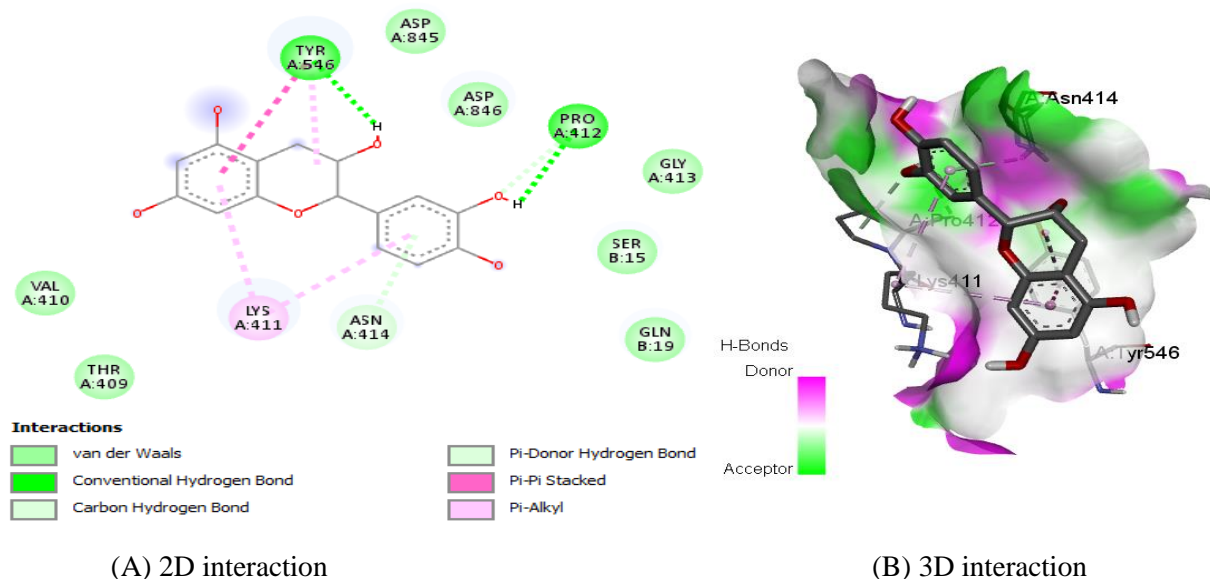


Figure 4. 12: Interaction of RdRp enzyme on CPD61 [(A) 2D interactions (B) 3D interactions].

CPD62

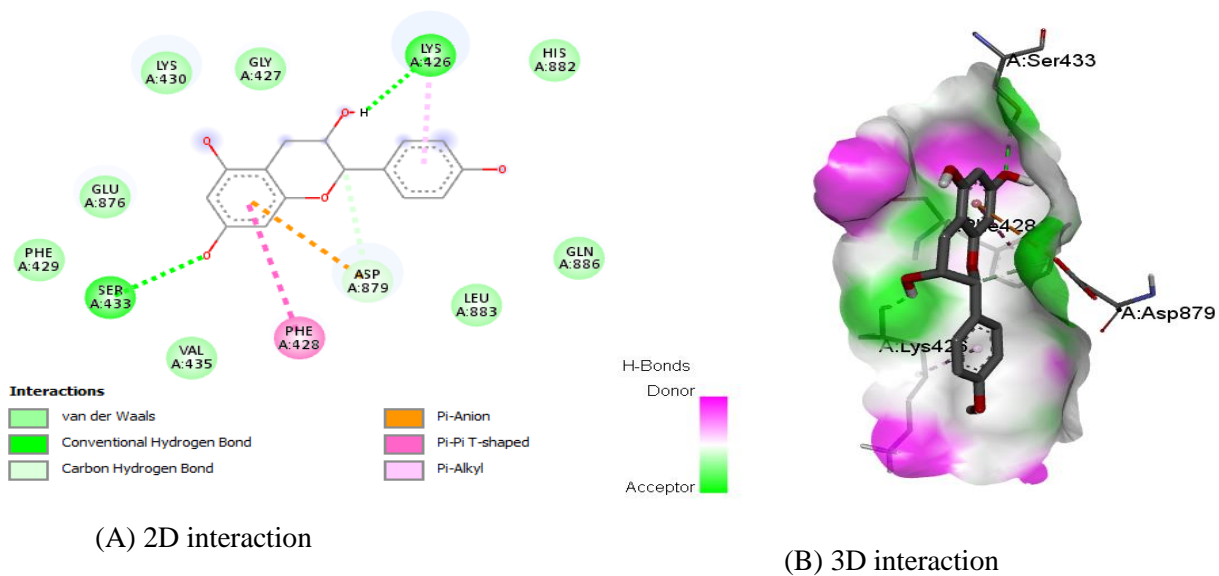


Figure 4. 13: Interaction of RdRp enzyme on CPD62 [(A) 2D interactions (B) 3D interactions].

CPD63

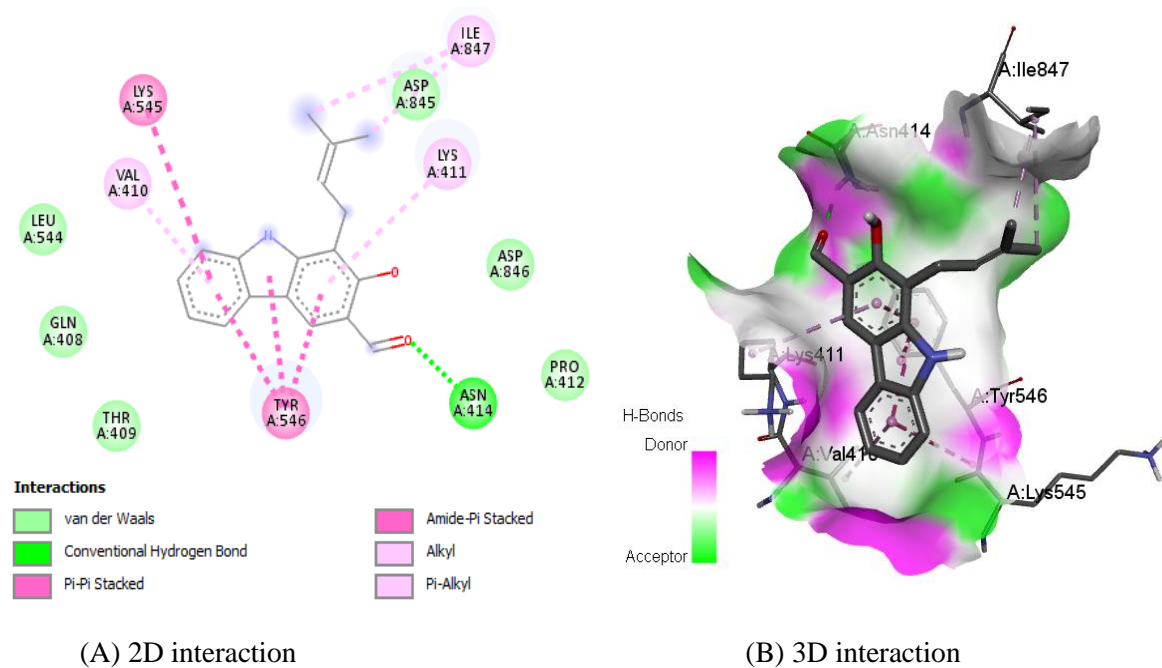


Figure 4. 14: Interaction of RdRp enzyme on **CPD63** [(A) 2D interactions (B) 3D interactions].

CPD64

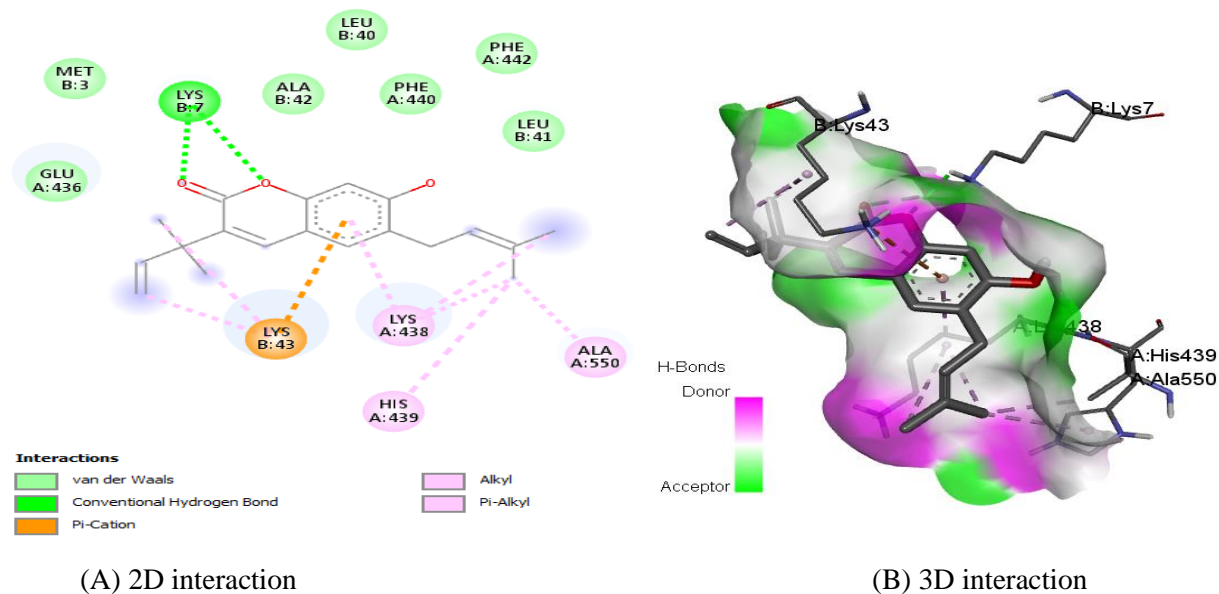


Figure 4. 15: Interaction of RdRp enzyme on **CPD64** [(A) 2D interactions (B) 3D interactions].

CPD65

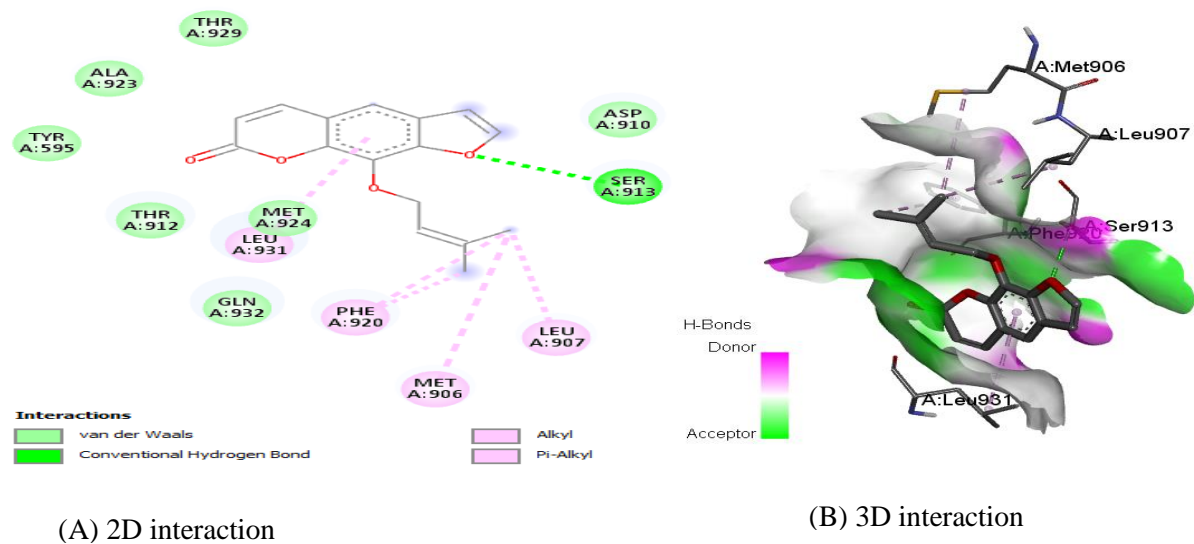


Figure 4. 16: Interaction of RdRp enzyme on **CPD65** [(A) 2D interactions (B) 3D interactions].

CPD66

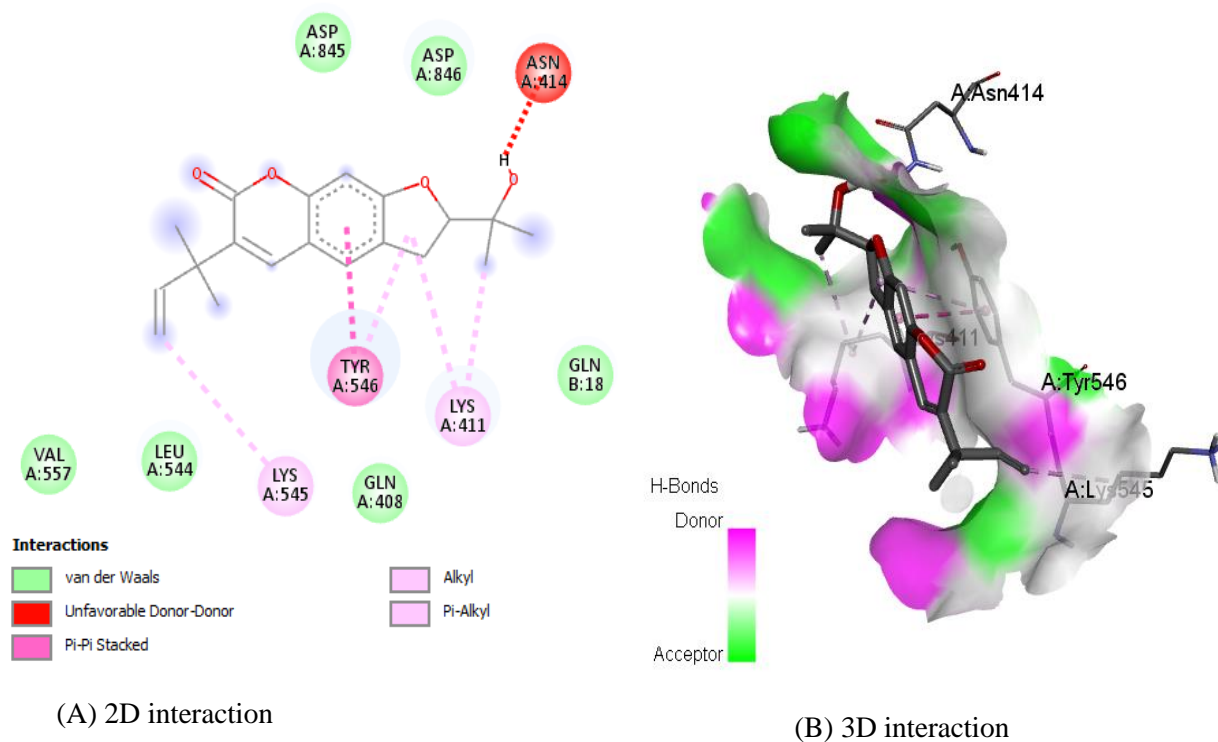
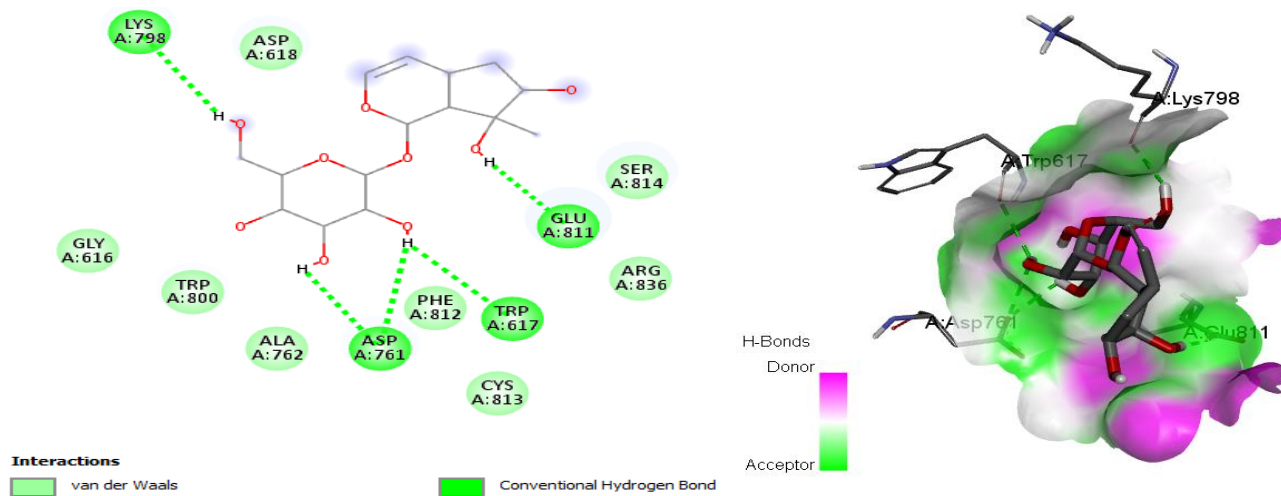


Figure 4. 17: Interaction of RdRp enzyme on **CPD66** [(A) 2D interactions (B) 3D interactions].

CPD67

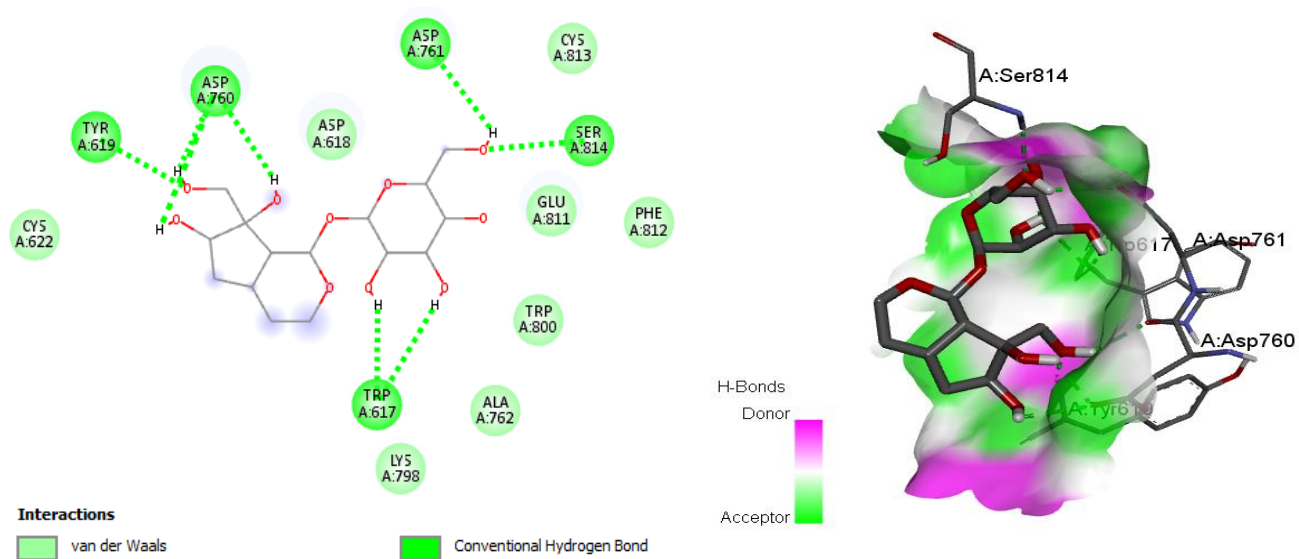


(A) 2D interaction

(B) 3D interaction

Figure 4. 18: Interaction of RdRp enzyme on **CPD67** [(A) 2D interactions (B) 3D interactions].

CPD68



(A) 2D interaction

(B) 3D interaction

Figure 4. 19: Interaction of RdRp enzyme on **CPD68** [(a) 2D interactions (b) 3D interactions].

CPD69

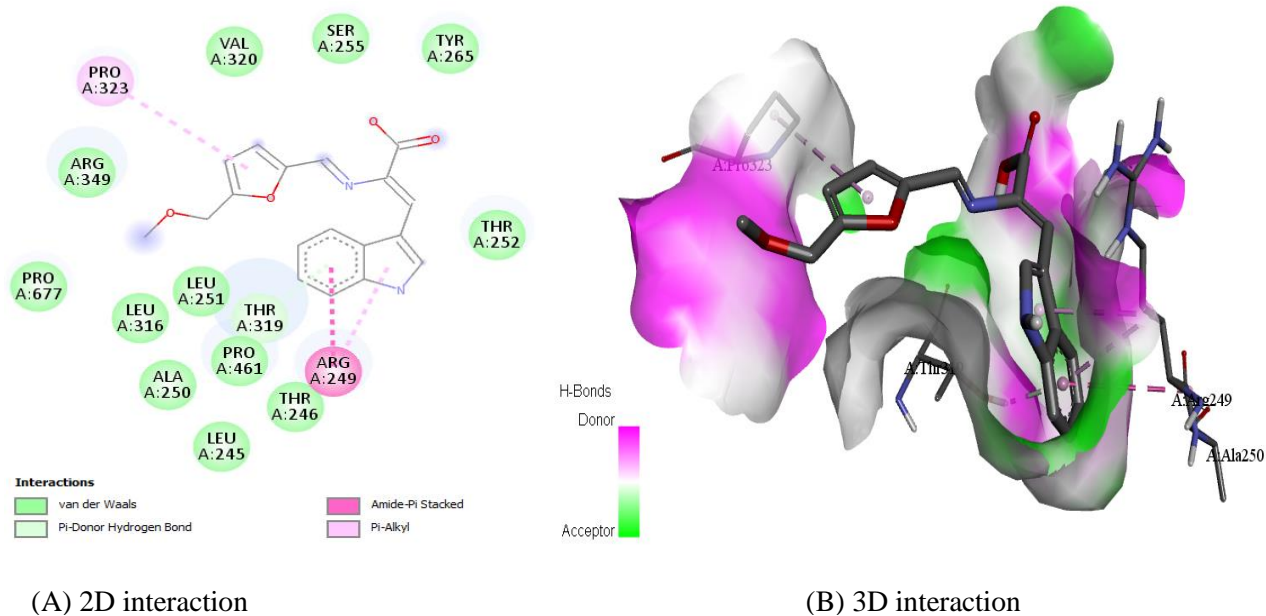


Figure 4. 20: Interaction of RdRp enzyme on **CPD69** [(A) 2D interactions (B) 3D interactions].

CPD70

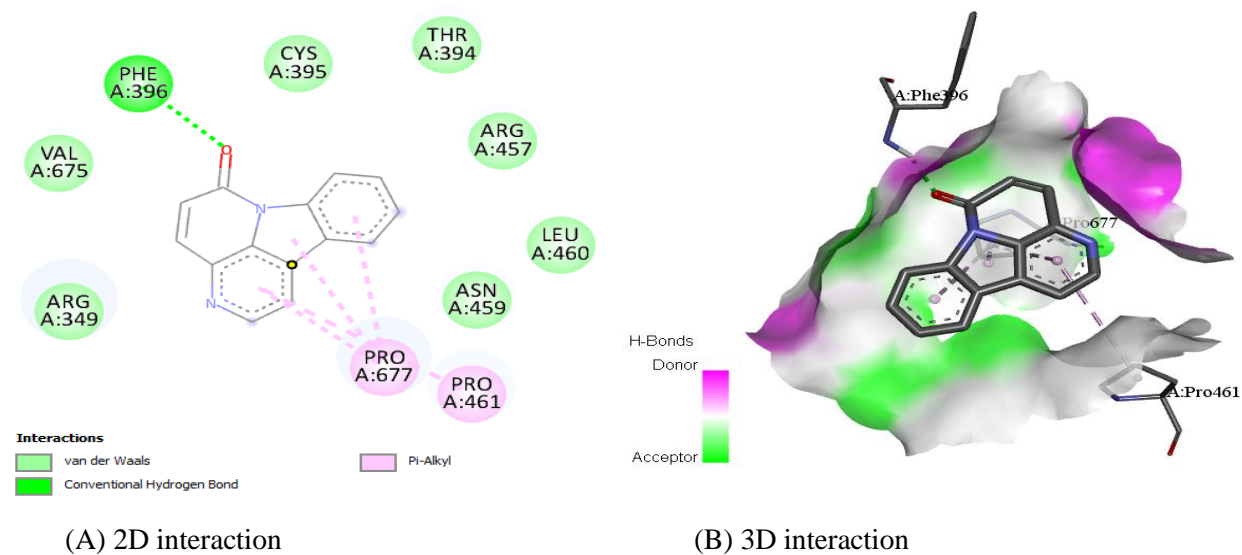


Figure 4. 21: Interaction of RdRp enzyme on **CPD70** [(A) 2D interactions (B) 3D interactions].

CPD71

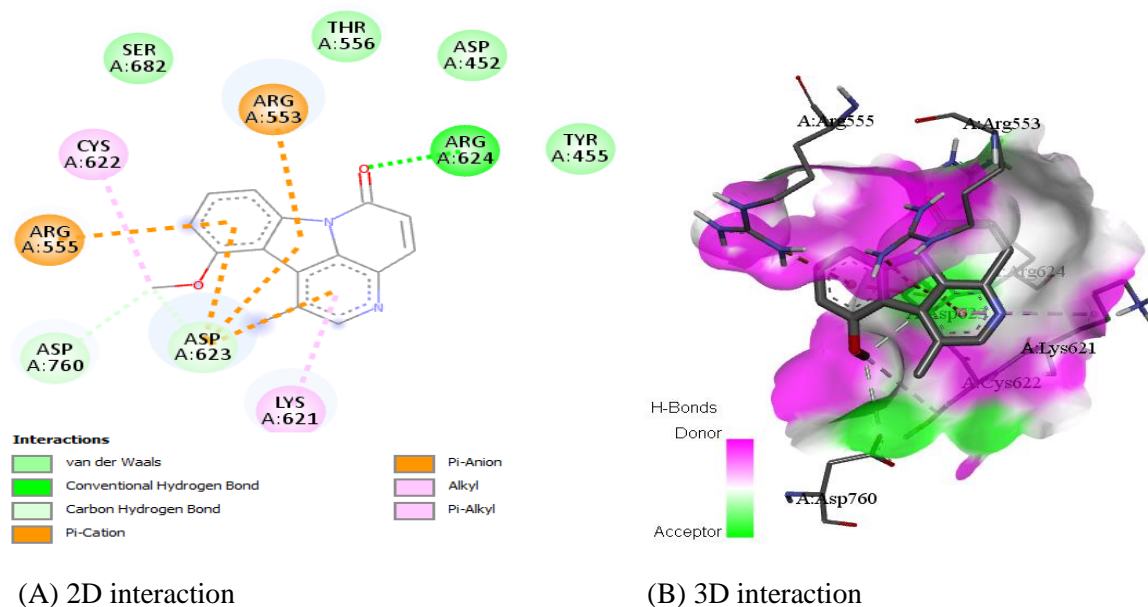


Figure 4. 22: Interaction of RdRp enzyme on CPD71 [(A) 2D interactions (B) 3D interactions].

4.2. Discussion

From the drug-likeness examination, the majority of the compounds tested obeyed Lipinski's rule of five except for nicotiflorin(59), which has three violations, 9 NHBDs (> 5), 15 NHBA (>10), and a molecular weight of 594.52 g/mol (>500 g/mol). According to Lipinski *et al.* (1997) it can be suggested that the 19 compounds of study have drug-like molecular nature.

Of the predicted physicochemical properties number of rotatable bonds, TPSA, molecular weight, and molar refractivity are based on drug absorption. The number of rotatable bonds of all studied compounds was < 6 which fulfills the criteria for good in vivo absorption of drugs by Lipinski's filter states that molecules show good GI absorption if they have ≤ 7 rotatable bonds (Ranjith and Ravikumar, 2019). All test molecules have different molecular refractivity (MR). Molecular refractivity from physicochemical properties represents the real volume of the molecules and London dispersive forces that act in the drug-receptor interaction. Of the studied molecules berbamine(52) has the highest MR value, 181.6, and bufotenin has the least, 62.6, this works similarly for the molecular weight of both molecules, 608.72 g/mol and 204.27 g/mol

respectively. The study result shows that molecular weight and molar refractivity of the molecules are in a direct relationship. Another important physicochemical property predicted is TPSA, which is a good descriptor of in vivo molecule absorption. A molecule's topological polar surface area is defined as the surface sum of all polar atoms or molecules, typically oxygen and nitrogen, as well as their connected hydrogen atoms. The molecules with a TPSA of 140 Å and above would be poorly absorbed (< 10% fractional absorption), while those below are well absorbed (Clark, 1999). TPSA value of the test compound from this study lies in a range of 34.37 to 249.2. The predicted value of it is less than 140 Å for the majority of the compounds except for nicotiflorin(59) with 249.2, CPD67 with 149.07, and CPD68 with 169.3. In agreement with GI absorption, this entails that all compounds except the above three may have good absorption properties.

Another predicted descriptor of pharmacokinetics is the P-GP substrate. P-GP (permeability glycoprotein) is found in a variety of pharmacokinetic-related organs and physical barriers, including the GI tract, the blood-brain barrier (BBB), the kidney, liver, endothelium, and the placenta (Prachayasittikul and Prachayasittikul, 2016). P-GP is good drug transporter that facilitates or renders the uptake or efflux of the drugs. P-GP substrate is a drug/compound that could be metabolized by P-GP. Pharmacokinetic prediction of 20 compounds revealed that CPD53, CPD54, CPD55, CPD56, CPD59, CPD67, and CPD68 are P-GP substrates meaning that they can be metabolized by P-GP (Hollenberg, 2002).

The skin permeability coefficient (Log Kp), is a multiple linear regression (Potts and Guy, 1992), the more negative the log Kp (with Kp in cm/s), the less skin permeant is the molecule. Skin permeability, LogKp, values found for 20 natural compounds evaluated in this study range from -10.53 to -4.26 cm/s (Table 4.3), indicating low skin permeability (Daina *et al.*, 2017).

Other important parameters from pharmacokinetics properties are CYP enzymes. CYP enzymes are a protein that catalyzes the oxidation and metabolism of a wide range of xenobiotics and endogenous chemicals and are also responsible for the bioactivation of drugs and toxicants to more reactive intermediates (Nelson, 2009). According to a previous study, CYP enzyme inhibition and induction are likely the most prevalent causes of drug interactions, which may result in toxic and undesirable side effects (Hollenberg, 2002). In the current study, the inhibition of important classes of CYP enzymes such as CYP1A2, CYP2C9, CYP2C19, CYP2D6, and

CYP3A4 was predicted for all compounds. The Swiss ADME model returns “Yes” or “No” if the compound under examination has a greater probability to be an inhibitor or non-inhibitor of Cytochrome P 450 isoenzymes (CYP1A2, CYP2c9, CYP2C19, CYP2D6, and CYP3A4). Among the studied natural compounds, berbamine(52), psilocibin(58), nicotiflorin(59), biscriptolepine(60), CPD61, CPD62, CPD67, and CPD68 have no inhibitory effect on predicted CYP enzymes, indicating no drug-drug interactions that may cause unpredicted adverse reactions (Nelson, 2009). In general, the predicted results might be useful inputs for future experimental investigations.

After the evaluations of the above exhaustive parameters of selected compounds, molecular docking was performed on 19 drug-like compounds against RdRp. But identification and characterization of the binding site should be performed before docking for more reliable and accurate molecular docking. The active sites for target-ligand binding interaction were predicted using the CASTP online bioinformatics tool. CASTP predicted active residues of the current study are the same as the predicted result in different works of literature as an active site with little distinctions by different site predicting software and molecular docking. For example, Saha *et al.* (2021) predicted a catalytic site with some same residue using CASTp software and Poustforoosh *et al.* (2021) predicted a relative binding site of RdRp using site map software.

The docking was performed in a grid map which was made on the predicted active site of RdRp. When a molecular docking simulation is run on AV, it generates a binding affinity value (kcal/mol) for each ligand, allowing the binding potential of ligands to be rated (Trott and Olson, 2010). The first pose of nine AV-generated poses is considered as optimal in all cases since it has the maximum binding affinity for the target protein. The target protein has the lowest binding affinity for the ninth pose. Based on this, the first pose and its binding affinity value were chosen for further investigation. To some extent, all the compounds interacted with the binding site of the target protein having minimum binding energy ranging from -5.3 to -9.0 Kcal/mol (Table 3.1). However, out of 20 compounds, nine compounds such as biscriptolepin (60), berbamin(52), CPD(63), Jatrorrhizine(55), Dicentrin(53) and (CPD(66), CPD(69), and CPD(70)) tightly bound and showed the best docking score of -9.0 kcal/mol, -8.8 kcal/mol, -8.2 kcal/mol, -7.7 kcal/mol, -7.4 kcal/mol, -7.1 kcal/mol and -6.8 kcal/mol, respectively, which is

better than that of remdesivir(-6.7 kcal/mol) suggesting that they can inhibit RdRp of SARS CoV-2).

From the interaction analysis, the main kind of interaction for all complexes is van der Waals interaction. The hydrogen bond and hydrophobic interactions between active substances and their receptors mainly stabilize the interaction. Studied compounds showed significant H-bond interactions with amino acid residues (Table 4.5), demonstrating a strong affinity between them except for CPD66 and CPD69. Detailed interaction analysis revealed that the complexes were stabilized by a variety of interactions. Also, some compounds interact with RdRp by electrostatic interaction including pi-anion and pi-cation. Unfavorable (donor-acceptor/acceptor - donor) interaction was also found between Dicentrin(53), psilocybin(58), and CPD66. The result indicated that amino acids only from chain A are involved in the interaction with all compounds except Psilocybin(58), and CPD64, which interacted with some residue from chain B. The ligands have a different binding lengths on protein, according to molecular interactions.

The docking and interaction pattern of the ligand molecules considered in the current study indicates that they are capable of interacting with the protein's catalytic region, limiting RdRp activity and preventing viral multiplication and transcription. Among the top nine poses berbamin(52) has hydrogen bonds with Arg-249, THR-319 and ARG-457 with bond length 3.01, 3.66 and 3.12 Å, Jatrorrhizine(55) has hydrogen bonds with ARG-349 and ARG-457 with bond length 3.32 and 3.57 and Dicentrin(53) has hydrogen bonds with ASN-414, SER-15 and B: GLN-18 with bond length 2.71, 3.53 and 3.48 Å respectively it has been reported that these compounds having a potential to reduce viral replication on previous SARS-CoVs by intercalating nucleic acid (Schmeller *et al.*, 1997; Wink, 2007). These interactions indicate the importance and impact of natural products on RdRp. The high affinity of biscriptolepin(60), berbamin(52), CPD63, Jatrorrhizine(55), Dicentrin(53), CPD61, and CPD66, CPD69, CPD70, to the active site of RNA-dependent RNA-polymerase gives us proof of the high potential anti-RdRP activity of these natural products to be further examined for the treatment of coronaviruses. Finally from toxicity evaluation of the compounds which show better binding energy than the control and have polar interaction, Biscryptolepine(60) and CPD61 (with zero toxicological endpoints), and CPD63 and CPD70 (with one toxicological endpoint) can be suggested may be suggested as a safe and potential inhibitor of RdRp.

CHAPTER FIVE

5. CONCLUSION AND RECOMMENDATIONS

5.1. Conclusion

To support the scientific community in the COVID-19 battle, the current study was designed to examine the potential of twenty selected natural compounds targeting RdRp of SARS CoV-2. The drug-likeness, physicochemical, pharmacokinetic, toxicity prediction, and molecular docking results of these natural compounds and one control drug (remdesivir) were presented. Out of them, only nicotiflorine(59) violates Lipinski's rule of five (Ro5), hence docking was performed on all except it. The study result revealed that natural compounds, biscriptolepin(60), berbamin(52), CPD63, Jatrorrhizine(55), Dicentrin(53), CPD61, and CPD66, CPD69, and CPD70, had better binding energies with the RdRp enzyme of SARS-CoV-2 than the control with good absorption.

From toxicity profile prediction LD50 values varied from 96 to 89470 mg/Kg. Acute toxicity predictions revealed that the compounds under consideration are not fatal; rather, they can be classified as nontoxic to harmful toxic classes, with dicentrin(53), coptisine (54), and palmatine (56) active for all predicted toxicological endpoints and psilocybin (58), biscriptolepine(60), CPD61, CPD62, CPD68, and CPD69 active for none.

Overall, the current study found that four of the investigated compounds, Biscriptolepine(60) and CPD61(C₁₅H₁₄O₆) with zero toxicological endpoints, and CPD63 (C₁₈H₁₇NO₂), and CPD70(C₁₄H₈N₂O) with one toxicological endpoint and high absorption have the ability to act as antiviral agents, preventing the virus from replicating.

5.2. Recommendations

In this study, molecular docking and ADMET study of some selected natural products in comparison with remdesivir were presented. The study result revealed some natural products have better binding energy than the control with less toxicity, hence hereby we recommend the following points to be further done on them such as:

- Molecular dynamics simulation is further to be done to assure their bonding strength on the active site of RdRp and stability of the complex.
- Since they show better binding affinity on the active site of RdRp suggesting they may be a good inhibitor of selected enzyme even better than remdesivir evaluation of their therapeutic potential is recommended.
- In general, these are only preliminary screening results to help in subsequent tests, which will begin with in vitro and in vivo research (in animal models or human clinical trials). Further in vitro and in vivo therapeutic testing of these products on COVID-19 is recommended.

RESEARCH FUND ACKNOWLEDGEMENT

This research project is funded by Adama Science and Technology University under the grant number ASTU/SM-R/553/22, Adama, Ethiopia.

REFERENCES

- Abubakar, M. B., Usman, D., Batiha, G. E.-S., Cruz-Martins, N., Malami, I., Ibrahim, K. G., Abubakar, B., Bello, M. B., Muhammad, A., & Gan, S. H. (2021). Natural products modulating angiotensin-converting enzyme 2 (ACE2) as potential COVID-19 therapies. *Frontiers in Pharmacology*, *12*.
- Alemu Tewabech, Shenkute Kebede, Eswaramoorthy, R., Girmay Solomon, Melaku Yadessa, & Endale Milkyas. (2020). Molecular docking analysis of antibacterial indole alkaloids from roots of *Brucea antidysentrica*. *Ethiopian Journal of Sciences and Sustainable Development*, *7(2)*, 1-13.
- Alfaro, M., Alfaro, I., & Angel, C. (2020). Identification of potential inhibitors of SARS-CoV-2 papain-like protease from tropane alkaloids from *Schizanthus porrigens*: A molecular docking study. *Chem Phys Lett*, *761*, 138068. <https://doi.org/10.1016/j.cplett.2020.138068>
- Assefa Etagegnehu, Alemayhu Israel, Endale Milkyas, & Mammo Fikre. (2016). Iridoid glycosides from the root of *Acanthus sennii*. *Journal of Pharmacy & Pharmacognosy Research*, *4(6)*, 231-237.
- Atanasov, A. G., Zotchev, S. B., Dirsch, V. M., & Supuran, C. T. (2021). Natural products in drug discovery: advances and opportunities. *Nature Reviews Drug Discovery*, *20(3)*, 200-216.
- Azam, S. S., & Abbasi, S. W. (2013). Molecular docking studies for the identification of novel melatonergic inhibitors for acetylserotonin-O-methyltransferase using different docking routines. *Theoretical Biology and Medical Modelling*, *10(1)*, 1-16.
- Banerjee, P., Eckert, A. O., Schrey, A. K., & Preissner, R. (2018). ProTox-II: a webserver for the prediction of toxicity of chemicals. *Nucleic acids research*, *46(W1)*, W257-W263. <https://doi.org/10.1093/nar/gky318>
- Basu, A., Sarkar, A., & Maulik, U. (2020). Molecular docking study of potential phytochemicals and their effects on the complex of SARS-CoV2 spike protein and human ACE2. *Sci Rep*, *10(1)*, 17699. <https://doi.org/10.1038/s41598-020-74715-4>

- Bell, E. W., & Zhang, Y. (2019). DockRMSD: an open-source tool for atom mapping and RMSD calculation of symmetric molecules through graph isomorphism. *Journal of cheminformatics*, *11*(1), 1-9.
- Berman, H. M., Henrick, K., & Nakamura, H. (2003). Announcing the worldwide Protein Data Bank Nature Structural Biology *10*(12), 980.
- Bindom, S. M., & Lazartigues, E. (2009). The sweeter side of ACE2: physiological evidence for a role in diabetes. *Molecular and cellular endocrinology*, *302*(2), 193-202.
- Bissantz, C., Folkers, G., & Rognan, D. (2000). Protein-based virtual screening of chemical databases. 1. Evaluation of different docking/scoring combinations. *Journal of medicinal chemistry*, *43*(25), 4759-4767.
- Borquaye, L. S., Gasu, E. N., Ampomah, G. B., Kyei, L. K., Amarh, M. A., Mensah, C. N., Nartey, D., Commodore, M., Adomako, A. K., & Acheampong, P. (2020). Alkaloids from *Cryptolepis sanguinolenta* as potential inhibitors of SARS-CoV-2 viral proteins: an in silico study. *BioMed research international*, 2020.
- Burrell, C. J., Howard, C. R., & Murphy, F. A. (2016). *Fenner and White's medical virology*. Academic Press.
- Ccsb-Scripps. (2021a). *AutoDock-vina/docking_flexible.RST at Develop · CCSB-Scripps/Autodock-Vina*. GitHub. Retrieved on 29-April-2022 from https://github.com/ccsb-scripps/AutoDock-Vina/blob/develop/docs/source/docking_flexible.rst
- Ccsb-Scripps. (2021b). *AutoDock-Vina/introduction.rst at Develop · CCSB-Scripps/Autodock-Vina*. GitHub. Retrieved on 29-April-2022 from <https://github.com/ccsb-scripps/AutoDock-Vina/blob/develop/docs/source/introduction.rst>
- CDC. (2021). *Older adults risks and vaccine information*. Centers for Disease Control and Prevention. Retrieved on 12-January-2022 from <https://www.cdc.gov/aging/covid19/covid19-older-adults.html>
- CDC. (2022a). *Symptoms of COVID-19*. Centers for Disease Control and Prevention. Retrieved on 27-march-2022 from <https://www.cdc.gov/coronavirus/2019-ncov/symptoms-testing/symptoms.html>
- CDC. (2022b). *Underlying medical conditions associated with higher risk for severe COVID-19: Information for Healthcare professionals*. Centers for Disease Control and Prevention.

- Retrieved on 17-February-2022 from <https://www.cdc.gov/coronavirus/2019-ncov/hcp/clinical-care/underlyingconditions.html>
- Chakravarti, R., Singh, R., Ghosh, A., Dey, D., Sharma, P., Velayutham, R., Roy, S., & Ghosh, D. (2021). A review on potential of natural products in the management of COVID-19. *RSC Advances*, *11*(27), 16711-16735.
- Chen, H., & Du, Q. (2020). Potential natural compounds for preventing SARS-CoV-2 (2019-nCoV) infection.
- Clark, D. E. (1999). Rapid calculation of polar molecular surface area and its application to the prediction of transport phenomena. 1. Prediction of intestinal absorption. *Journal of pharmaceutical sciences*, *88*(8), 807-814.
- Cragg, G. M., & Newman, D. J. (2013). Natural products: A continuing source of novel drug leads. *Biochim. Biophys. Acta - Gen. Subj*, *1830*(60), p. 3670-3695.
- Da Silva, F. M. A., Da Silva, K. P. A., De Oliveira, L. P. M., Costa, E. V., Koolen, H. H., Pinheiro, M. L. B., De Souza, A. Q. L., & De Souza, A. D. L. (2020). Flavonoid glycosides and their putative human metabolites as potential inhibitors of the SARS-CoV-2 main protease (Mpro) and RNA-dependent RNA polymerase (RdRp). *Memórias do Instituto Oswaldo Cruz*, *115*.
- Daina, A., Michielin, O., & Zoete, V. (2017). SwissADME: a free web tool to evaluate pharmacokinetics, drug-likeness and medicinal chemistry friendliness of small molecules. *Scientific Reports*, *7*(1), 1-13.
- Dias, D. A., Urban, S., & Roessner, U. (2012). A Historical overview of natural products in drug discovery. *Metabolites*, *2*(2), p. 303–336.
- Dong, Y., Shamsuddin, A., Campbell, H., & Theodoratou, E. (2021). Current COVID-19 treatments: Rapid review of the literature. *Journal of global health*, *11*.
- Drwal, M. N., Banerjee, P., Dunkel, M., Wettig, M. R., & Preissner, R. (2014). ProTox: a web server for the in silico prediction of rodent oral toxicity. *Nucleic acids research*, *42*(W1), W53-W58.
- Edwards, K. M., & Orenstein, W. A. (2022). COVID-19: Vaccines. *Up To Date*. <https://www.uptodate.com/contents/covid-19-vaccines>.
- Fattorusso, E., & Tagliatela-Scafati, O. (2007). *Modern alkaloids: structure, isolation, synthesis, and biology*. John Wiley & Sons.

- Garg, S., Anand, A., Lamba, Y., & Roy, A. (2020). Molecular docking analysis of selected phytochemicals against SARS-CoV-2 M(pro) receptor. *Vegetos*, 33(4), 766-781. <https://doi.org/10.1007/s42535-020-00162-1>
- Gordon, D., Jang, G., Bouhaddou, M., Xu, J., Obernier, K., & White, K. (2020). O' Meara MJ, Rezelj VV, Guo JZ, Swaney DL, et al: A SARS-CoV-2 protein interaction map reveals targets for drug repurposing. *nature*, 583, 459-468.
- Guex, N., & Peitsch, M. C. (1997). SWISS-MODEL and the Swiss-Pdb Viewer: an environment for comparative protein modeling. *electrophoresis*, 18(15), 2714-2723.
- Guyasa Babe, Melaku Yadessa, & Endale Milkyas. (2018). Antibacterial activity of two flavans from the stem bark of *Embelia schimperi*. *Advances in Pharmacological Sciences*, 2018.
- Harapan, H., Itoh, N., Yufika, A., Winardi, W., Keam, S., Te, H., Megawati, D., Hayati, Z., Wagner, A. L., & Mudatsir, M. (2020). Coronavirus disease 2019 (COVID-19): A literature review. *Journal of infection and public health*, 13(5), 667-673.
- Hernández-Santoyo, A., Tenorio-Barajas, A. Y., Altuzar, V., Vivanco-Cid, H., & Mendoza-Barrera, C. (2013). Protein-protein and protein-ligand docking. *Protein engineering-technology and application*, 63-81.
- Hesse, M. (2002). *Alkaloids: Nature's curse or blessing?* John Wiley & Sons.
- Hoffmann, M., Kleine-Weber, H., Schroeder, S., Krüger, N., Herrler, T., Erichsen, S., Schiergens, T. S., Herrler, G., Wu, N.-H., & Nitsche, A. (2020). SARS-CoV-2 cell entry depends on ACE2 and TMPRSS2 and is blocked by a clinically proven protease inhibitor. *cell*, 181(2), 271-280. e278.
- Hollenberg, P. F. (2002). Characteristics and common properties of inhibitors, inducers, and activators of CYP enzymes. *Drug metabolism reviews*, 34(1-2), 17-35.
- Hu, B., Guo, H., Zhou, P., & Shi, Z.-L. (2021). Characteristics of SARS-CoV-2 and COVID-19. *Nature Reviews Microbiology*, 19(3), 141-154.
- Huang, C., Wang, Y., Li, X., Ren, L., Zhao, J., Hu, Y., Zhang, L., Fan, G., Xu, J., Gu, X., Cheng, Z., Yu, T., Xia, J., Wei, Y., Wu, W., Xie, X., Yin, W., Li, H., Liu, M., Xiao, Y., Gao, H., Guo, L., Xie, J., Wang, G., Jiang, R., Gao, Z., Jin, Q., Wang, J., & Cao, B. (2020). Clinical features of patients infected with 2019 novel coronavirus in Wuhan, China. *The lancet*, 395(10223), 497-506. [https://doi.org/10.1016/S0140-6736\(20\)30183-5](https://doi.org/10.1016/S0140-6736(20)30183-5)

- Huey, R., Morris, G. M., & Forli, S. (2012). Using AutoDock 4 and AutoDock vina with AutoDockTools: a tutorial. *The Scripps Research Institute Molecular Graphics Laboratory*, 10550, 92037.
- Hui, D. S., Azhar, E. I., Madani, T. A., Ntoumi, F., Kock, R., Dar, O., Ippolito, G., Mchugh, T. D., Memish, Z. A., & Drosten, C. (2020). The continuing 2019-nCoV epidemic threat of novel coronaviruses to global health—The latest 2019 novel coronavirus outbreak in Wuhan, China. *International journal of infectious diseases*, 91, 264-266.
- Imai, Y., Kuba, K., Ohto-Nakanishi, T., & Penninger, J. M. (2010). Angiotensin-converting enzyme 2 (ACE2) in disease pathogenesis. *Circulation Journal*, 74(3), 405-410.
- Ishikawa, Y. (2017). *Add missing residues*. ResearchGate. Retrieved on 13-February-2022 from <https://www.researchgate.net/post/Add-missing-residues/59677b4d48954ca8de05a7a2/citation/download>.
- John, R. H., & Philip, D. H. (2021). *Get to know an enzyme: CYP1A2*. Pharmacy Times. Retrieved on 03-May-2022 from <https://www.pharmacytimes.com/view/2007-11-8279>
- Kaapro, A., & Ojanen, J. (2002). Protein docking. URL <http://www.lce.hut.fi/teaching/S-114.500/k2002/Protodock.pdf>.
- Kanehisa, M., Goto, S., Hattori, M., Aoki-Kinoshita, K. F., Itoh, M., Kawashima, S., Katayama, T., Araki, M., & Hirakawa, M. (2006). From genomics to chemical genomics: new developments in KEGG. *Nucleic acids research*, 34(suppl_1), D354-D357.
- Kim, C.-H. (2021). Anti-SARS-CoV-2 natural products as potentially therapeutic agents. *Frontiers in Pharmacology*, 12.
- Kim, D., Lee, J.-Y., Yang, J.-S., Kim, J. W., Kim, V. N., & Chang, H. (2020). The architecture of SARS-CoV-2 transcriptome. *cell*, 181(4), 914-921. e910.
- Kim, S., Chen, J., Cheng, T., Gindulyte, A., He, J., He, S., Li, Q., Shoemaker, B. A., Thiessen, P. A., Yu, B., Zaslavsky, L., Zhang, J., & Bolton, E. E. (2021). PubChem in 2021: new data content and improved web interfaces. *Nucleic acids research*, 49(D1), D1388-D1395. <https://doi.org/10.1093/nar/gkaa971>
- Kramer, A., Schwebke, I., & Kampf, G. (2006). How long do nosocomial pathogens persist on inanimate surfaces? A systematic review. *BMC infectious diseases*, 6(1), 1-8.
- Kuba, K., Imai, Y., & Penninger, J. M. (2006). Angiotensin-converting enzyme 2 in lung diseases. *Current opinion in pharmacology*, 6(3), 271-276.

- Kumar, S., Nyodu, R., Maurya, V. K., & Saxena, S. K. (2020). Morphology, genome organization, replication, and pathogenesis of severe acute respiratory syndrome coronavirus 2 (SARS-CoV-2). In *Coronavirus Disease 2019 (COVID-19)* (pp. 23-31). Springer.
- Kuntz, I. D. (1992). Structure-based strategies for drug design and discovery. *Science*, 257(5073), 1078-1082.
- Letko, M., Marzi, A., & Munster, V. (2020). Functional assessment of cell entry and receptor usage for SARS-CoV-2 and other lineage B betacoronaviruses. *Nat Microbiol.* 2020; 5: 562–9. In: PUBMED.
- Lipinski, C. A., Lombardo, F., Dominy, B. W., & Feeney, P. J. (1997). Experimental and computational approaches to estimate solubility and permeability in drug discovery and development settings. *Advanced drug delivery reviews*, 23(1-3), 3-25.
- Liu, C., Zhou, Q., Li, Y., Garner, L. V., Watkins, S. P., Carter, L. J., Smoot, J., Gregg, A. C., Daniels, A. D., & Jervey, S. (2020). Research and development on therapeutic agents and vaccines for COVID-19 and related human coronavirus diseases. In: ACS Publications.
- Liu, H., Jiang, Y., Li, M., Yu, X., Sui, D., & Fu, L. (2019). Ginsenoside Rg3 attenuates angiotensin II-mediated renal injury in rats and mice by upregulating angiotensin-converting enzyme 2 in the renal tissue. *Evidence-based Complementary and Alternative Medicine*, 2019.
- Lokhande, K. B., Doiphode, S., Vyas, R., & Swamy, K. V. (2021). Molecular docking and simulation studies on SARS-CoV-2 Mpro reveals Mitoxantrone, Leucovorin, Birinapant, and Dynasore as potent drugs against COVID-19. *Journal of Biomolecular Structure and Dynamics*, 39(18), 7294-7305.
- Lu, R., Zhao, X., Li, J., Niu, P., Yang, B., Wu, H., Wang, W., Song, H., Huang, B., & Zhu, N. (2020). Genomic characterisation and epidemiology of 2019 novel coronavirus: implications for virus origins and receptor binding. *The lancet*, 395(10224), 565-574.
- Lucas-Gómez, I., López-Fernández, A., González-Pérez, B. K., Andrea, M., Calderón, A. V., & Gayosso-Morales, M. A. (2020). Docking study for Protein Nsp-12 of SARS-CoV with Betalains and Alfa-Bisabolol. *arXiv preprint arXiv:2012.14504*.

- Malami, I., Abdul, A. B., Abdullah, R., Bt Kassim, N. K., Waziri, P., & Christopher Etti, I. (2016). In silico discovery of potential uridine-cytidine kinase 2 inhibitors from the rhizome of *Alpinia mutica*. *Molecules*, *21*(4), 417.
- Manhas, A. (2016). *Docking and missing residues of proteins?* ResearchGate. Retrieved 29-March-2022 from https://www.researchgate.net/post/Docking_and_missing_residues_of_proteins/57f0c0605b4952b619341b21/citation/download.
- Marchan, J. (2020). Conserved HLA binding peptides from five non-structural proteins of SARS-CoV-2—An in silico glance. *Human immunology*, *81*(10-11), 588-595.
- Mendelsohn, L. D. (2004). ChemDraw 8 Ultra, Windows and Macintosh Versions. *Journal of chemical information and computer sciences*, *44*(6), 2225-2226. <https://doi.org/10.1021/ci040123t>
- Morris, G. M., & Lim-Wilby, M. (2008). Molecular docking. In *Molecular modeling of proteins* (pp. 365-382). Springer.
- Morris, G. M., & Lim-Wilby, M. (2009). AutoDock4 and AutoDockTools4: Automated docking with selective receptor flexibility. *Journal of computational chemistry*, *30*(16).
- Müller, C., Schulte, F. W., Lange-Grünweller, K., Obermann, W., Madhugiri, R., Pleschka, S., Ziebuhr, J., Hartmann, R. K., & Grünweller, A. (2018). Broad-spectrum antiviral activity of the eIF4A inhibitor silvestrol against corona-and picornaviruses. *Antiviral research*, *150*, 123-129.
- Nelson, D. R. (2009). The cytochrome p450 homepage. *Human genomics*, *4*(1), 1-7.
- O'Boyle, N. M., Banck, M., James, C. A., Morley, C., Vandermeersch, T., & Hutchison, G. R. (2011). Open Babel: An open chemical toolbox. *Journal of cheminformatics*, *3*(1), 33. <https://doi.org/10.1186/1758-2946-3-33>
- Ohashi, H., Watashi, K., Saso, W., Shionoya, K., Iwanami, S., Hirokawa, T., Shirai, T., Kanaya, S., Ito, Y., & Kim, K. S. (2020). Multidrug treatment with nelfinavir and cepharanthine against COVID-19. *bioRxiv*.
- Okpara, M., & Jamabo, M. (2020). Understanding COVID-19 - A Molecular Perspective.
- Pandeya, K. B., Ganeshpurkar, A., & Mishra, M. K. (2020). Natural RNA dependent RNA polymerase inhibitors: Molecular docking studies of some biologically active alkaloids of

- Argemone mexicana. *Med Hypotheses*, 144, 109905.
<https://doi.org/10.1016/j.mehy.2020.109905>
- Panyatip, P., Nunthaboot, N., & Puthongking, P. (2020). In Silico ADME, Metabolism Prediction and Hydrolysis Study of Melatonin Derivatives. *International Journal of Tryptophan Research*, 13, 1178646920978245.
- Pathak, M., Ojha, H., Tiwari, A. K., Sharma, D., Saini, M., & Kakkar, R. (2017). Design, synthesis and biological evaluation of antimalarial activity of new derivatives of 2, 4, 6-s-triazine. *Chemistry Central Journal*, 11(1), 1-11.
- Peiris, J. S., Yuen, K. Y., Osterhaus, A. D., & Stöhr, K. (2003). The severe acute respiratory syndrome. *New England journal of medicine*, 349(25), 2431-2441.
- Poustforoosh, A., Hashemipour, H., Tüzün, B., Pardakhty, A., Mehrabani, M., & Nematollahi, M. H. (2021). Evaluation of potential anti-RNA-dependent RNA polymerase (RdRP) drugs against the newly emerged model of COVID-19 RdRP using computational methods. *Biophysical chemistry*, 272, 106564.
- Prachayasittikul, V., & Prachayasittikul, V. (2016). P-glycoprotein transporter in drug development. *EXCLI journal*, 15, 113.
- Rahman, S., Rahman, M. M., Miah, M., Begum, M. N., Sarmin, M., Mahfuz, M., Hossain, M. E., Rahman, M. Z., Chisti, M. J., & Ahmed, T. (2022). COVID-19 reinfections among naturally infected and vaccinated individuals. *Scientific Reports*, 12(1), 1-10.
- Ramawat, K. G. (2009). Herbal Drugs: Ethnomedicine to Modern Medicine. *Springer-Verlag: Berlin, Heidelberg, Germany*, 22, p. 32.
- Ranjith, D., & Ravikumar, C. (2019). SwissADME predictions of pharmacokinetics and drug-likeness properties of small molecules present in *Ipomoea mauritiana* Jacq. *Journal of Pharmacognosy and Phytochemistry*, 8(5), 2063-2073.
- Rashid, M. A. (2013). Recent trends in natural product research and Bangladesh perspective. *Biochem Pharmacol*, 2(5), p. 179.
- Sadeghi, M., Moradi, M., Madanchi, H., & Johari, B. (2021). In silico study of garlic (*Allium sativum* L.)-derived compounds molecular interactions with α -glucosidase. *In Silico Pharmacology*, 9(1), 1-8.
- Saha, S., Nandi, R., Vishwakarma, P., Prakash, A., & Kumar, D. (2021). Discovering Potential RNA Dependent RNA Polymerase Inhibitors as Prospective Drugs Against COVID-19:

- An in silico Approach. *Front Pharmacol*, 12, 634047.
<https://doi.org/10.3389/fphar.2021.634047>
- Satarker, S., & Nampoothiri, M. (2020). Structural proteins in severe acute respiratory syndrome coronavirus-2. *Archives of medical research*, 51(6), 482-491.
- Schmeller, T., Latz-Brüning, B., & Wink, M. (1997). Biochemical activities of berberine, palmatine and sanguinarine mediating chemical defence against microorganisms and herbivores. *Phytochemistry*, 44(2), 257-266.
- Schrödinger, L., & DeLano, W. (2020). *PyMOL*. Retrieved from <http://www.pymol.org/pymol>
- Selvaraj, J., Rekha, U. V., Jh, S. F., Sivabalan, V., Ponnulakshmi, R., Vishnupriya, V., Kullappan, M., Sreekandan, R. N., & Mohan, S. K. (2021). Molecular docking analysis of SARS-CoV-2 linked RNA dependent RNA polymerase (RdRp) with compounds from *Plectranthus amboinicus*. *Bioinformation*, 17(1), 167-170.
<https://doi.org/10.6026/97320630017167>
- Shin, J. S., Jung, E., Kim, M., Baric, R. S., & Go, Y. Y. (2018). Saracatinib inhibits middle east respiratory syndrome-coronavirus replication in vitro. *Viruses*, 10(6), 283.
- Sousa, S. F., Fernandes, P. A., & Ramos, M. J. (2006). Protein–ligand docking: current status and future challenges. *Proteins: Structure, Function, and Bioinformatics*, 65(1), 15-26.
- Su, S., Wong, G., Shi, W., Liu, J., Lai, A. C., Zhou, J., Liu, W., Bi, Y., & Gao, G. F. (2016). Epidemiology, genetic recombination, and pathogenesis of coronaviruses. *Trends in microbiology*, 24(6), 490-502.
- SYSTEMES, D. (2016). BIOVIA Discovery Studio. In *Dassault Syst mes BIOVIA, Discovery Studio Modeling Environment, Release 2017*: Dassault Syst mes.
- Takahashi, S., Yoshiya, T., Yoshizawa-Kumagaye, K., & Sugiyama, T. (2015). Nicotianamine is a novel angiotensin-converting enzyme 2 inhibitor in soybean. *Biomedical Research*, 36(3), 219-224.
- Tallei, T. E., Tumilaar, S. G., Niode, N. J., Fatimawali, Kepel, B. J., Idroes, R., Effendi, Y., Sakib, S. A., & Emran, T. B. (2020). Potential of Plant Bioactive Compounds as SARS-CoV-2 Main Protease (M(pro)) and Spike (S) Glycoprotein Inhibitors: A Molecular Docking Study. *Scientifica (Cairo)*, 2020, 6307457.
<https://doi.org/10.1155/2020/6307457>

- Tamene Dandena, & Endale Milkyas. (2019). Antibacterial activity of coumarins and carbazole alkaloid from roots of *clausena anisata*. *Advances in Pharmacological Sciences*, 2019.
- Tan, T. K., Rijal, P., Rahikainen, R., Keeble, A. H., Schimanski, L., Hussain, S., Harvey, R., Hayes, J. W., Edwards, J. C., & McLean, R. K. (2021). A COVID-19 vaccine candidate using SpyCatcher multimerization of the SARS-CoV-2 spike protein receptor-binding domain induces potent neutralising antibody responses. *Nature communications*, 12(1), 1-16.
- Tazzini, N. (2014). *Flavonoids: chemical structure, classification, and examples*. Retrieved on 05-April-2022 from <https://www.tuscany-diet.net/2014/01/22/flavonoids-definition-structure-classification/>
- Te Velthuis, A. J., Arnold, J. J., Cameron, C. E., Van Den Worm, S. H., & Snijder, E. J. (2010). The RNA polymerase activity of SARS-coronavirus nsp12 is primer dependent. *Nucleic acids research*, 38(1), 203-214.
- Thoms, M., Buschauer, R., Ameismeier, M., Koepke, L., Denk, T., Hirschenberger, M., Kratzat, H., Hayn, M., Mackens-Kiani, T., & Cheng, J. (2020). Structural basis for translational shutdown and immune evasion by the Nsp1 protein of SARS-CoV-2. *Science*, 369(6508), 1249-1255.
- Tian, W., Chen, C., Lei, X., Zhao, J., & Liang, J. (2018). CASTp 3.0: computed atlas of surface topography of proteins. *Nucleic acids research*, 46(W1), W363-W367.
- To, K., Tong, J. H., Chan, P. K., Au, F. W., Chim, S. S., Allen Chan, K., Cheung, J. L., Liu, E. Y., Tse, G. M., & Lo, A. W. (2004). Tissue and cellular tropism of the coronavirus associated with severe acute respiratory syndrome: an in-situ hybridization study of fatal cases. *The Journal of Pathology: A Journal of the Pathological Society of Great Britain and Ireland*, 202(2), 157-163.
- Trott, O., & Olson, A. J. (2010). AutoDock Vina: improving the speed and accuracy of docking with a new scoring function, efficient optimization, and multithreading. *Journal of computational chemistry*, 31(2), 455-461.
- Tutunchi, H., Naeini, F., Ostadrahimi, A., & Hosseinzadeh-Attar, M. J. (2020). Naringenin, a flavanone with antiviral and anti-inflammatory effects: A promising treatment strategy against COVID-19. *Phytotherapy Research*, 34(12), 3137-3147.

- Vakser, I. A. (2014). Protein-protein docking: From interaction to interactome. *Biophysical journal*, 107(8), 1785-1793.
- Venkataraman, S., Prasad, B. V., & Selvarajan, R. (2018). RNA dependent RNA polymerases: insights from structure, function and evolution. *Viruses*, 10(2), 76.
- Verdecchia, P., Cavallini, C., Spanevello, A., & Angeli, F. (2020). The pivotal link between ACE2 deficiency and SARS-CoV-2 infection. *European journal of internal medicine*, 76, 14-20.
- Vincent, S., Arokiyaraj, S., Saravanan, M., & Dhanraj, M. (2020). Molecular Docking Studies on the Anti-viral Effects of Compounds From Kabasura Kudineer on SARS-CoV-2 3CLpro [Original Research]. *Frontiers in Molecular Biosciences*, 7. <https://doi.org/10.3389/fmolb.2020.613401>
- Wen, C.-C., Kuo, Y.-H., Jan, J.-T., Liang, P.-H., Wang, S.-Y., Liu, H.-G., Lee, C.-K., Chang, S.-T., Kuo, C.-J., & Lee, S.-S. (2007). Specific plant terpenoids and lignoids possess potent antiviral activities against severe acute respiratory syndrome coronavirus. *Journal of medicinal chemistry*, 50(17), 4087-4095.
- WHO. (2020a). *Archived: Who timeline - covid-19*. World Health Organization. Retrieved on 1-January-2022 from <https://www.who.int/news/item/27-04-2020-who-timeline---covid-19>
- WHO. (2020b). Novel Coronavirus (2019-nCoV): situation report, 11.
- WHO. (2022). *Who coronavirus (COVID-19) dashboard*. World Health Organization. Retrieved ON 11-may-2022 from <https://covid19.who.int/>
- Wink, M. (2007). Molecular modes of action of cytotoxic alkaloids: from DNA intercalation, spindle poisoning, topoisomerase inhibition to apoptosis and multiple drug resistance. *The Alkaloids: Chemistry and Biology*, 64, 1-47.
- Wong, S. E., & Lightstone, F. C. (2011). Accounting for water molecules in drug design. *Expert opinion on drug discovery*, 6(1), 65-74.
- Wu, F., Zhao, S., Yu, B., Chen, Y.-M., Wang, W., Song, Z.-G., Hu, Y., Tao, Z.-W., Tian, J.-H., & Pei, Y.-Y. (2020). A new coronavirus associated with human respiratory disease in China. *nature*, 579(7798), 265-269.
- Wu, Y., Crich, D., Pegan, S. D., Lou, L., Hansen, M. C., Booth, C., Desrochers, E., Mullinix, L. N., Starling, E. B., & Chang, K. Y. (2021). Polyphenols as Potential Inhibitors of SARS-CoV-2 RNA Dependent RNA Polymerase (RdRp). *Molecules*, 26(24), 7438.

- Yin, W., Mao, C., Luan, X., Shen, D.-D., Shen, Q., Su, H., Wang, X., Zhou, F., Zhao, W., & Gao, M. (2020). Structural basis for inhibition of the RNA-dependent RNA polymerase from SARS-CoV-2 by remdesivir. *Science*, 368(6498), 1499-1504.
- Zhou, P., Yang, X.-L., Wang, X.-G., Hu, B., Zhang, L., Zhang, W., Si, H.-R., Zhu, Y., Li, B., & Huang, C.-L. (2020). A pneumonia outbreak associated with a new coronavirus of probable bat origin. *nature*, 579(7798), 270-273.
- Zhu, N., Zhang, D., Wang, W., Li, X., Yang, B., Song, J., Zhao, X., Huang, B., Shi, W., & Lu, R. (2020). A novel coronavirus from patients with pneumonia in China, 2019. *New England journal of medicine*.
- Zothantluanga, J. H. (2021). Molecular Docking Simulation Studies, Toxicity Study, Bioactivity Prediction, and Structure-Activity Relationship Reveals Rutin as a Potential Inhibitor of SARS-CoV-2 3CL pro. *Journal of Scientific Research*, 65(05), 96-104. <https://doi.org/10.37398/jsr.2021.650511>

APPENDICES

Appendix 1: Vina Dock Results in Respect to Binding Energy

Berbamine (52)

```
Command Prompt
Detected 4 CPUs
Reading input ... done.
Setting up the scoring function ... done.
Analyzing the binding site ... done.
Using random seed: -613576432
Performing search ...
0% 10 20 30 40 50 60 70 80 90 100%
|----|----|----|----|----|----|----|----|----|----|
*****
done.
Refining results ... done.

mode | affinity | dist from best mode
| (kcal/mol) | rmsd l.b. | rmsd u.b.
-----+-----+-----+-----
1 | -8.8 | 0.000 | 0.000
2 | -8.8 | 23.030 | 26.905
3 | -8.7 | 23.538 | 28.554
4 | -8.3 | 23.549 | 28.192
5 | -8.2 | 23.332 | 27.355
6 | -8.2 | 21.484 | 26.197
7 | -7.9 | 24.340 | 29.095
8 | -7.9 | 2.620 | 7.325
9 | -7.9 | 30.207 | 34.580
Writing output ... done.

C:\Users\tare\Desktop\Berbamine (52)>
```

Dicentrin (53)

```
Command Prompt
Detected 4 CPUs
Reading input ... done.
Setting up the scoring function ... done.
Analyzing the binding site ... done.
Using random seed: 1694184856
Performing search ...
0% 10 20 30 40 50 60 70 80 90 100%
|----|----|----|----|----|----|----|----|----|----|
*****
done.
Refining results ... done.

mode | affinity | dist from best mode
| (kcal/mol) | rmsd l.b. | rmsd u.b.
-----+-----+-----+-----
1 | -7.1 | 0.000 | 0.000
2 | -6.8 | 30.250 | 32.475
3 | -6.4 | 28.830 | 32.260
4 | -6.3 | 45.010 | 46.971
5 | -6.2 | 48.842 | 52.551
6 | -6.2 | 28.659 | 30.858
7 | -6.2 | 11.992 | 15.393
8 | -6.1 | 45.046 | 47.085
9 | -6.1 | 54.989 | 56.707
Writing output ... done.

C:\Users\tare\Desktop\Dicentrin (53)>
```

Jatrorrhizine (55)

```
Command Prompt
Detected 4 CPUs
Reading input ... done.
Setting up the scoring function ... done.
Analyzing the binding site ... done.
Using random seed: 141339696
Performing search ...
0% 10 20 30 40 50 60 70 80 90 100%
|----|----|----|----|----|----|----|----|----|----|
*****
done.
Refining results ... done.

mode | affinity | dist from best mode
| (kcal/mol) | rmsd l.b. | rmsd u.b.
-----+-----+-----+-----
1 | -8.0 | 0.000 | 0.000
2 | -7.5 | 19.750 | 23.149
3 | -7.2 | 31.084 | 33.216
4 | -7.2 | 25.134 | 27.277
5 | -7.2 | 27.338 | 29.126
6 | -7.1 | 21.809 | 23.942
7 | -7.0 | 21.245 | 23.562
8 | -6.9 | 23.689 | 26.592
9 | -6.9 | 23.845 | 26.550
Writing output ... done.

C:\Users\tare\Desktop\Coptisine (54)>
```

Coptisine (54)

```
Command Prompt
Detected 4 CPUs
Reading input ... done.
Setting up the scoring function ... done.
Analyzing the binding site ... done.
Using random seed: 809394088
Performing search ...
0% 10 20 30 40 50 60 70 80 90 100%
|----|----|----|----|----|----|----|----|----|----|
*****
done.
Refining results ... done.

mode | affinity | dist from best mode
| (kcal/mol) | rmsd l.b. | rmsd u.b.
-----+-----+-----+-----
1 | -7.4 | 0.000 | 0.000
2 | -6.8 | 25.014 | 27.501
3 | -6.7 | 25.157 | 27.700
4 | -6.6 | 25.349 | 28.052
5 | -6.6 | 28.404 | 30.951
6 | -6.4 | 43.272 | 45.942
7 | -6.4 | 24.226 | 27.684
8 | -6.3 | 25.115 | 27.664
9 | -6.3 | 22.040 | 25.323
Writing output ... done.

C:\Users\tare\Desktop\Jatrorrhizine (55)>
```

Palmatine (56)

```

C:\> Command Prompt
Detected 4 CPUs
Reading input ... done.
Setting up the scoring function ... done.
Analyzing the binding site ... done.
Using random seed: -1456835000
Performing search ...
0% 10 20 30 40 50 60 70 80 90 100%
|----|----|----|----|----|----|----|----|----|----|
|*****|
done.
Refining results ... done.

mode |  affinity | dist from best mode
      | (kcal/mol) | rmsd l.b. | rmsd u.b.
-----+-----+-----+-----
1     |    -6.1   |    0.000   |    0.000
2     |    -6.1   |    1.133   |    8.336
3     |    -6.1   |    7.291   |   9.911
4     |    -6.1   |   22.127   |   23.752
5     |    -6.0   |   31.347   |   32.192
6     |    -5.9   |   25.656   |   30.467
7     |    -5.9   |   19.309   |   21.495
8     |    -5.9   |   37.806   |   41.791
9     |    -5.8   |   28.236   |   30.924
Writing output ... done.

C:\Users\tare\Desktop\Palmatine (56)>

```

Bufotenin (57)

```

C:\> Command Prompt
Detected 4 CPUs
Reading input ... done.
Setting up the scoring function ... done.
Analyzing the binding site ... done.
Using random seed: -895806976
Performing search ...
0% 10 20 30 40 50 60 70 80 90 100%
|----|----|----|----|----|----|----|----|----|----|
|*****|
done.
Refining results ... done.

mode |  affinity | dist from best mode
      | (kcal/mol) | rmsd l.b. | rmsd u.b.
-----+-----+-----+-----
1     |    -5.3   |    0.000   |    0.000
2     |    -5.1   |   56.794   |   58.529
3     |    -4.9   |   36.757   |   38.589
4     |    -4.9   |   57.742   |   58.744
5     |    -4.9   |    9.354   |   10.842
6     |    -4.9   |   57.798   |   60.400
7     |    -4.8   |    8.631   |    9.828
8     |    -4.8   |   45.582   |   47.220
9     |    -4.8   |   27.606   |   29.436
Writing output ... done.

C:\Users\tare\Desktop\new final\Bufotenin (57)>

```

silocybin (58)

```

C:\> Command Prompt
Detected 4 CPUs
Reading input ... done.
Setting up the scoring function ... done.
Analyzing the binding site ... done.
Using random seed: -1783734664
Performing search ...
0% 10 20 30 40 50 60 70 80 90 100%
|----|----|----|----|----|----|----|----|----|----|
|*****|
done.
Refining results ... done.

mode |  affinity | dist from best mode
      | (kcal/mol) | rmsd l.b. | rmsd u.b.
-----+-----+-----+-----
1     |    -5.9   |    0.000   |    0.000
2     |    -5.7   |   37.617   |   39.366
3     |    -5.6   |   27.343   |   29.357
4     |    -5.5   |   31.185   |   32.886
5     |    -5.4   |    3.656   |    6.129
6     |    -5.4   |   34.583   |   35.803
7     |    -5.3   |   36.903   |   38.092
8     |    -5.3   |   37.455   |   39.581
9     |    -5.2   |    3.530   |    4.346
Writing output ... done.

C:\Users\tare\Desktop\Psilocybin (58)>

```

Biscryptolepine (60)

```

C:\> Command Prompt
Detected 4 CPUs
Reading input ... done.
Setting up the scoring function ... done.
Analyzing the binding site ... done.
Using random seed: -337394960
Performing search ...
0% 10 20 30 40 50 60 70 80 90 100%
|----|----|----|----|----|----|----|----|----|----|
|*****|
done.
Refining results ... done.

mode |  affinity | dist from best mode
      | (kcal/mol) | rmsd l.b. | rmsd u.b.
-----+-----+-----+-----
1     |    -9.0   |    0.000   |    0.000
2     |    -8.9   |   19.985   |   24.988
3     |    -8.9   |   20.209   |   24.672
4     |    -8.7   |    4.036   |    5.824
5     |    -8.6   |    1.177   |    7.325
6     |    -8.6   |    1.566   |    7.216
7     |    -8.3   |   31.542   |   35.025
8     |    -8.3   |   31.430   |   34.470
9     |    -8.1   |   31.184   |   34.047
Writing output ... done.

C:\Users\tare\Desktop\Biscryptolepine (60)>

```

CPD61

```

Command Prompt
Detected 4 CPUs
Reading input ... done.
Setting up the scoring function ... done.
Analyzing the binding site ... done.
Using random seed: 199898908
Performing search ...
0% 10 20 30 40 50 60 70 80 90 100%
|----|----|----|----|----|----|----|----|----|----|
|*****|
done.
Refining results ... done.

mode | affinity | dist from best mode
      | (kcal/mol) | rmsd l.b. | rmsd u.b.
-----+-----+-----+-----
1      -7.1      0.000      0.000
2      -6.8      25.385     27.933
3      -6.7      33.670     36.550
4      -6.4      31.687     34.260
5      -6.4      36.215     38.637
6      -6.3      32.023     35.527
7      -6.3      25.287     27.964
8      -6.3      41.104     43.175
9      -6.2      26.533     28.645
Writing output ... done.

C:\Users\tare\Desktop\CPD61>

```

➤ CPD63

```

Command Prompt
Detected 4 CPUs
Reading input ... done.
Setting up the scoring function ... done.
Analyzing the binding site ... done.
Using random seed: -1506949096
Performing search ...
0% 10 20 30 40 50 60 70 80 90 100%
|----|----|----|----|----|----|----|----|----|----|
|*****|
done.
Refining results ... done.

mode | affinity | dist from best mode
      | (kcal/mol) | rmsd l.b. | rmsd u.b.
-----+-----+-----+-----
1      -7.7      0.000      0.000
2      -7.3      37.438     41.360
3      -7.1      3.381      5.440
4      -6.8      34.275     37.646
5      -6.6      34.031     37.247
6      -6.6      1.881      4.897
7      -6.6      31.376     33.274
8      -6.5      21.925     24.610
9      -6.5      31.349     33.463
Writing output ... done.

C:\Users\tare\Desktop\CPD63>

```

CPD62

```

Command Prompt
Detected 4 CPUs
Reading input ... done.
Setting up the scoring function ... done.
Analyzing the binding site ... done.
Using random seed: 415706960
Performing search ...
0% 10 20 30 40 50 60 70 80 90 100%
|----|----|----|----|----|----|----|----|----|----|
|*****|
done.
Refining results ... done.

mode | affinity | dist from best mode
      | (kcal/mol) | rmsd l.b. | rmsd u.b.
-----+-----+-----+-----
1      -6.6      0.000      0.000
2      -6.5      31.565     34.153
3      -6.3      1.540      6.755
4      -6.3      25.175     27.809
5      -6.3      1.863      6.750
6      -6.2      12.433     14.453
7      -6.2      34.496     36.859
8      -6.2      17.735     19.746
9      -6.2      26.420     28.688
Writing output ... done.

C:\Users\tare\Desktop\CPD62>

```

CPD64

```

Command Prompt
Detected 4 CPUs
Reading input ... done.
Setting up the scoring function ... done.
Analyzing the binding site ... done.
Using random seed: -1324758264
Performing search ...
0% 10 20 30 40 50 60 70 80 90 100%
|----|----|----|----|----|----|----|----|----|----|
|*****|
done.
Refining results ... done.

mode | affinity | dist from best mode
      | (kcal/mol) | rmsd l.b. | rmsd u.b.
-----+-----+-----+-----
1      -6.5      0.000      0.000
2      -6.4      35.949     39.158
3      -6.4      27.904     30.954
4      -6.3      43.594     45.819
5      -6.3      27.729     30.681
6      -6.2      30.305     32.346
7      -6.0      52.761     56.420
8      -6.0      32.231     37.228
9      -6.0      44.304     46.950
Writing output ... done.

C:\Users\tare\Desktop\CPD64>

```

CPD65

```

C:\Users\tare\Desktop\CPD65>
Detected 4 CPUs
Reading input ... done.
Setting up the scoring function ... done.
Analyzing the binding site ... done.
Using random seed: -296492872
Performing search ...
0% 10 20 30 40 50 60 70 80 90 100%
|----|----|----|----|----|----|----|----|----|----|
*****
done.
Refining results ... done.

mode |  affinity | dist from best mode
      | (kcal/mol) | rmsd l.b. | rmsd u.b.
-----+-----+-----+-----
1      -6.2      0.000      0.000
2      -6.2      27.985     30.962
3      -6.2      27.974     30.790
4      -6.2      15.911     18.548
5      -6.1      45.108     48.594
6      -6.1      30.449     33.346
7      -6.1      27.446     30.113
8      -6.1      41.717     44.432
9      -6.0      27.285     30.324
Writing output ... done.

C:\Users\tare\Desktop\CPD65>

```

CPD66

```

C:\Users\tare\Desktop\CPD66>
Detected 4 CPUs
Reading input ... done.
Setting up the scoring function ... done.
Analyzing the binding site ... done.
Using random seed: 721766760
Performing search ...
0% 10 20 30 40 50 60 70 80 90 100%
|----|----|----|----|----|----|----|----|----|----|
*****
done.
Refining results ... done.

mode |  affinity | dist from best mode
      | (kcal/mol) | rmsd l.b. | rmsd u.b.
-----+-----+-----+-----
1      -6.8      0.000      0.000
2      -6.8      1.678      3.154
3      -6.5      5.624     12.697
4      -6.5     43.570     46.166
5      -6.4     45.161     46.517
6      -6.3     32.245     34.063
7      -6.3     20.981     25.222
8      -6.2     32.809     36.399
9      -6.2     21.970     26.263
Writing output ... done.

C:\Users\tare\Desktop\CPD66>

```

CPD67

```

C:\Users\tare\Desktop\CPD67>
Detected 4 CPUs
Reading input ... done.
Setting up the scoring function ... done.
Analyzing the binding site ... done.
Using random seed: 795790464
Performing search ...
0% 10 20 30 40 50 60 70 80 90 100%
|----|----|----|----|----|----|----|----|----|----|
*****
done.
Refining results ... done.

mode |  affinity | dist from best mode
      | (kcal/mol) | rmsd l.b. | rmsd u.b.
-----+-----+-----+-----
1      -6.1      0.000      0.000
2      -6.0     27.529     29.665
3      -5.9     19.389     22.355
4      -5.9     15.142     17.486
5      -5.8     20.519     23.843
6      -5.8     22.256     24.499
7      -5.8     33.705     37.199
8      -5.8      2.586      3.990
9      -5.7      2.619      5.481
Writing output ... done.

C:\Users\tare\Desktop\CPD67>

```

CPD68

```

C:\Users\tare\Desktop\CPD68>
Detected 4 CPUs
Reading input ... done.
Setting up the scoring function ... done.
Analyzing the binding site ... done.
Using random seed: 708681144
Performing search ...
0% 10 20 30 40 50 60 70 80 90 100%
|----|----|----|----|----|----|----|----|----|----|
*****
done.
Refining results ... done.

mode |  affinity | dist from best mode
      | (kcal/mol) | rmsd l.b. | rmsd u.b.
-----+-----+-----+-----
1      -6.3      0.000      0.000
2      -6.1      2.760      4.174
3      -5.9     27.217     29.141
4      -5.9      8.968     12.356
5      -5.9      2.963      6.020
6      -5.8     29.096     32.312
7      -5.8     30.050     32.967
8      -5.7      2.082      5.811
9      -5.7      2.295      3.810
Writing output ... done.

C:\Users\tare\Desktop\CPD68>

```

CPD69

```

Command Prompt
Detected 4 CPUs
Reading input ... done.
Setting up the scoring function ... done.
Analyzing the binding site ... done.
Using random seed: -797560036
Performing search ...
0% 10 20 30 40 50 60 70 80 90 100%
|---|---|---|---|---|---|---|---|---|---|
|-----|-----|-----|-----|-----|-----|-----|-----|
*****
done.
Refining results ... done.

mode | affinity | dist from best mode
      | (kcal/mol) | rmsd l.b. | rmsd u.b.
-----+-----+-----+-----
1      -6.8      0.000      0.000
2      -6.4     30.522     32.558
3      -6.4     55.198     56.514
4      -6.3     29.817     31.995
5      -6.2     52.170     53.494
6      -6.2     52.774     54.117
7      -6.2     30.907     33.142
8      -6.1     48.967     51.636
9      -6.1     29.854     32.336
Writing output ... done.

C:\Users\tare\Desktop\CPD69>

```

CPD70

```

Command Prompt
Detected 4 CPUs
Reading input ... done.
Setting up the scoring function ... done.
Analyzing the binding site ... done.
Using random seed: 57190876
Performing search ...
0% 10 20 30 40 50 60 70 80 90 100%
|---|---|---|---|---|---|---|---|---|---|
|-----|-----|-----|-----|-----|-----|-----|-----|
*****
done.
Refining results ... done.

mode | affinity | dist from best mode
      | (kcal/mol) | rmsd l.b. | rmsd u.b.
-----+-----+-----+-----
1      -6.8      0.000      0.000
2      -6.7     51.513     52.111
3      -6.6     36.022     38.249
4      -6.5     51.365     52.529
5      -6.5      1.383      4.265
6      -6.5      1.372      4.369
7      -6.3     34.180     36.589
8      -6.2     34.192     36.017
9      -6.2     32.230     34.010
Writing output ... done.

C:\Users\tare\Desktop\CPD70>

```

CPD71

```

Command Prompt
Detected 4 CPUs
Reading input ... done.
Setting up the scoring function ... done.
Analyzing the binding site ... done.
Using random seed: 1655386328
Performing search ...
0% 10 20 30 40 50 60 70 80 90 100%
|---|---|---|---|---|---|---|---|---|---|
|-----|-----|-----|-----|-----|-----|-----|-----|
*****
done.
Refining results ... done.

mode | affinity | dist from best mode
      | (kcal/mol) | rmsd l.b. | rmsd u.b.
-----+-----+-----+-----
1      -6.6      0.000      0.000
2      -6.5     33.446     35.939
3      -6.4     17.185     18.658
4      -6.4     34.506     36.967
5      -6.4      1.372      1.943
6      -6.3     17.274     19.151
7      -6.2     34.404     36.877
8      -6.1     24.176     25.786
9      -6.1     19.114     20.196
Writing output ... done.

C:\Users\tare\Desktop\CPD71>

```

Remdesivir

```

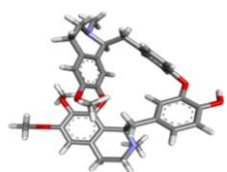
Command Prompt
Detected 4 CPUs
Reading input ... done.
Setting up the scoring function ... done.
Analyzing the binding site ... done.
Using random seed: 1879893656
Performing search ...
0% 10 20 30 40 50 60 70 80 90 100%
|---|---|---|---|---|---|---|---|---|---|
|-----|-----|-----|-----|-----|-----|-----|-----|
*****
done.
Refining results ... done.

mode | affinity | dist from best mode
      | (kcal/mol) | rmsd l.b. | rmsd u.b.
-----+-----+-----+-----
1      -6.7      0.000      0.000
2      -6.7     17.952     22.926
3      -6.6     19.474     22.549
4      -6.4     38.170     41.468
5      -6.3     20.105     24.886
6      -6.2     38.865     42.263
7      -6.1      2.544      5.127
8      -6.1     19.863     23.764
9      -6.1     35.759     40.724
Writing output ... done.

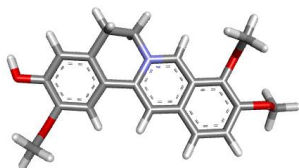
C:\Users\tare\Desktop\Remdesivir>

```

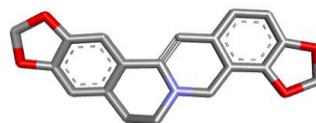
Appendix 2. Three-dimensional structure of target compounds.



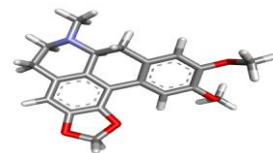
Berbamine(52)



Jatrorrhizine(55)



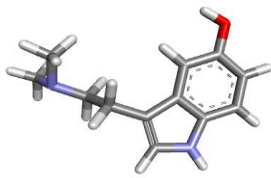
Dicentrine(53)



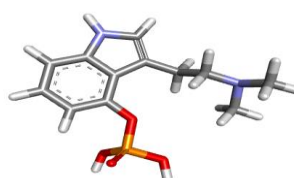
Coptisin(54)



Palmatine(56)



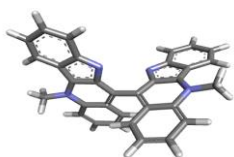
Bufotenin(57)



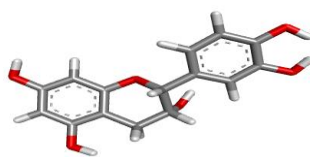
Psilocybin(58)



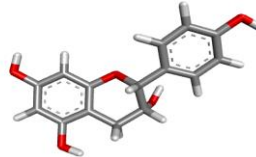
Nicotiflorin(59)



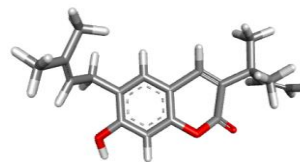
Biscryptolepine(60)



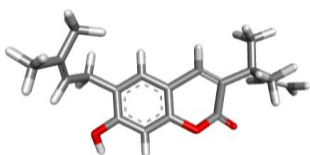
CPD61



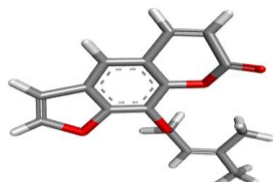
CPD62



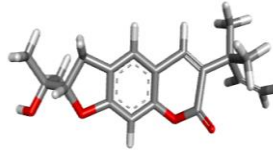
CPD63



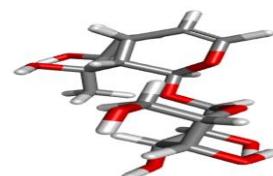
CPD64



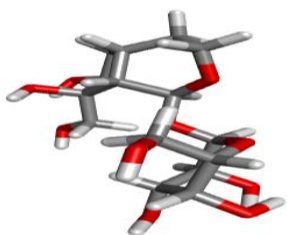
CPD65



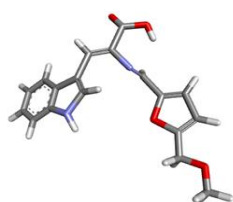
CPD66



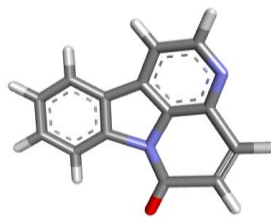
CPD67



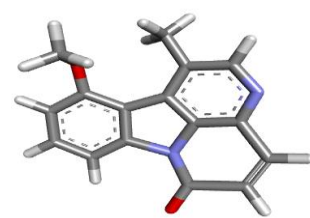
CPD68



CPD69



CPD70



CPD71